THE TRAFFICKING OF AMPHIREGULIN IN POLARIZED EPITHELIAL CELLS

By

Jonathan D. Gephart

Dissertation

Submitted to the Faculty of the

Graduate School of Vanderbilt University

in partial fulfillment of the requirements

for the degree of

DOCTOR OF PHILOSOPHY

In

Cell and Developmental Biology

August, 2011

Nashville, Tennessee

Approved:

Professor Steve Hanks

Professor Ethan Lee

Professor Anna Means

Professor Todd Graham

Professor Robert Coffey

To my wonderful wife Corey,

and our two amazing daughters,

Skylar and Harper

ACKNOWLEDGEMENTS

I would like to first and foremost thank my wonderful wife Corey for all her patience, support, and encouragement over the years. She has always been there for me in good and bad times. Her belief in me has provided the necessary strength to accomplish my goals. Without her, I would have nothing.

I would like to thank Dr. Robert J Coffey for all his support and guidance during my graduate education. I always knew Bob had my back and was supportive of all my endeavors. Bob never placed limits on what I could try in the lab but instead encouraged me to be bold in my experiments. Bob's love and dedication to science is an inspiration.

I would like to thank the many members of the Coffey lab who have all been great to work with over the years. Ramona Graves Deal is an excellent lab manager and is always willing to help out however she can. The Coffey lab would crumble without Ramona. Galina Bogatcheva is full of experience and wise advice. I could always turn to Galina when I had questions about how science should be done. Cunxi Li is a great scientist and was an invaluable resource on protein trafficking. Jeff Franklin was my scientific rock in the lab, someone I could always turn to for any problem. Jeff's guidance over the course of my graduate education has had profound influence on my scientific development.

Bhumi Singh has been a great lab partner in the study of EGFR ligand trafficking. Bhumi is an excellent scientist and had great influence on my experimental directions at the tail end of my graduate work. Having Bhumi to

discuss science with across the bench made the lab much more enjoyable. Jim Higginbotham was essential to the advancement of my work. Jim's help with cell line generation made it possible for me to create so many different cell populations in a reasonable amount of time. I enjoyed working with Jim on the exosome project and all our discussions in the cell culture room. Michelle Demory Beckler has been a pleasure to work with on AREG. Michelle was kind enough to read and edit portions of this dissertation, a task I greatly appreciated. I wish her all the best in her future work on AREG. Also many thanks to all the other members of the lab that I did not work directly with but enjoyed our non-scientific interactions over the years.

I would like to thank members of the Goldenring lab for all their help with reagents in my times of desperation. When I could not find something in our lab or did not want to order it for a single experiment, I could always get a sample from the Goldenring lab. I would like to especially thank Joe Roland for all his help and guidance. Joe had a profound influence on how I think about science and how I have developed as a scientist.

I would like to thank my committee members for all their guidance during my education. During every committee meeting, my committee would provide me with extremely helpful and constructive criticism that would always get my projects back on track. One of my regrets during my graduate education is not meeting with my committee more often. Had I done so, I may have reached my defense earlier. Finally, I would like to thank the US taxpayer, whose hard work generated the wealth and taxes that allowed me to obtain this education.

TABLE OF CONTENTS

LIST OF TABLES

LIST OF FIGURES

LIST OF ABBREVIATIONS

ACD – AREG Cytoplasmic Domain

AP – Adaptor Protein

Ap – Apical

APC - Adenomatous Polyposis Coli

AREG – Amphiregulin

ARH – Autosomal Recessive Hypercholesterolemia Protein

BL – Basolateral

CaRT – Cargo Recognition and Targeting

CK2 – Casein Kinase 2

CL – Cleared Lysate

Co-IP – Co-Immunoprecipitate

CRC – Colorectal Cancer

Crb – Crumbs

Dlg – Discs Large

DUB – De-ubiquitylating enzyme

EC – Extracellular Cadherin

ECM – Extracellular Matix

EGF – Epidermal Growth Factor

EGFR – Epidermal Growth Factor Receptor

EREG – Epiregulin

ER – Endoplasmic Reticulum

ESCRT – Endosomal Sorting Complex Required for Transport

FAVS – Fluorescence-Activated Vesicle Sorting

GAT – GGA and TOM (target of myb)

GAE – γ-adaptin ear

GAP – GTPase-Activating Protein

GEF – Guanine Nucleotide Exchange Factor

GGA – Golgi-localized, γ-ear-containing Arf-binding proteins

GPI – Glycosylphosphatidylinositol

HB-EGF – Heparin-Binding EGF-like Growth Factor

ILV – Intralumenal Vesicle

IP – Immunoprecipitation

JAMs – Junctional Adhesion Molecules

KD – Knock Down

LBPA – Lyso-Bisphosphatidic Acid

LDL – Low Density Lipoprotein

Lgl – Lethal Giant Larvae

LRR – Leucine Rich Repeat

MAGI-3 – Membrane Associated Guanylate Kinase Inverted-3

MCS – Multiple Cloning Site

MVB – Multivesicular Body

NGFR – 75-kD Human Nerve Growth Factor Receptor

NKD2 – Naked 2

PALS1 – Protein Associated with LIN-7

PATJ – PALS1 Associated Tight Junction Protein

Par – Partitioning Defect

PDZ – Postsynaptic density-95, Discs large, Zonula occludens 1

aPKC – atypical Protein Kinase C

TEER – Transepithelial Electrical Resistance

TGFα – Transforming Growth Factor-α

TGN – Trans Golgi Network

TL – Total Lysate

TM165 – Transmembrane Protein 165

VHS – Vps27, Hrs, Stam

ZO – Zona Occludin

CHAPTER I

BIOLOGY OF THE POLARIZED EPITHELIUM

Epithelial cells make up the epithelial tissue or epithelium that covers all external and internal organs of multicellular organisms. There are four principal types of epithelium: simple columnar, simple squamous, transitional, and stratified squamous (Lodish, 2003). One of the most important functions of the epithelium is the creation of a selectively permeable barrier that separates chemically and functionally distinct compartments. This compartmentalization allows for different functions and reactions to proceed simultaneously within an organism. Accordingly, epithelial cells contain four distinct structural elements to create and maintain epithelial polarity: the apical membrane, the tight junction, the adherens junction, and the basolateral (BL) membrane (Figure 1) (St Johnston and Ahringer, 2010). These cellular regions are biochemically and functionally divergent polarized membrane surfaces with distinct protein and lipid compositions (Martin-Belmonte and Mostov, 2008).

The Apical Membrane

The apical membrane is the surface of the cell exposed to the lumen or external environment. Because this environment can vary dramatically depending on the location of the cell, there is great variety in the composition of apical membranes. Apical membranes often contain structural elements that

interact with the external environment and these structures vary depending on the cell location and function. For example, the apical membranes of intestinal and kidney cells contain protrusions of microvilli, collectively termed a brush border, which increases the absorptive capacity of the cell (Nambiar et al., 2010). The apical membrane is also the location of the primary cilium that acts as a "cellular antenna" for a variety of sensory and signaling mechanisms (Singla and Reiter, 2006). Because this membrane is the interface between the external environment and the interior of an organism, endocytosis at the apical membrane is much more regulated then the BL membrane, such that the rate of endocytosis at the apical surface is only 20% the rate of endocytosis at the BL surface (Mostov et al., 2000). The apical membrane is enriched in glycosphingolipids, which may function to protect the cell from the harsh environment of the lumen, and depleted in phosphatidylcholine (Simons and van Meer, 1988; van Meer and Simons, 1988). The protein components of the apical membrane include ion channels and transporters that regulate nutrient and water uptake as well as hydrolases involved in digestive and protective functions (Rodriguez-Boulan and Nelson, 1989). Maintaining the appropriate protein and lipid composition of the apical membrane is critical for proper cellular function.

Tight Junctions

Tight junctions perform multiple functions in polarized epithelial cells. Tight junctions are the major paracellular barrier between the external and internal milieu (Denker and Nigam, 1998). The apical membrane is physically separated

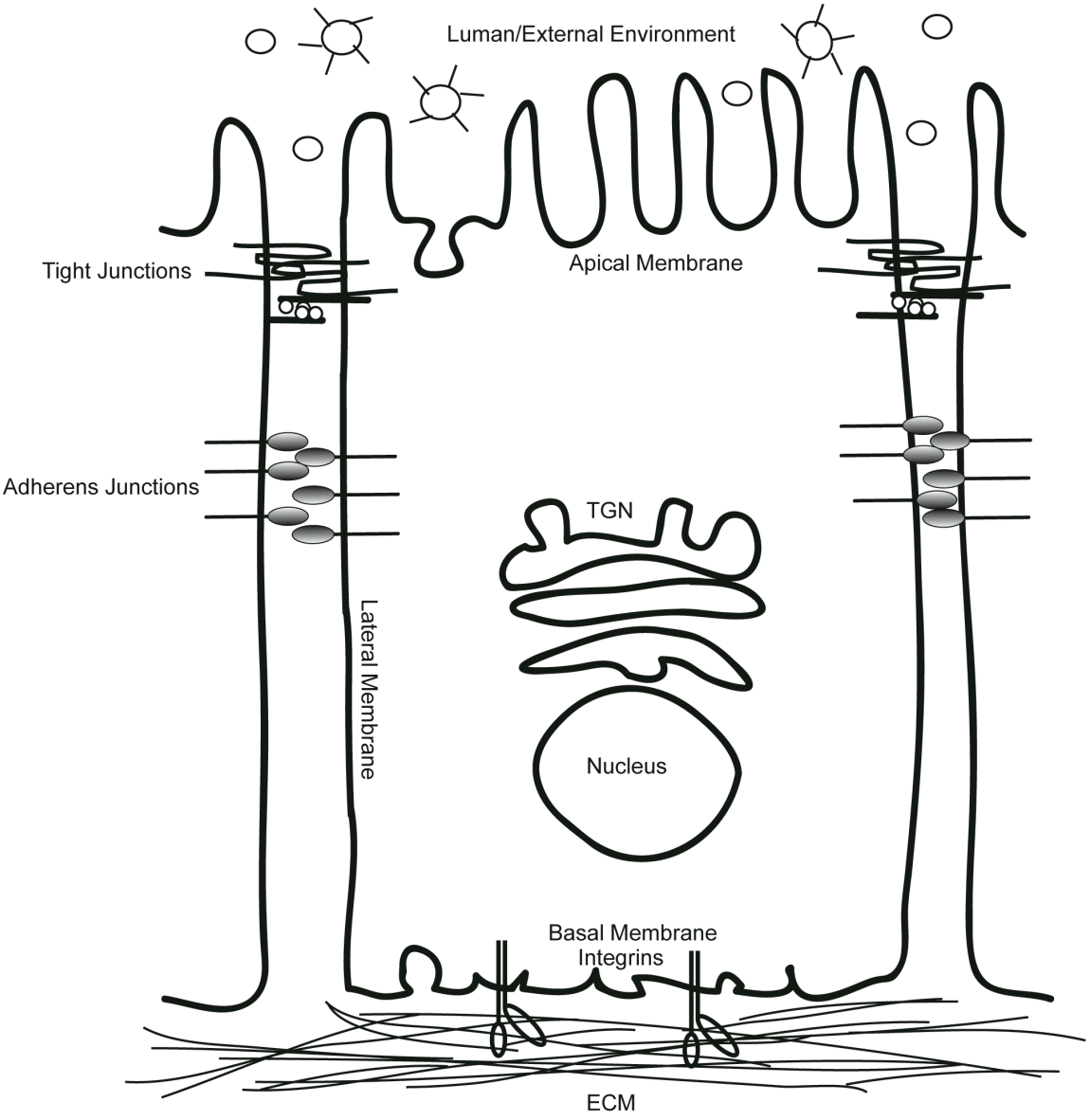

Figure 1. Basic schematic of a polarized epithelial cell. Epithelial cells form a selectively permeable barrier that facilitates the creation of chemically and functionally distinct compartments within an organism. To cope with the disparate environments created by this compartmentalization, epithelial cells must establish biochemically and functionally diverse membrane surfaces with distinct lipid and protein compositions. The apical membrane faces the lumen or external environment; the lateral membrane faces neighboring cells; the basal membrane faces the ECM. Tight junctions form a selective paracellular barrier that regulates intramembrane diffusion. Adherens junctions mediate cell-cell interactions and integrins mediate cell-ECM interactions, both involved in mechanical attachment and orientation cues.

from the lateral membrane by the tight junctions, which act as a fence to prevent the diffusion of lipids within the exoplasmic leaflet and maintain the polarity of the cell surface (Aijaz et al., 2006). Tight junctions are comprised of the tetraspan adhesion proteins occludin and claudin and the single pass transmembrane proteins junctional adhesion molecules (JAMs) and coxsackievirus and adenovirus receptor (CAR) (Figure 2) (Aijaz et al., 2006). These adhesion proteins are clustered together at the tight junctions by ZO-1 and ZO-2, which bind to the cytoplasmic domains of occludin and the claudins, linking them to the underlying actin cytoskeleton (St Johnston and Ahringer, 2010). Together these proteins form a “fence” to separate the apical membrane from the lateral membrane and a selective paracellular “gate” acting to regulate ion permeability (Kohler and Zahraoui, 2005; Marchiando et al., 2010).

Occludin, the first tight junction protein to be identified, clearly localizes to the tight junction but its function is poorly defined (Schneeberger and Lynch, 2004). Occludin is expressed from a single gene that produces five isoforms by alternative splicing (Aijaz et al., 2006). Occludin consists of four transmembrane domains with two extracellular loops and the N- and C- terminal domains both localized in the cytoplasm. The C-terminal domain is rich in serine, threonine, and tyrosine residues that are phosphorylated and regulate occludin integration into the tight junction and occludins barrier function (Raleigh et al., 2011; Sakakibara et al., 1997; Schneeberger and Lynch, 2004). Occludin functions as part of the intramembrane diffusion barrier, or “fence”, that separates the apical and lateral membrane domains (Balda et al., 1996). Increased expression of

occludin within a polarized cell line results in an increased transepithelial electrical resistance (TEER), suggesting a role in electrical barrier function and regulating the paracellular diffusion of small hydrophilic molecules (Aijaz et al., 2006; McCarthy et al., 1996). However, occludin null mice exhibit normal tight junction morphology and normal barrier function in the intestinal epithelium (Saitou et al., 2000). The role of occludin in the tight junction will become more clearly defined as more is learned about its regulation and interactions with other tight junction proteins.

Claudins are the major structural component of the tight junctions and determine the ion selectivity of the paracellular barrier (Balda and Matter, 2008). Claudins are tetraspan transmembrane proteins, with 24 family members expressed in a tissue-specific manner. The two extracellular loops of claudins, the large first loop and the small second loop, have great variability among family members and form intercellular hetero- and homotypic interactions in varying combinations, creating diverse ion selectivity barriers (Aijaz et al., 2006; Tsukita et al., 2001). The C-terminal cytoplasmic domain, the most heterogeneous region of the claudin isoforms, can be phosphorylated and contains a PDZ binding-motif, suggesting a role for the C-terminal domain in claudin isoform regulation and targeting (Angelow et al., 2008). Over expression of claudins in fibroblasts can induce the formation of tight junction strands, supporting the importance of claudins in tight junction structure (Furuse et al., 1998). Future studies on how the claudin extracellular loops regulate ion selectivity and the regulatory role of

the C-terminal domain will reveal how different claudin isoforms function in various epithelial tissues.

The role of the single pass transmembrane proteins JAMs and CAR at the tight junction is not clear. Both proteins have two immunoglobulin folds in their extracellular domains that form intercellular homophilic interactions (Coyne and Bergelson, 2005; Ebnet et al., 2004; Tomko et al., 1997). CAR and the four isoforms of JAMs (A-D) localize to the tight junctions and interact with ZO-1 through the PDZ binding motifs within their cytoplasmic domains (Cohen et al., 2001; Ebnet et al., 2004). Expression of CAR can reduce the passage of macromolecules and ions across a cellular monolayer, suggesting a role in tight junction permeability (Cohen et al., 2001). JAMs associate with polarity proteins as well as ZO-1 and may play a role in cell polarity as opposed to tight junction permeability (Ebnet et al., 2004). Future investigations into these proteins should clarify the roles they play at the tight junctions.

In addition to providing a physical barrier, the tight junction is the location of membrane domain orientation cues essential for establishment and maintenance of cellular polarity. These membrane domain orientation cues define which membrane is apical and which is BL. Three complexes are responsible for providing intrinsic membrane domain orientation cues: the Crumbs complex, consisting of crumbs (Crb), protein associated with LIN-7 (PALS1), and PALS1 associated tight junction protein (PATJ); the partitioning defect (Par) complex, consisting of Par3, Par6, and atypical protein kinase C (aPKC); and the Scribble complex, consisting of scribble, lethal giant larvae (Lgl),

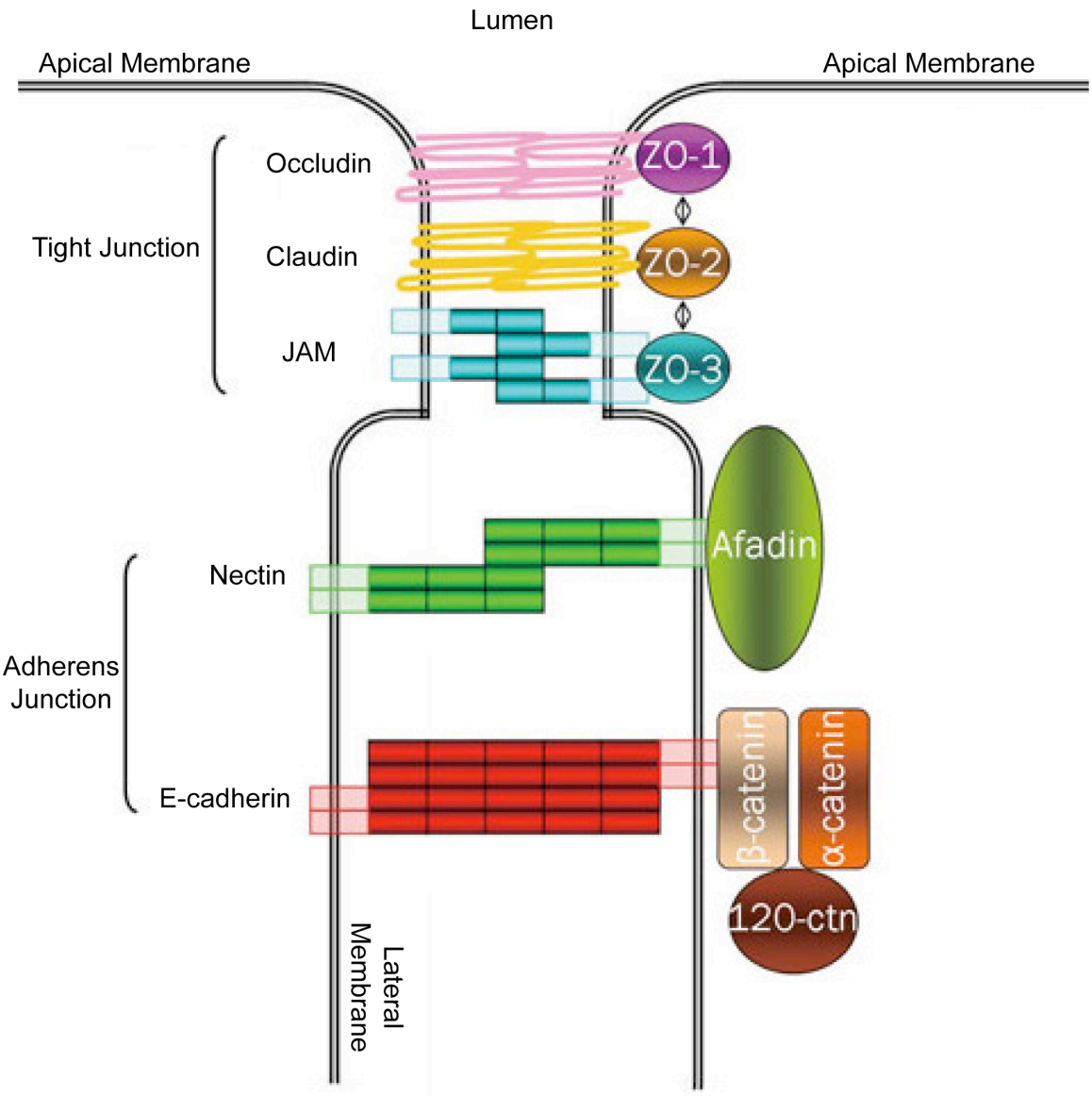

Figure 2. Components of the tight junctions and adherens junctions. An illustration of the transmembrane and cytoplasmic proteins that comprise the tight and adherens junctions. The tight junctions are the paracellular barrier separating the external environment from the interstitium and consist of claudins, occludin, JAMs, and CAR (not shown). The adherens junctions mediate cell-cell interactions through the transmembrane proteins nectin and E-cadherin. E-cadherin binds the catenins, α- β- and p120, with its cytoplasmic domain and mediates actin dynamics. Afadin links nectin to the actin cytoskeleton. Figure adapted from (Coradini et al., 2011)

and discs large (Dlg) (Pieczynski and Margolis, 2011). In mammalian epithelial cells, the Crumbs and Par complexes localize to the apical side of the tight junctions while the Scribble complex localizes to the lateral membrane (Figure 3) (Margolis and Borg, 2005). Through protein-protein interactions and phosphorylation these three complexes antagonize each other to form the boundary between the apical and BL domains at the tight junctions.

The Crumbs Complex

There are three isoforms of Crb in humans (Crb1-3), with Crb3 involved in epithelial polarity and tight junction formation. Crb3 is a transmembrane protein with PDZ and FERM binding domains and is located on the apical surface and tight junctions of polarized epithelial cells (Makarova et al., 2003). Over expression of Crb3 results in expansion of the apical membrane and reduction of the BL membrane in polarized cells and can lead to the formation of tight junctions in non-polarized cells (Fogg et al., 2005; Roh et al., 2003). This suggests a role for Crbs3 in defining the apical membrane.

PALS1 is a cytosolic protein localized to the tight junction and contains six distinct protein interacting domains including a PDZ domain and a L27 domain important for epithelial polarity (Pieczynski and Margolis, 2011). Crb3 binds the PDZ domain of PALS1 while PATJ binds the L27 domain (Bachmann et al., 2001; Li et al., 2004b). The N-terminus of PALS1 also binds the PDZ domain of Par6, linking the Par and Crumbs complexes (Wang et al., 2004). Knockdown of PALS1 results in a loss of PATJ expression and reduced interaction of Par6 and

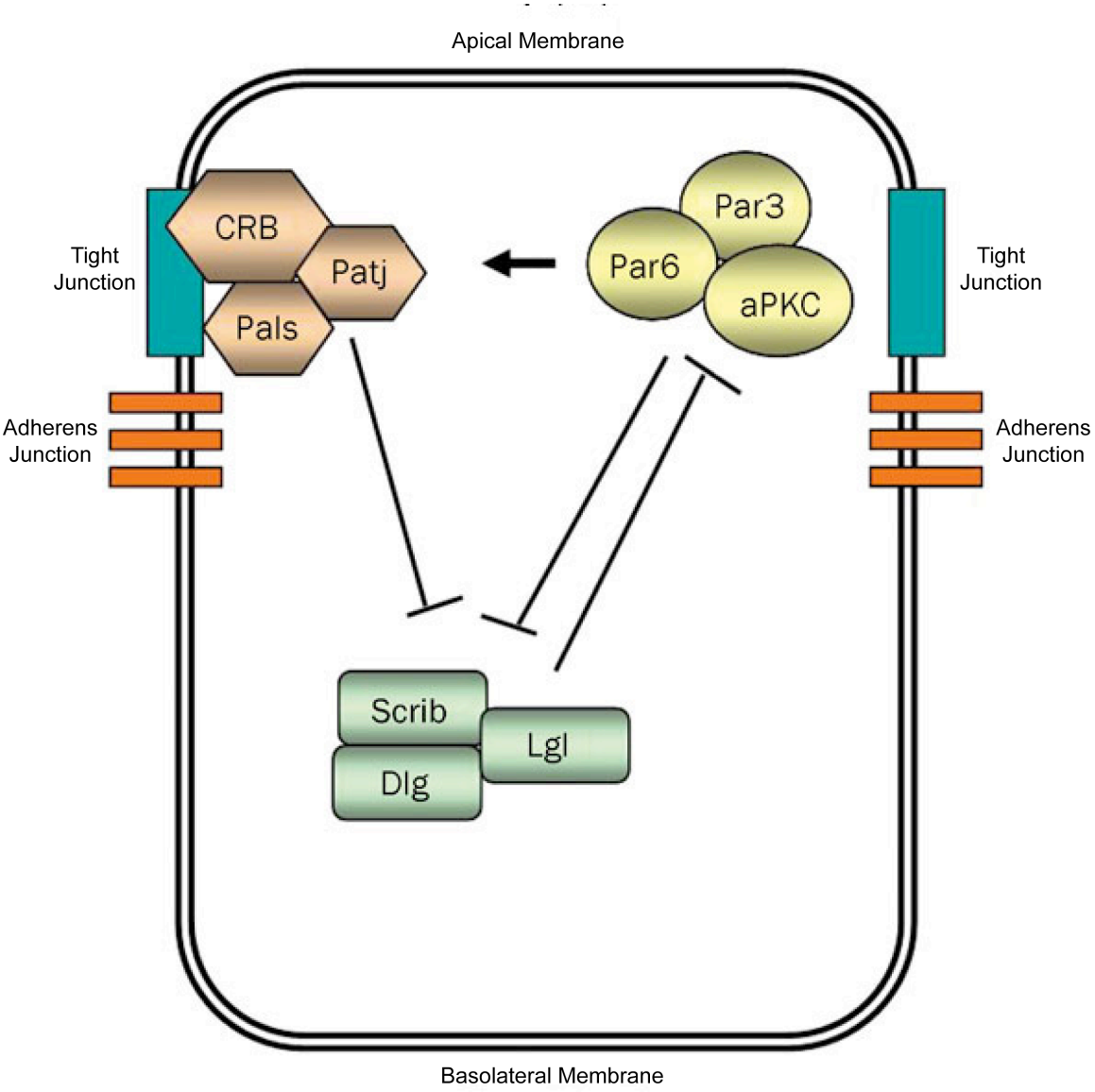

Figure 3. Schematic of the three polarity complexes responsible for establishment and maintenance of polar membrane domains. The Crumbs complex (CRB/Patj/Pals), localized to the apical surface and tight junctions, promotes apical membrane expansion. The Scribbled complex (Scrib/Dlg/Lgl) localizes to the lateral membrane and promotes lateral membrane expansion. The Par complex (Par3/Par6/aPKC) localizes to the tight junctions and acts as the mediator between the Crumbs and Scribbled complexes. Figure adapted from (Coradini et al., 2011).

Crb3 but does not affect Crb3 expression or localization (Straight et al., 2004). These data suggest PALS1 is essential in cell polarity by stabilizing PATJ at the tight junction and providing a bridge between the Crumbs and Par complexes.

The main role of PATJ is as a molecular scaffold. PATJ contains 10 PDZ domains and a N-terminal L27 domain (Pieczynski and Margolis, 2011). PATJ interacts with PALS1 through the L27 domain and with ZO-3 and claudin-1 thought PDZ domains, directly linking the Crumbs complex with the tight junction (Roh et al., 2002a; Roh et al., 2002b). PATJ is also bound by the protein angiomotin, which associates with the Cdc42 GTPase-Activating Protein (GAP) Rich1, linking the Crumbs complex with Cdc42 regulation at the tight junction (Wells et al., 2006). This regulation of Cdc42 at the tight junction may affect the ability of Cdc42 to interaction with Par6 (Garrard et al., 2003). The three proteins that make up the Crumbs complex localize to the apical side of the tight junction and regulate the identity of the apical membrane (Mellman and Nelson, 2008).

The Par Complex

The Par complex (Par3/Par6/aPKC) localizes to the tight junction and binds both and acts as mediator between the Crumbs and Scribbled complexes (Mellman and Nelson, 2008). Par3 is a multidomain scaffolding protein that contains three PDZ domains that bind Par6, aPKC, and JAM tight junction proteins. Par3 is required for the localization of the other Par complex proteins and is necessary for the formation of tight junctions (Chen and Macara, 2005; Pieczynski and Margolis, 2011). There are two Par3 proteins expressed in

humans, Par3A and Par3B. Par3A is the most important for polarity and expresses three isoforms in epithelial cells (Gao et al., 2002). Localization of Par3 to the tight junction and its association with Par6, Par5, aPKC, and the Crumbs complex are all regulated by phosphorylation of Par3 by aPKC or the polarity kinase Par1 (Pieczynski and Margolis, 2011). Par3 also spatially regulates the activity of Rac1 by interacting with the Rac1 guanine nucleotide exchange factor (GEF) Tiam1/2 (Chen and Macara, 2005). This enhancement of Rac1 activity at the tight junction is necessary for assembly of tight junctions, but can be inhibited by Rho kinase phosphorylation of Par3 (Chen and Macara, 2005; Nakayama et al., 2008). The localization and regulation of Par3 through these various phosphorylation events is critical for tight junction formation and epithelial polarity.

Par6 is a multifunction protein that allows the Par complex to interact with both the Crumbs and Scribbled complexes. Par6 contains a PDZ domain allowing interaction with Crb3 and PALS1 of the Crumbs complex, while through an alternative interaction it can also bind Dlg of the Scribbled complex (Pieczynski and Margolis, 2011). These interactions may be regulated by GTP-Cdc42, which binds the Par6 simi-CRIB and PDZ domains, altering the ability of Par6 to bind components of the Crumbs complex (Garrard et al., 2003). Par6 is the link between the other component of the Par complex, binding and activating aPKC, which phosphorylates Par3 and results in Par3 binding the PDZ and simi-CRIB domain of Par6 in a tripartite complex (Pieczynski and Margolis, 2011; Yamanaka et al., 2001). The platform provided by Par6 for aPKC is critical in

locating aPKC within proximity of two substrates important for polarity and tight junction formation, Par3 and Lgl (Hirose et al., 2002; Yamanaka et al., 2003). aPKC is thought to regulate the location of these two substrates, with phosphorylation of Par3 locating it to the tight junction and phosphorylation of Lgl incorporating it into the Scribbled complex (Hirose et al., 2002; Pieczynski and Margolis, 2011; Plant et al., 2003). The regulatory roles played by aPKC are essential for epithelial cell polarity.

The term “complex” may be inaccurate to describe the association between Par3, Par6, and aPKC. They are most likely in constant flux between the Crumbs and Scribbled complexes, regulating both complexes through recruitment of various proteins and phosphorylation events that mediate the establishment of apical and lateral surfaces.

The Scribbled Complex

The Scribbled complex (Scribbled/Lgl/Dlg) is located along the lateral membrane and is required to define the lateral surface through exclusion of apical membrane proteins (Bilder and Perrimon, 2000; St Johnston and Ahringer, 2010). There is little evidence that the Scribbled complex is actually a “complex” because not all the components are known to directly interact, with the exception of scribbled and Lgl (Kallay et al., 2006). However, the Scribbled complex proteins have complete or partial cellular colocalization and mutations of each protein in the complex result in a similar phenotype (St Johnston and Ahringer, 2010). These results suggest that scribbled, Lgl and Dlg work cooperatively.

Scribbled is a large cytosolic scaffold protein that contains 16 leucine rich repeats (LRRs) and four PDZ domains (Pieczynski and Margolis, 2011). Scribbled localization to the lateral membrane is dependent on the LRRs and the junctional protein E-cadherin (Navarro et al., 2005). While loss of scribbled has been shown to result in expansion of the apical membrane, knockdown of scribbled delays, but does not prevent polarization (Bilder and Perrimon, 2000; Qin et al., 2005). The main role of scribbled appears to be stabilization of the E-cadherin-catenin interaction, supporting a role for scribbled as a tumor suppressor (Qin et al., 2005).

Another component of the Scribbled complex, Lgl, interacts with scribbled and Par6/aPKC, physically linking the Scribbled and Par complexes. Phosphorylation of Lgl by aPKC restricts Lgl to the lateral membrane (Plant et al., 2003). Lgl and aPKC may antagonize each other since over expression of Lgl results in the same phenotype as aPKC knockout and Lgl can rescue the apical expansion caused by aPKC over expression (Chalmers et al., 2005). In addition, Lgl has been shown to interact with syntaxin-4, a component of the BL exocytic machinery, revealing a possible role for Lgl in BL trafficking and polarity (Musch et al., 2002).

The third component of the Scribbled complex, Dlg, has been linked to the complex genetically, but not physically. A direct link between Dlg and scribbled or Lgl has yet to be confirmed, although Dlg has been shown to interact with a variety of other proteins making the role of Dlg in polarity unclear (Pieczynski and Margolis, 2011). Dlg has been demonstrated to interact with APC and scribbled

with E-cadherin-catenin, and these associations could link Dlg and scribbled (Matsumine et al., 1996; Qin et al., 2005). Future studies may provide a more direct link between Dlg and the other components of the Scribbled complex.

The complexity of the three polarity complexes, Crumbs, Par and Scribbled, is immense and we have only a cursory understanding of how these three complexes mutually regulate the function and location of each other. Currently, the exact mechanisms by which these complexes regulate the different membrane domains remain unknown (Mellman and Nelson, 2008). However, as more is learned about the different components of these complexes, the pieces of the puzzle will fall into place.

The Adherens Junctions

Below the tight junctions in the lateral membrane of the cell are the adherens junctions, which are dynamic mediators of cell-cell contact (Figure 2). The adherens junction serves three functions: provide mechanical attachment between cells within a monolayer, provide domain orientation cues at points of cell-cell contact in establishment of apical BL polarity, and provide junction points for the cortical domain polarization in planar cell polarity (Baum and Georgiou 2011). Adherens junctions are composed of the type-1 transmembrane proteins cadherin and nectin, both of which interact with junctional proteins on adjacent cells as well as with a number of intracellular proteins through their cytoplasmic domains to regulate junctional maintenance, turnover, and function.

The core of the adherens junction is E-cadherin, a member of the classical cadherin family of transmembrane glycoproteins, which mediates Ca^{2+}-dependent homophilic interactions with cadherins on adjacent cells (Hartsock and Nelson, 2008). The extracellular domain of E-cadherin consists of five extracellular cadherin (EC1-EC5) domains that interact in a Ca^{2+}-dependent manner (Pokutta et al., 1994; Ringwald et al., 1987). The EC domains can form cis- and trans- homophilic interactions, with the trans-interactions being mediated through the EC1 domain (Patel et al., 2006). The trans-interactions are reported to be weak and are compensated for through the formation of cis-dimers that trans-oligomerize with the cis-dimerized cadherins on adjacent cells to form strong adherens junctions (Nelson, 2008).

In addition to intercellular interactions, E-cadherin mediates intracellular interactions through its cytoplasmic domain. The cytoplasmic domain of E-cadherin is bound by p120-catenin in the juxtamembrane region and by β-catenin in the C-terminal catenin binding domain (Aberle et al., 1994; Yap et al., 1998). A reported function of p120-catenin is to stabilize E-cadherin at the adherens junction by regulating E-cadherin turnover. Knockdown of p120-catenin results in elimination of E-cadherin and loss of adherens junctions (Davis et al., 2003). Alteration or loss of p120-catenin expression has been reported in a number of cancers, suggesting p120-catenin can act as a tumor suppressor (Thoreson and Reynolds, 2002). While β-catenin has many implications in cancer via inducing transcription of certain oncogenes, its role in adherens junctions may be to link E-cadherin to the actin cytoskeleton through α-catenin, an association that may be

very dynamic (Rimm et al., 1995). In addition, E-cadherin may regulate cytosolic levels of β-catenin by sequestering β-catenin to the adherens junctions, a process that is regulated by either phosphorylation of E-cadherin to increase β-catenin binding or by phosphorylation of β-catenin that decreases binding to E-cadherin (Hartsock and Nelson, 2008). Alpha-catenin does not interact directly with E-cadherin, but instead interacts with β-catenin and actin (Aberle et al., 1994; Rimm et al., 1995). The interaction between these two catenins is thought to physically link E-cadherin to the actin cytoskeleton; however, this quaternary complex cannot be reconstituted *in vitro* (Yamada et al., 2005). Alternatively, α-catenin may regulate actin dynamics at the adherens junctions. Alpha-catenin can exist as a monomer, which binds to β-catenin or as a homodimer, which binds and bundles actin. When actin is bound by α-catenin, Arp2/3 is forced to dissociate from actin thereby preventing actin branching. Accordingly, the increased local concentration of α-catenin at the adherens junctions via interaction with β-catenin/E-cadherin would promote actin bundling at the cell junctions and prevent Arp2/3-induced branching (Drees et al., 2005). Combined, these reports support a major function of the adherens junction, in addition to providing cell-cell adhesion, as regulator of the local concentration of α- and β-catenin, which affects actin dynamics and β-catenin induced gene transcription.

Another component of the adherens junction is the single pass transmembrane protein nectin, which contains three Ig-like domains in the extracellular region and a PDZ binding motif in the cytoplasmic domain (Takai and Nakanishi, 2003). There are four members of the nectin family that form

homo-cis-dimers and homo- and hetero- trans-dimers in a Ca^{2+}-independent manner (Reymond et al., 2001; Satoh-Horikawa et al., 2000). Nectin is recruited to the adherens junctions through interaction with the PDZ domain of the actin binding protein afadin (Mandai et al., 1997; Takahashi et al., 1999). Afadin links nectin to the actin cytoskeleton and possibly to E-cadherin through an interaction with α-catenin (Takai and Nakanishi, 2003). There is also evidence that suggests nectin is the initial adhesion molecule to form cell-cell adhesions and recruits E-cadherin through the afadin-α-catenin interaction to form mature adherens junctions (Tachibana et al., 2000). Nectin may provide the physical link between the actin cytoskeleton and the adherens junction since a physical link has not been established between E-cadherin and actin.

The Basolateral Membrane

The basal and lateral membranes of the cell are often combined and defined as the basolateral (BL) membrane. In a polarized columnar epithelial cell, the lateral membrane is the “side” surface of the cell juxtaposed to neighboring cells and is the site of cell-cell interactions. The basal membrane is the “bottom” surface of the cell and the site of cell-matrix interactions (Figure 1). Cell-matrix interactions are critical for cell survival and provide orientation cues (Rodriguez-Boulan and Nelson, 1989). The lateral membrane is enriched in proteins that mediate cell-cell interactions and domain orientation cues, as previously described, while the basal membrane is devoid of cell-cell interaction proteins and enriched in extracellular matrix (ECM) receptors.

The cell attaches and interacts with the ECM through focal adhesions that mainly consists of the integrin family of cell adhesion receptors. Integrins are made up of α- and β-subunits, of which there are 18 α-subunits and 8 β-subunits. The α- and β-subunits can form non-covalently linked heterodimers at the cell surface to provide the cell with a diverse family of 24 integrin heterodimers. The different combinations of α- and β-subunits is what provides integrins with their binding diversity (Dubash et al., 2009). The integrin extracellular domain binds to different components of the ECM, while the short cytoplasmic domain interacts with proteins linked to the actin cytoskeleton. The complexity and diversity of the proteins that function on the cytoplasmic side of the focal adhesion is immense, with more then 50 proteins identified so far (Zamir and Geiger, 2001).

Integrins are bidirectional signaling proteins. Intracellular signals can be transferred to integrin receptors resulting in activation or inactivation of the ECM binding domain (inside-out signaling). The extracellular domain of integrins can, in turn, relay a signal it receives from the ECM to the inside of the cell, resulting in an intracellular signaling cascade (outside-in signaling) (Hynes, 2002). The signals received from an integrin can mediate numerous cell-signaling pathways that control cell survival, division, differentiation, and migration (Zaidel-Bar et al., 2007; Zamir and Geiger, 2001).

In addition to mediating cell-cell and cell-ECM interaction, BL membrane proteins function in cellular communication and homeostasis. The BL membrane contains growth factor receptors and ligands that function to mediate signal reception and transduction. The BL membrane is the main site for the cell to

send and receive information to and from the surrounding interstitium. The BL membrane also contains ion channels and ATPases that function to generate an ion gradient. These channels and pumps work in concert with their counterparts in the apical membrane to create a suitable environment for cell and tissue homeostasis (Rodriguez-Boulan and Nelson, 1989).

Polarized Sorting Signals

In order to maintain these distinct membrane surfaces with specialized proteins and functions the polarized cell must sort, deliver, and retain membrane components to the correct location for proper cellular function. This is accomplished using signals contained within the proteins structure, either in the extracellular, transmembrane, or cytoplasmic domains (Carmosino et al., 2010). Signals present in the extracellular and transmembrane domains predominantly mediate protein delivery to the apical surface, while signals within the cytoplasmic domain typically drive proteins to the endosomal system or the BL surface and are involved in internalization. Cytoplasmic BL sorting signals have been shown to be dominant over extracellular apical sorting signals (Weisz and Rodriguez-Boulan, 2009).

Apical sorting signals mainly consist of extracellular protein modifications or a transmembrane structural determinant, such as a glycosylphosphatidylinositol (GPI) linkage to the membrane. The transmembrane or GPI-linkage determinants result in apical sorting of proteins by assisting in the incorporation of the protein into lipid rafts. The sphingolipid- and cholesterol-rich

lipid rafts tend to possess longer hydrophobic tails, making the raft domains of the membrane “taller” than non-raft domains. Proteins with large transmembrane domains find it energetically favorable to incorporate into these taller membrane domains and are sorted to the apical membrane.

GPI-anchored proteins are also incorporated into lipid rafts, although GPI-anchored proteins are present on both the apical and BL surface. An additional criterion for apical sorting of GPI-anchored proteins is oligomerization within the lipid raft (Paladino et al., 2004; Paladino et al., 2007). Apically targeted GPI-anchored proteins are reportedly delivered directly to the apical surface and are not transcytosed from the BL surface (Paladino et al., 2006).

Post-translational N- and O-linked glycosylation of the extracellular domain has been demonstrated to play a role in apical sorting (Potter et al., 2006). This was initially demonstrated with growth hormone that is normally secreted from both apical and BL surfaces of polarized cells, but is preferentially delivered apically when N-glycosylated (Scheiffele et al., 1995). O-glycosylation of the juxtamembrane stalk of p75 NGFR is important for its apical delivery (Yeaman et al., 1997). One possible explanation of how glycosylation assists in apical delivery is that proper folding and maturation of the protein requires these post-translational modifications. Glycosylation may also assist in the recognition of the protein by an as yet unidentified sorting receptor (Weisz and Rodriguez-Boulan, 2009).

Sorting signals contained within the cytoplasmic domains are composed of short linear sequence motifs and are involved in internalization, sorting to the BL

surface, and delivery to endosomes. Consensus motifs have been identified, but are not always exact, with a few residues being the most important, typically bulky hydrophobic or charged residues (Bonifacino and Traub, 2003). The best-characterized cytoplasmic domain sorting motifs contain critical tyrosine or leucine residues.

Consensus tyrosine-based motifs are [FY]XNPXY and YXXΦ, where Φ is a bulky hydrophobic residue (Leu, Ile, Met, or Phe). These motifs have been shown to be involved in delivery to the BL surface, the lysosome, and internalization (Chen et al., 1990; Gough et al., 1999; Hunziker et al., 1991; Marks et al., 1995). The [FY]XNPXY signal has been shown to be critical for the rapid internalization of transmembrane proteins, but has not been reported to be involved in other intracellular sorting events (Bonifacino and Traub, 2003). Transmembrane proteins that contain [FY]XNPXY motifs include low density lipoprotein (LDL) receptor, epidermal growth factor receptor (EGFR), insulin receptor, and integrin-β1, although not all have been demonstrated to be active internalization motifs (Bonifacino and Traub, 2003). The most extensive studies of this motif have been on the LDL receptor due to its importance in disease (Hobbs et al., 1992). Replacement of the phenylalanine, asparagine, proline, or tyrosine residues in the LDL receptor motif resulted in reduced internalization (Chen et al., 1990). The LDL receptor signal is also transplantable, capable of replacing the endogenous signal within the transferrin receptor (Collawn et al., 1991).

The YXXΦ motif has also been shown to be involved in BL sorting as well as internalization and delivery to the lysosome (Gough et al., 1999; Sorkin et al., 1996; Thomas et al., 1993). This functional flexibility is conferred by varying the localization of the motif within the cytoplasmic domain and by heterogeneous composition of the residues that make up the motif with the exception of the tyrosine, which is critical (Bonifacino and Traub, 2003; Williams and Fukuda, 1990). Addition of a glycine residue before the tyrosine specifies lysosomal targeting while different residues in the Φ position can also determine localization (Gough and Fambrough, 1997; Harter and Mellman, 1992). This motif has been shown to interact with the medium subunit (see below) of adaptor proteins (Aguilar et al., 2001; Ohno et al., 1995; Owen and Evans, 1998; Rous et al., 2002).

Consensus leucine-based sorting motifs are [DE]XXXL[LI], DXXLL, EEEXXXXXL, and EEXXXL. Similar to tyrosine-based signals, leucine-based sorting signals are diverse in their composition and function, acting as endosomal/lysosomal, internalization, and BL sorting signals (Deora et al., 2004; Dietrich et al., 1994; Johnson and Kornfeld, 1992b; Matter et al., 1994; Miranda et al., 2001). Leucine-based sorting signals were discovered after tyrosine-based sorting signals. The first leucine-based signal identified was a di-leucine signal [DE]XXXL[LI] in a protein that when truncated to not contain any tyrosine residues in the cytoplasmic domain was still delivered to the lysosome (Letourneur and Klausner, 1992). These same studies demonstrated the importance of both leucine residues for proper lysosome localization with the first

leucine more critical than the second. Replacement of the first leucine with an isoleucine impairs signal function while replacement of the second leucine with an isoleucine maintains a functional signal (Letourneur and Klausner, 1992). The acidic residues N-terminal to the di-leucine residues are also important for internalization and targeting to the endosomal system, possibly by providing a necessary structure for signal recognition or binding to the adaptor protein (Kelly et al., 2008; Pond et al., 1995).

The DXXLL consensus motif is involved in TGN to endosome transport and is conserved in all metazoans (Bonifacino and Traub, 2003; Johnson and Kornfeld, 1992a). This motif tends to be located toward the carboxy-terminus of the cytoplasmic domain, although this localization may not be critical for its function (Braulke and Bonifacino, 2009). Both of the leucine residues are critical as well as the aspartic acid residue, which cannot even tolerate an isoelectric or isosteric substitution (Chen et al., 1997).

The EEEXXXXXL and EEXXXL mono-leucine motifs are both involved in BL sorting of transmembrane proteins (Deora et al., 2004; Wehrle-Haller and Imhof, 2001). To date, the EEEXXXXXL motif has been found in only two proteins, CD147 and stem cell factor, while the EEXXXL motif exists in amphiregulin (AREG) and is described in chapter 2 of this dissertation (Deora et al., 2004; Wehrle-Haller and Imhof, 2001). Further studies are needed to determine how these motifs function and proteins that recognize these signals.

Cargo Adaptor Proteins

Sorting motifs are recognized by heterotetrameric cargo adaptor protein complexes (AP-1A, AP-1B, AP-2, AP-3A, AP-3B, AP-4) and the monomeric Golgi-localized, γ-ear-containing Arf-binding proteins (GGAs 1-3), which selectively incorporate cargo proteins and facilitate vesicle formation (Robinson, 2004). The main functions of these adaptor proteins are to bind to the membrane, recognize and bind cargo, and recruit clathrin and other proteins involved in vesicle formation. The heterotetrameric cargo adaptor proteins are 300 kDa and are composed of two large subunits (γ/β1, α/β2, δ/β3A, δ/β3B, ε/β4), one medium subunit (μ1A, μ1B, μ2, μ3A, μ3B, μ4), and one small subunit (σ1-σ4) (Figure 4). The large subunits are responsible for binding the heterotetramer to the target membrane (γ, α, δ, ε) and binding clathrin though clathrin box motifs (β1, β2, β3). The medium subunit contains a binding pocket that recognizes and binds the sorting signal within a cargo protein. The small subunit functions to stabilize the complex (Owen et al., 2004).

Adaptor proteins localize to different membranes on the cell surface or organelles of the cell, depending on their function (Figure 4 and 5). Localization of adaptor proteins can be directed by membrane phosphoinositide composition. For example, AP-2 localization to the phosphatidylinositol (4,5)-bisphosphate [PIP2] enriched inner leaflet of the plasma membrane is mediated by the PIP2 binding sites contained in the α and μ2 subunits of AP-2 (Gaidarov and Keen, 1999; Jost et al., 1998; Rohde et al., 2002). The μ1B subunit of AP-1B contains a three amino acid sequence necessary for localization of AP-1B to the

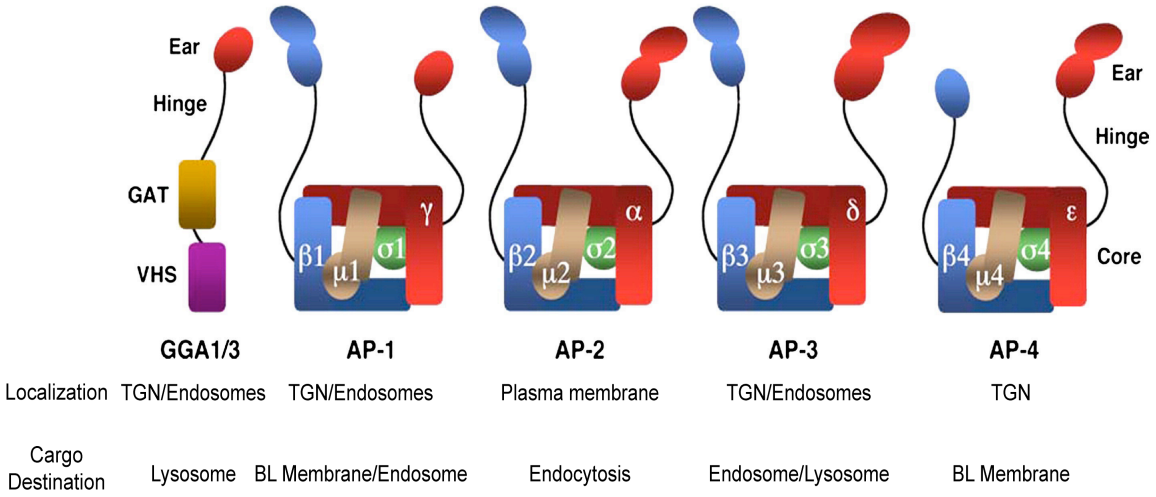

Figure 4. Cargo adaptor proteins. An illustration of the four cargo adaptor heterotetramer protein complexes and a GGA monomer protein. Each AP complex consists of two large subunits (γ/β1, α/β2, δ/β3A, δ/β3B, ε/β4), one medium subunit (μ1A, μ1B, μ2, μ3A, μ3B, μ4), and one small subunit (σ1-σ4). Listed below each AP complex is where the AP is localized in the cell and the destination of the sorted cargo. Figure adapted from (Braulke and Bonifacino, 2009).

phosphatidylinositol 3,4,5-trisphosphate [PI(3,4,5)P3] enriched recycling endosomes (Fields et al., 2010). Golgi-associated type II phosphatidylinositol 4 kinase-α (PI4KIIα) generates phosphatidylinositol 4 phosphate [PI(4)P] at the Golgi and is required for recruitment of AP-1 to the Golgi (Wang et al., 2003). In addition to phosphoinositides, the ADP-ribosylation factor (ARF) family of small GTPases is also involved in membrane recruitment of adaptor proteins (D'Souza-Schorey and Chavrier, 2006). Activated GTP-bound Arf1 recruits AP-1, AP-4, and GGAs to the TGN membrane and AP-3 to the endosomal membrane (Boehm et al., 2001; Boman et al., 2000; Ooi et al., 1998; Stamnes and Rothman, 1993). Once localized to the proper membrane/organelle the adaptor protein can perform its function.

AP-1 has two isoforms, the ubiquitously expressed AP-1A (γ, β1, μ1A, σ1) and epithelial specific AP-1B (γ, β1, μ1B, σ1). These two isoforms differ only by their medium subunits, μ1A and μ1B, which are 79% identical (Ohno et al., 1999). AP-1A localizes to the trans Golgi network (TGN) and along with the GGA proteins is involved in vesicle formation for transport between the TGN and endosomes (Doray et al., 2002b). The epithelial specific AP-1B is localized to recycling endosomes near the TGN and sorts proteins to the BL surface via two routes, biosynthetically and recycling (Figure 5) (Cancino et al., 2007; Folsch et al., 2003; Gravotta et al., 2007). In the biosynthetic route, proteins are delivered to the recycling endosome from the TGN. Once in the recycling endosome, the proteins are recognized by AP-1B and incorporated into vesicles destined for the BL surface (Gonzalez and Rodriguez-Boulan, 2009). In the recycling route,

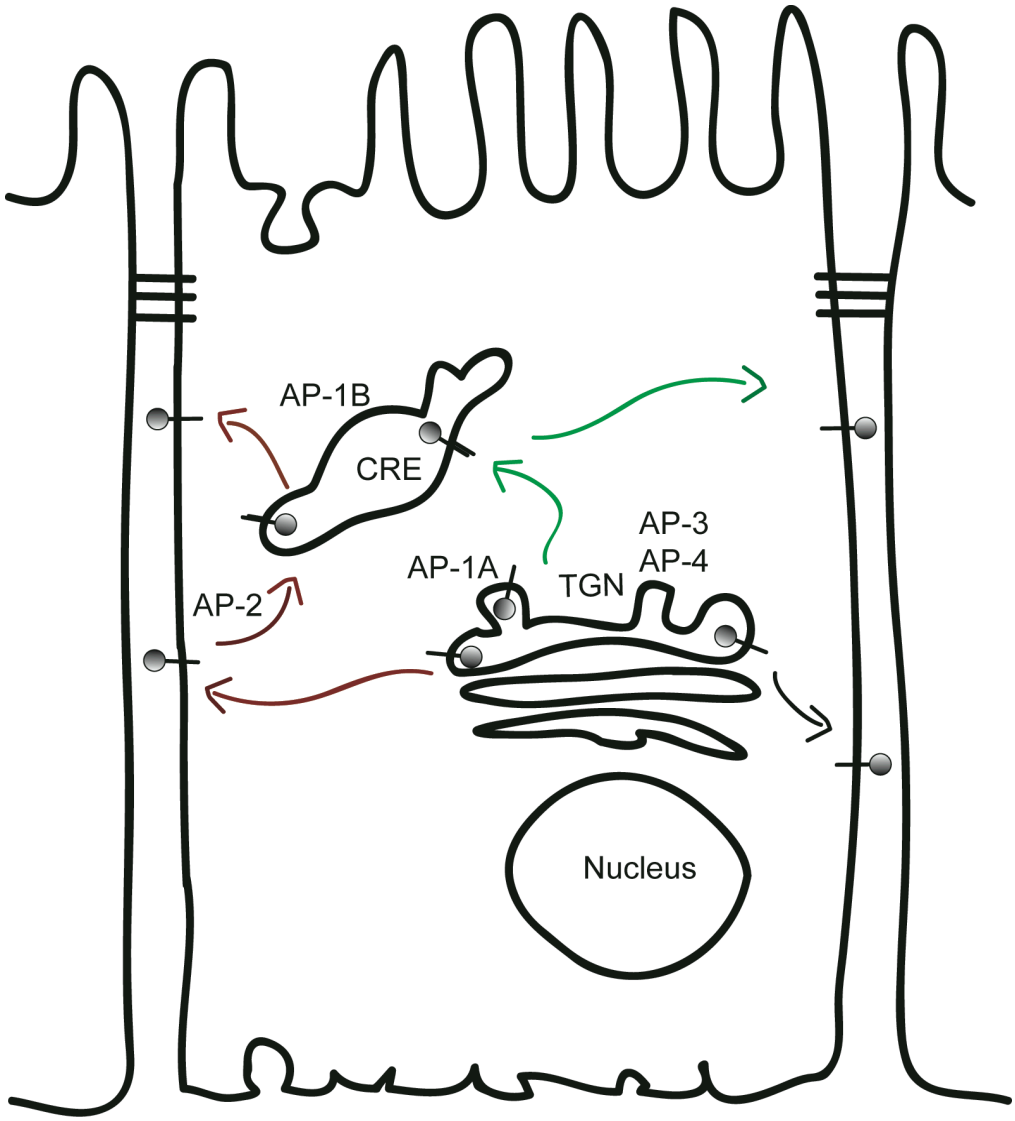

Figure 5. Possible routes taken by BL membrane proteins. There are three possible routes taken by a protein to obtain and maintain BL polarity. The direct biosynthetic route taken to the BL surface, represented by the black arrow, is delivery from the TGN to the BL surface. A second biosynthetic route to the BL surface, represented by the green arrows, is via the common recycling endosome (CRE) and is AP-1B dependent. The recycling route, represented by the red arrows, delivers BL proteins to the CRE after endocytosis and returns them back to the BL surface from the CRE. Proteins that follow the red route can be delivered to the BL surface in an AP-1B-independent manner but depend on AP-1B for recycling back to the BL surface and maintenance of steady-state polar distribution. Adaptor proteins AP-1A, AP-3, and AP-4 are located at the TGN. AP-1B is localized to the CRE. AP-2 is located at the plasma membrane.

proteins are endocytosed from the cell surface and delivered to the recycling endosome where they are recognized by AP-1B for return to the BL surface. Proteins, such as LDL receptor, transferrin receptor, and AREG that are AP-1B dependent for steady state polarized distribution are initially delivered to the BL surface via an AP-1B independent biosynthetic route (Cancino et al., 2007; Gan et al., 2002; Gravotta et al., 2007). However, over time these proteins lose polarity because they are mis-recycled to the apical surface in AP-1B deficient cells. The medium μ1B subunit has been demonstrated to contain a tyrosine motif binding pocket, mutation of which impairs the BL sorting of some but not all AP-1B-dependent BL proteins (Sugimoto et al., 2002).

AP-2 (α, β2, μ2, σ2), the most well characterized adaptor protein, is localized to the plasma membrane and regulates receptor-mediated endocytosis (Nakatsu and Ohno, 2003). Yeast two-hybrid and structural analyses of AP-2 have identified the medium subunit, μ2, as the site of interaction with YXXΦ tyrosine-based sorting motifs (Ohno et al., 1995; Owen and Evans, 1998). The structural analysis of μ2 revealed a hydrophobic binding pocket that facilitated the formation of hydrogen bonds with the tyrosine hydroxyl group in the sorting signal. Importantly, it was found that the size and composition of this binding pocket precludes the phosphorylation of the tyrosine (Owen and Evans, 1998). AP-2 also interacts with di-leucine-based sorting signals [DE]XXXL[LI]. This interaction takes place between the two leucine residues and a hydrophobic pocket of the σ2 subunit. There is also a positively charged patch of amino acids

between the α and σ2 subunits that accommodates hydrophilic residues upstream of the leucine residues on the cargo protein (Kelly et al., 2008).

Sorting signal recognition by AP-2 may be regulated by phosphorylation of the adaptor protein. Within the inactive AP-2 complex, the β2 subunit blocks both the di-leucine binding interface on the σ2 subunit and the YXXΦ binding pocket in the μ2 subunit. When the β2 subunit dissociates from σ2 it reveals the σ2 binding interface, an event that may be regulated by phosphorylation of tyrosine 6 on β2. However, the μ2 binding pocket remains blocked (Kelly et al., 2008; Traub, 2009). Opening of the μ2 binding pocket is regulated by adaptor-associated kinase AAK1-mediated phosphorylation of μ2 on threonine 156 and is further stabilized by interaction of μ2 with PIP2 (Honing et al., 2005; Olusanya et al., 2001; Ricotta et al., 2002). These two steps allow for a strong binding interaction between μ2 and the YXXΦ motif while not enhancing binding of di-leucine motifs to the σ2 binding interface (Honing et al., 2005). All of this taken together suggests these two phosphorylation events may be important regulatory mechanisms for motif recognition by AP-2.

AP-3 has two isoforms, the ubiquitous AP-3A (δ, β3A, μ3A, σ3) and neuronal specific AP-3B (δ, β3B, μ3B, σ3) (Nakatsu and Ohno, 2003). AP-3A is localized to endosomes where it is present on budding vesicles enriched in lysosomal proteins (Peden et al., 2004). Patients with Hermansky-Pudlak syndrome (HPS) have a mutant form of β3A, resulting in an increase in lysosomal proteins on the cell surface (Dell'Angelica et al., 1999b). Additionally, yeast two-hybrid analysis indicated μ3A preferentially binds tyrosine-based

lysosomal targeting motifs, all implicating AP-3A in sorting from the endosome to the lysosome (Dell'Angelica et al., 1999b). Unlike AP-1 and AP-2, the role of clathrin in AP-3A vesicles is not clear. Components of AP-3 were initially identified as not enriched in clathrin-coated vesicles, but were later shown to interact with clathrin via β3 (Dell'Angelica et al., 1998; Simpson et al., 1996). Subsequent studies quantitated only 46% of AP-3 positive membranes to be associated with clathrin coats, compared to 91% of AP-1 positive membranes (Peden et al., 2004). Taken together, AP-3A appears to play a role in endosome to lysosome transport in clathrin-dependent and clathrin-independent pathways. AP-3B has two subunits, β3B and μ3B, that are only expressed in neurons. Deletion of μ3B in mice results in spontaneous epileptic seizures and a reduced number of synaptic vesicles in excitatory and inhibitory terminals of the hippocampus (Nakatsu et al., 2004). These results indicate a role for AP-3B in synaptic vesicle formation.

AP-4 (ε, β4, μ4, σ4) is ubiquitously expressed at low levels and is located at the TGN in an ARF-regulated manner (Boehm et al., 2001; Hirst et al., 1999). The μ4 subunit can bind certain canonical YXXΦ motifs, particularly signals within lysosomal proteins, although this interaction is not as strong as μ2 or μ3A (Aguilar et al., 2001). A novel YXXΦ motif, YX[FYL][FL]E, is tightly bound by μ4, while not bound by μ1, μ2, or μ3 (Burgos et al., 2010). The μ4 binding pocket requires the same conserved residues as μ2 to bind canonical YXXΦ motifs, but binding to the YX[FYL][FL]E motif takes place on a different face of the μ4 pocket than the YXXΦ binding with μ2 (Aguilar et al., 2001; Burgos et al., 2010; Owen

and Evans, 1998). AP-4 is the only adaptor protein that does not contain a clathrin-binding domain and does not associate with clathrin-coated vesicles as determined by EM (Dell'Angelica et al., 1999a; Hirst et al., 1999). AP-4 has been speculated to participate in transport from the TGN to the endosomal/lysosomal system, however siRNA against μ4 does not impair lysosomal transport (Aguilar et al., 2001; Burgos et al., 2010; Simmen et al., 2002). However, AP-4 has been shown to sort proteins to the BL surface of polarized MDCK cells, making it and AP-1B the only adaptor proteins demonstrated to sort BL proteins (Folsch, 2005; Simmen et al., 2002).

The most recent studies on AP-4 have focused in neuronal cells, which similar to epithelial cells, form distinct polarized membrane domains. Proteins delivered to the epithelial apical surface are delivered to the neuronal axonal domain, whereas proteins that are delivered to the epithelial BL surface are delivered to the neuronal somatodendritic domain (Dotti and Simons, 1990; Jareb and Banker, 1998). In neurons, AMPA receptors are normally delivered to the somatodendritic domain. However, these receptors are not properly delivered in mice carrying a null mutation for β4, providing further evidence AP-4 acts as a BL sorting adaptor protein (Matsuda et al., 2008). Homozygous deletion of the gene encoding the ε subunit results in cerebral palsy due to a deficiency in AP-4 (Moreno-De-Luca et al., 2011). The difficulties in pinpointing a function for AP-4 in fibroblasts and epithelial cells and the recent findings in neurons may indicate the main function for AP-4 is in the neurons.

Golgi-localized, γ-ear-containing Arf-binding proteins (GGAs) are monomeric clathrin adaptor proteins involved in TGN to endosomal transport (Bonifacino, 2004). There are three ubiquitously expressed GGA proteins (GGA1-3) that localize to the TGN in an ARF-dependent manner (Boman et al., 2000). GGAs consist of three tandem domains, VHS (Vps27, Hrs, Stam), GAT (GGA and TOM (target of myb)) and GAE (γ-adaptin ear), connected by two linker sequences (Figure 4). The 140-residue VHS domain binds DXXLL motifs contained within the cytoplasmic domains of lysosomal proteins (Takatsu et al., 2001; Zhu et al., 2001). The VHS domain can also bind a DXXLL motif within the hinge segment of GGA1 and GGA3, an autoinhibitory mechanism regulated by casein kinase 2 (CK2) (Doray et al., 2002a). The VHS domain interaction with the DXXLL motif is specific, in that it will not interact with tyrosine- or di-leucine-based motifs devoid of acidic residues (Puertollano et al., 2001). A short 20-residue linker connects the VHS and GAT domains. The 150-residue GAT domain contains a binding site for GTP-bound ARF proteins, a necessary interaction for proper localization of GGAs to the TGN (Dell'Angelica et al., 2000). The GAT domain is followed by the long unstructured hinge segment that connects the GAT and GAE domains. In addition to containing the aforementioned autoregulatory DXXLL domain, the hinge segment also contains a clathrin box motif (Zhu et al., 2001). The hinge segment can also bind the γ-ear domain of AP-1, indicating an interaction between GGAs and AP-1. Cargo that is mutated such that it cannot interact with GGAs is poorly incorporated into AP-1 vesicles, suggesting a mechanism by which GGAs identify and bind cargo that is

then presented to AP-1 for incorporation into vesicles (Doray et al., 2002b). The 124-residue GAE domain binds the consensus motif DFGXΦ, which is contained within the unstructured regions of accessory proteins. The accessory proteins may be involved in processes such as membrane deformation and tethering/fusion events (Bonifacino, 2004). The current understanding of GGAs and their interaction with AP-1 supports the idea that the two work together to select cargo destined for the lysosome and provide a foundation for the recruitment of accessory and scaffolding proteins to facilitate vesicle biogenesis at the TGN.

Polarized Delivery of the EGFR and the EGFR Ligands

One family of proteins that is distributed to the cell surface in a polarized manner is the EGFR and its cognate ligands (Harris et al., 2003). EGFR is a transmembrane receptor tyrosine kinase involved in proliferation, migration, and cell survival and is critical for epithelial wound repair and homeostasis (Jost et al., 2000; Konturek et al., 1995; Wells, 1999). Seven mammalian EGFR ligands have been identified (EGF, AREG, transforming growth factor-α (TGFα), heparin-binding EGF-like growth factor (HB-EGF), betacellulin (BTC), epiregulin (EREG), and epigen), all of which are produced as type 1 transmembrane proteins and delivered to the cell surface where they are cleaved by metalloproteases to release a mature soluble ligand (Figure 6) (Harris et al., 2003). The soluble ligands can bind and activate the EGFR with differing affinities and intensities in

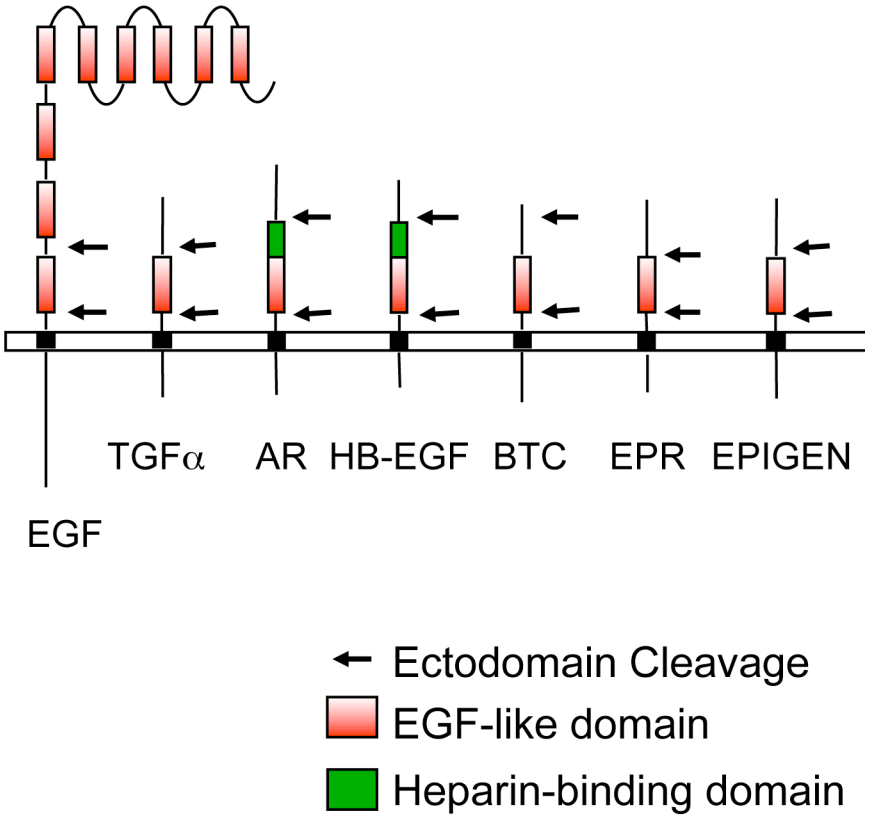

Figure 6. EGFR ligands. There are seven ligands that bind and activate the EGFR. All of these ligands are produced as type-1 transmembrane proteins that are cleaved from the cell surface by metalloproteases to release a soluble mature ligand. Figure adapted from (Harris et al., 2003).

a paracrine, autocrine, or juxtacrine manner (Harris et al., 2003; Shoyab et al., 1989). The cellular signaling pathways activated downstream of the EGFR are ligand-dependent (Chung et al., 2005; Luetteke et al., 1999; Luetteke et al., 1993).

In polarized epithelial cells, EGFR is selectively delivered to the BL surface (Hobert and Carlin, 1995). The EGFR is a large type 1 transmembrane glycoprotein with a 622-amino acid extracellular ligand binding domain, 23-amino acid transmembrane domain, and a 541-amino acid cytoplasmic domain (Carpenter, 1987). The cytoplasmic domain contains a tyrosine kinase domain and multiple tyrosine autophosphorylation sites responsible for the biologic activity of the receptor (Schlessinger, 2000). The C-terminal region of the EGFR cytoplasmic domain contains a canonical YXXΦ internalization signal that is recognized by AP-2 (Sorkin et al., 1996). The information responsible for BL delivery of the EGFR is also contained within the cytoplasmic

domain, removal of which results in apical expression of the EGFR (Hobert and Carlin, 1995). This BL sorting information is present in the juxtamembrane region of the cytoplasmic domain and consists of a non-canonical BL sorting motif within a 22-residue stretch and was initially thought to lack a critical tyrosine or di-leucine motif (Hobert et al., 1997). This 22-residue stretch is predicted to form two α-amphipathic helices with three hydrophobic leucine residues on one face and charged residues on the opposite face of each helix (Hobert et al., 1997). These helices could provide a binding interface similar to what may be present within the cytoplasmic domain of AREG.

The same group later published a more precise study of the EGFR BL sorting motif that narrowed down the critical residues within the 22-residue stretch to include two leucine residues within the first helix and a proline rich motif consisting of PXXP in the second helix, constituting two separate signals with the proline-based motif being the dominant signal (He et al., 2002). An alternative explanation to the proline residues acting as a sorting signal is that mutation of the proline residues destroys important structural elements necessary for recognition of the two α-amphipathic helices described in the initial paper, although there is no evidence to support this hypothesis. Additionally, the EGFR was recently demonstrated to be AP-1B-dependent for polar distribution in LLC-PK1 cells (Ryan et al., 2010). The di-leucine motif was shown to bind AP-1B in an *in vitro* peptide pulldown assay, supporting the leucine residues as the critical determinants for polar distribution of the EGFR (Ryan et al., 2010).

The ligand EGF is delivered to both surfaces of MDCK cells, but is selectively cleaved by BL metalloproteases, leading to apically retained EGF (Dempsey et al., 1997). EGF is the largest of the EGFR ligands, with nine EGF-like repeats in the extracellular domain and a 154-residue cytoplasmic domain, considerably larger than the typical 20 to 40-residue EGFR ligand cytoplasmic domain (Table 1) (Harris et al., 2003). While EGF is delivered to both surfaces, the cytoplasmic domain of EGF contains a PXXP motif, mutation of which results in loss of EGF at the BL surface but not the apical surface (Groenestege et al., 2007). This supports the dogma that PXXP is a bonafide BL sorting signal, although EGF also contains di-leucine residues N-terminal to the PXXP, similar

to the EGFR. It is possible that these di-leucine residues are the critical residues and mutation of the proline simply affects the structure of the cytoplasmic domain, a hypothesis unsupported by experimental evidence. Questions still remain regarding the role of proline residues in BL transport, such as can the PXXP motif itself provide BL sorting information or must it be in the context of the surrounding residues? How do PXXP motifs bind adaptor proteins? More analysis of the PXXP motif in the EGF and EGFR cytoplasmic domains is needed before a definitive sorting signal can be declared.

TGFα is delivered to the BL surface of polarized epithelial cells with the help of the myristoylated cargo recognition and targeting (CaRT) protein Naked2 (NKD2) (Dempsey and Coffey, 1994; Li et al., 2004a). ProTGFα is a 160-amino acid type one transmembrane glycoprotein with a 39-residue palmitoylated cytoplasmic domain (Table 1) (Bringman et al., 1987; Lee et al., 1995). The BL sorting motif of TGFα consists of two elements in the cytoplasmic domain, a non-canonical di-leucine motif and an 8-residue segment of the juxtamembrane domain (Dempsey et al., 2003). Removal of only the 8-residue juxtamembrane segment or site-directed mutagenesis of just the di-leucine residues results in loss of polarized delivery. This suggests both regions contain some information important for the polarized distribution of TGFα. However, if the cytoplasmic domain is truncated to only 8-residues, BL distribution is maintained. This is interesting because the truncated mutant lacks the di-leucine motif but does not lose polar distribution, whereas site-directed mutagenesis of the two leucine residues, which still contains the 8-residue juxtamembrane region, results in loss

of polar distribution. How these two regions of the TGFα cytoplasmic domain assist in BL delivery is unclear.

TGFα is palmitoylated on two cysteine residues towards the C-terminus of the cytoplasmic domain (Shum et al., 1996). Palmitoylation of the cytoplasmic domain positions the domain in a unique manner, anchoring the C-terminus into the membrane. This orientation could possibly contribute to the interaction between TGFα and NKD2, although site-directed mutagenesis of the two cysteine residues did not affect NKD2-TGFα interaction by yeast two-hybrid analysis (Li et al., 2004a). However the interaction between NKD2 and TGFα was reduced by site-directed mutagenesis of the di-leucine motif and the juxtamembrane domain, supporting the role of these two regions in BL delivery of TGFα (Li et al., 2004a). TGFα is the only EGFR ligand known to be trafficked by NKD2, which functions by coating TGFα-containing vesicles after emergence from the TGN and delivering them to the BL corner of polarized MDCK cells where they fuse with the plasma membrane in a NKD2 myristoylation-dependent manner (Li et al., 2004a). Knockdown of NKD2 by shRNA reduces cell surface expression of TGFα and leads to accumulation of TGFα-containing vesicles in the cytoplasm (Li et al., 2007). NKD2 is a critical component for the proper delivery of TGFα to the BL surface.

The very C-terminal portion of TGFα contains a PDZ recognition motif that is bound by the PDZ protein MAGI-3 (Franklin et al., 2005). MAGI-3 was identified in a yeast two-hybid screen for interacting proteins of the TGFα cytoplasmic domain. A model was proposed that different PDZ proteins

recognize this motif as TGFα passes through the secretory pathway, “handing off” TGFα along the way. In this model the PDZ protein syntenin binds TGFα early in the secretory pathway in the endoplasmic reticulum (ER) (Fernandez-Larrea et al., 1999). TGFα is then “handed off” to another PDZ protein, the myristoylated and palmitoylated GRASP55, in the cis-Golgi (Kuo et al., 2000). At this point NKD2 may be next in line to take the TGFα “baton” at the TGN and escort TGFα containing vesicles to the BL surface. At the cell surface, TGFα interacts with another PDZ protein, MAGI-3, which assists TGFα traffic efficiently to the cell surface (Franklin et al., 2005). It is unknown if TGFα is the only EGFR ligand to be handed off through the secretory pathway. AREG does contain a possible PDZ recognition motif at its C-terminus, but removal of this sequence has no effect on AREG delivery and no PDZ domain-containing proteins have been identified to interact with the AREG cytoplasmic domain.

The latest EGFR ligand to be studied for a BL sorting motif is EREG. It has been determined through unpublished work in the Coffey lab that EREG is delivered to the BL surface of polarized MDCK cells. Removal of the cytoplasmic domain results in almost exclusively apical expression of EREG. Replacement of the apically expressed NGFR cytoplasmic domain with the EREG cytoplasmic domain results in BL expression of NGFR. Cytoplasmic domain truncation mutants of EREG revealed a tyrosine motif similar to YXXΦ, with valine in the Φ position (Table 1). Site-directed mutagenesis of the single tyrosine in this motif resulted in apical expression of EREG, similar to removal of the entire

Table 1. The EGFR ligands' cytoplasmic domains. Amino acid compositions of the seven EGFR ligands' cytoplasmic domains are listed with identified BL sorting determinants in **bold**. The length of each domain is indicated on the right.

EGFR Ligand	Cytoplasmic Domain Amino Acid Composition	Length
EGF	AHYYRTQKLLSKN**PKNP**YEESSRDVRSRRP ADTEDGMSSCPQPWFVVIKEHQDLKNGGQ PVAGEDGQAADGSMQPTSWRQEPQLCGM GTEQGCWIPVSSDKGSCPQVMERSFHMPS YGTQTLEGGVEKPHSLLSANPLWQQRALDP PHQMELTQ	154
TGFα	**HCCQVRKH**CEWCRALICRHEKPSA**LL**KGRTACCHSETVV	39
AREG	QLRRQYVRKYEGEA**EE**RKK**L**RQENGNVHAIA	31
HB-EGF	RYHRRGGYDVENEEKVKLGMTNSH	24
BTC	TCCHPLRKRRKRKKKEEEMETLGKDITPINEDIEETNIA	39
EREG	CRWYRNRKSKEPKKE**Y**ERVTSGDPELPQV	29
Epigen	RCINLKSPYIICSGGSPL	18

cytoplasmic domain. Analysis of the EREG cytoplasmic domain reveals a possible PXXP motif similar to EGFR and EGF. However, the EREG motif is at the C-terminus of the cytoplasmic domain as opposed to the juxtamembrane region and is not downstream of a di-leucine motif like in EGFR and EGF. Site-directed mutagenesis of this motif did not affect EREG BL delivery, indicating PXXP alone is not a BL sorting motif. The location in relation to the membrane and surrounding amino acids may be important determinants for PXXP to act as a BL sorting signal. However, the fact that PXXP is not functioning as a BL sorting signal in EREG supports my theory that mutation of the PXXP motif in EGFR and EGF affects the structure of the cytoplasmic domain and that PXXP is not an actual signal recognized by adaptor proteins.

EGFR ligands that have not been studied for BL sorting motifs include HB-EGF, BTC, and epigen. A cursory analysis of HB-EGF reveals a mono-leucine-based signal (EEKVKL) very similar to the one identified in chapter 2 of this dissertation for AREG (EERKKL). Future analysis of HB-EGF will determine if this signal is involved in BL delivery of HB-EGF. Interestingly, HB-EGF was the first ligand identified to be present in exosomes. AREG was later determined to be in exosomes and play an important role in cellular invasion (Higginbotham et al., 2011). The fact that both of these proteins contain an EEXXXL motif could be an important determinant of how they are trafficked to exosomes. This motif is similar to the DXXLL motif described earlier for targeting to the lysosome, and may serve a similar function in diverting proteins from the lysosome to a multi-vesicular body destined to fuse with the plasma membrane and release

exosomes. If one extends the similarities within the AREG (YEGEAEERKKL) and HB-EGF (YDVENEEKVKL) cytoplasmic domains they both contain the amino acid sequence YaXaXaabXbL, where “a” represents an acidic residue and “b” represents a basic residue. This charged region flanked by tyrosine and leucine, two residues shown to be critical in signal recognition, could play an important role in the trafficking of these two proteins.

Loss of Polarity in Disease

Our understanding of how proteins are delivered in a polarized cell is critical to understanding the basis for a number of human diseases. When proteins important for the function of a cell or organ are not properly delivered, the homeostasis of the organism can be disrupted. This is especially true in organs vital for overall homeostasis such as the kidney and liver.

Isolated recessive renal hypomagnesemia is a disorder of the kidney characterized by excessive Mg^{2+} wasting (Groenestege et al., 2007). In the kidney, EGF is delivered to both the apical and BL surface of polarized epithelial cells (Dempsey et al., 1997). A mutation of the PXXP motif to PXXL results in loss of BL delivery, restricting the ligand from activating the BL localized EGFR (Groenestege et al., 2007). Loss of EGFR signaling prevents activation and cell surface expression of the Mg^{2+} permeable channel TRPM6, reducing Mg^{2+} reabsorption in the distal convoluted tubule and resulting in renal Mg^{2+} loss (Thebault et al., 2009). Maintenance of Mg^{2+} homeostasis in the body is critical for normal functioning of the immune system, neuromuscular excitability, and

neuroprotection; loss of homeostasis can contribute to hypertension and metabolic syndrome (Cao et al., 2008a).

Familial hypercholesterolaemia is an inherited disease caused by mutations within the LDL receptor. In the liver, the LDL receptor functions in removal and catabolism of plasma LDL. Individuals with dysfunctional LDL receptors are unable to properly clear cholesterol carrying LDL from the plasma and develop premature coronary heart disease (Hobbs et al., 1992). To function properly the LDL receptor must be delivered in a polarized manner to the proper sinusoidal surface of hepatocytes (Koivisto et al., 2001). In 1992 there were more than 150 known mutations to the LDL receptor that impaired its function to the point of causing hypercholesterolaemia (Hobbs et al., 1992). One of the mutations is a G34D mutation within the GYXY BL sorting motif in the C-terminal portion of the LDL receptor, resulting in receptors that were no longer expressed in a polarized manner at steady state (Koivisto et al., 2001). Receptors with this mutation were delivered to the sinusoidal surface in hepatocytes but were post-endocytically missorted to the apical surface, resulting in decreased clearance of LDL (Koivisto et al., 2001). While the receptors were initially delivered to the proper cell surface, they were not properly recycled back, resulting in a diminished number of receptors available to clear the LDL.

Diseases like hypercholesterolaemia and renal hypomagnesemia reveal the delicate balance of homeostasis in the body and demonstrate how important maintenance of polarity is within the cell. The existence of diseases like these confirms the need to study the complexities of the polarized epithelial cell. The

cell is not a static structure but is in constant flux and renewal. The more we learn about each individual component of the cell, like polarized delivery of AREG, the closer we get to understanding the entirety of the cell and how it functions.

In the following chapters, I will describe how the EGFR ligand AREG is trafficked in polarized epithelial cells. In chapter 2, I will demonstrate that AREG delivery to the BL surface is driven by a dominant BL sorting signal in the cytoplasmic domain. The main sorting signal present in the AREG cytoplasmic domain consists of a mono-leucine preceded by an acidic cluster. The steady state polarized distribution of AREG is dependent on the epithelial-specific adaptor protein AP-1B. The data in chapter 2 support the hypothesis that AP-1B facilitates the recycling of AREG to the BL surface and loss of AP-1B results in mis-recycling of AREG to the apical surface. Chapter 2 identifies a novel BL sorting signal in the AREG cytoplasmic domain and shows that AREG is the sole EGFR ligand dependent on AP-1B for its polarized distribution.

Chapter 3 will introduce exosomes and discuss AREG in exosomes. Exosomal AREG is in a signaling competent topology and AREG is enriched in exosomes from cells with a mutant KRAS, suggesting a difference in exosome composition between normal and transformed cells. AREG western blots of exosome preparations reveal a post-translational modification of AREG not seen in AREG IP or total lysate western blots. Hypothesizing this modification is ubiquitin, I demonstrate that AREG can be ubiquitylated *in vitro* and provide

supporting data for the hypothesis that ubiquitylation is necessary for efficient delivery to exosomes. The data in chapter 3 provide a foundation for future work on how AREG is delivered to exosomes and how exosomes may act as a novel EGFR ligand signaling platform.

Chapter 4 will discuss the techniques used to discover AREG-interacting proteins. Two methods, a split ubiquitin yeast two-hybrid screen and a crosslinked AREG IP mass spectral analysis, were performed to identify interacting proteins for AREG. The main focus of these screens was to identify proteins involved in the delivery of AREG to the BL surface. Chapter 4 includes the list of identified proteins and highlights several interesting candidates for future work. While these screens did not uncover any interacting proteins that regulate BL delivery of AREG, they do provide a set of data that may prove useful in future work in the Coffey lab.

The data presented in this dissertation expands our knowledge of how AREG is trafficked in polarized epithelial cells and opens new areas for future study. Now that we know AREG is AP-1B dependent for its polarized distribution, identification of the signal recognized by AP-1B will add to our understanding of how this critical adaptor protein functions. Identification of the signal recognized during AREG endocytosis from the cell surface and regulation of internalization will increase our understanding of how EGFR ligands are regulated. Revealing that AREG can be ubiquitylated suggests this modification may play an important role in regulating AREG. Good science not only answers questions but also poses new ones, and I think my work accomplishes both of those tasks.

CHAPTER II

THE CYTOPLASMIC DOMAIN OF AMPHIREGULIN CONTAINS A NOVEL MONO-LEUCINE-BASED BASOLATERAL SORTING MOTIF

Introduction

The *AREG* gene, localized to chromosomal region 4q13-4q21, encodes a 252-amino acid type one transmembrane glycoprotein (Plowman et al., 1990). The AREG precursor protein consists of a signal sequence, pro-peptide domain, heparin-binding domain, EGF-like consensus motif, transmembrane domain, and cytoplasmic domain (Figure 7). The 81-residue pro-peptide domain is N-glycosylated and provides structural elements to the heparin-binding domain necessary for proper folding and secretion of mature AREG (Thorne and Plowman, 1994). If the pro-peptide is removed from AREG, the protein is not properly secreted and is degraded, unless the heparin-binding domain is removed as well (Thorne and Plowman, 1994). The heparin-binding domain is enriched in basic residues and constitutes the N-terminal region of the mature secreted AREG ligand. The ability of the heparin-binding domain to interact with heparin-sulfated proteoglycans in the ECM has been proposed to be a factor in AREG-induced lung branching morphogenesis and cellular proliferation (Schuger et al., 1996). The heparin-binding domain may act to store the ligand in the ECM or present the ligand in a fashion that mediates more efficient binding to the EGFR. The EGF-like consensus motif consists of six cysteine residues in the

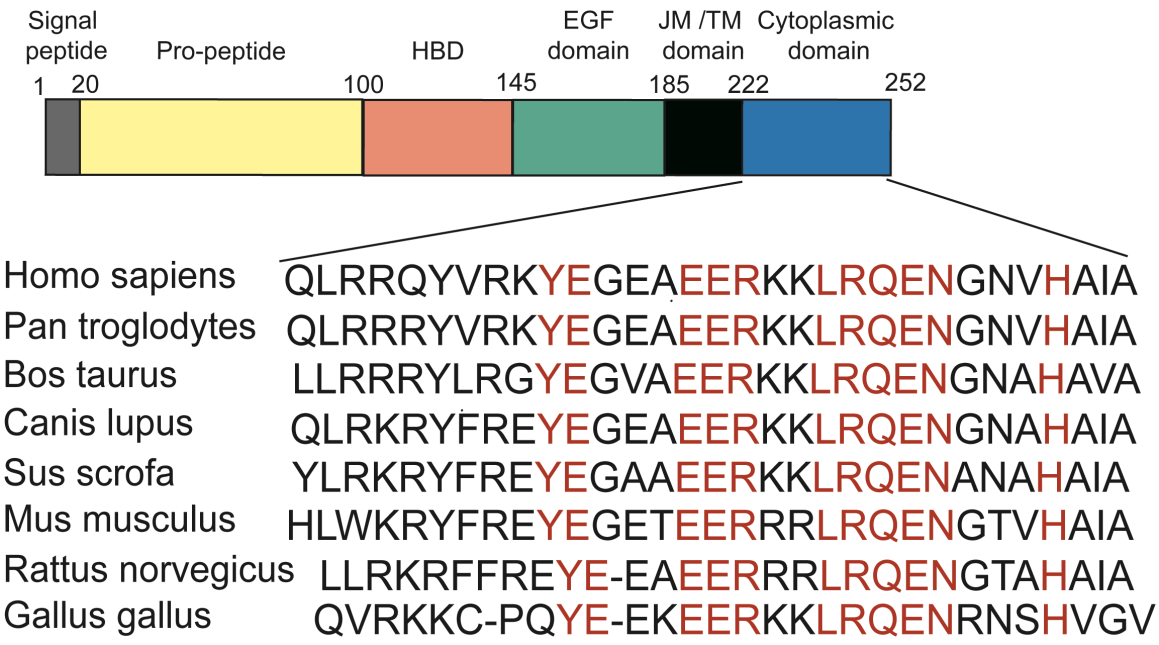

Figure 7. Schematic diagram of full-length AREG and amino acid composition of the AREG cytoplasmic domain. AREG is synthesized as a 252- amino acid type 1 transmembrane glycoprotein. Beginning with a signal sequence (1-19), AREG contains an N-glycosylated pro-peptide domain (20-100) that is required for proper folding and secretion. Following the pro-peptide is mature AREG (101-184) consisting of a heparin-binding domain (HBD) and an EGF domain. The EGF domain contains the conserved spacing of six cysteine residues that is preserved amongst all EGFR ligands. The 31-amino acid cytoplasmic domain (222-252) is aligned with other species with the conserved residues highlighted in red.

conserved spacing $CX_7CX_4CX_{10}CX_1CX_8C$ that form di-sulfide bonds to provide the necessary structure for binding and activating the EGFR (Shoyab et al., 1989). However, AREG does lack a critical leucine residue that is conserved in EGF, TGFα, and HB-EGF and may explain the lower binding affinity AREG has for the EGFR (Shoyab et al., 1989). The transmembrane domain anchors the protein to the membrane while the cytoplasmic domain contains critical information necessary for the proper localization of AREG to the BL surface of polarized epithelial cells (Brown et al., 2001; Damstrup et al., 1999). Each domain within the AREG precursor protein provides a necessary function for proper AREG secretion and activation of the EGFR.

Once delivered to the BL surface, mature soluble AREG, which includes the heparin-binding domain and the EGF-like motif, is released from the precursor protein by the metalloprotease ADAM17/TACE (Sahin et al., 2004). Metalloprotease processing of AREG results in multiple soluble and membrane forms (Figure 8) (Brown et al., 1998). The predominant membrane form detected in cell lysates is the 50 kDa full length N-glycosylated precursor protein. This form can be processed by metalloproteases to produce either a soluble 43 kDa form that still contains the pro-protein domain or 28 kDa and 26 kDa membrane forms. The 28 kDa and 26 kDa membrane forms no longer contain the pro-protein domain and differ in size due to processing of the N-terminal 6-residues within the heparin-binding domain. Since the pro-protein domain is no longer present on these two membrane forms and the pro-protein domain is necessary

for proper secretion, this processing event most likely occurs at the cell surface (Brown et al., 1998; Thorne and Plowman, 1994).

The 28 kDa and 26 kDa membrane forms are also the predominant forms detected in exosomes (Higginbotham et al., 2011). How AREG is delivered to exosomes is a topic of future study and the presence of forms lacking the pro-protein domain indicates delivery to exosomes may be enhanced by removal of the pro-protein domain. The presence of these two forms in exosomes and the requirement of the pro-protein domain for proper secretion also indicates the route to the exosome is via the cell surface where the removal of the pro-protein domain is thought to take place (Brown et al., 1998; Thorne and Plowman, 1994).

The 28 kDa and 26 kDa membrane forms can be processed to release 21 kDa and 19 kDa soluble forms, which correspond to the 84- and 78-residue soluble bioactive ligands initially identified as AREG (Brown et al., 1998; Shoyab et al., 1988; Shoyab et al., 1989). If not released as soluble isoforms, the heparin-binding domain of the 28 kDa and 26 kDa membrane forms can be removed to produce a 16 kDa membrane form that can be released as a 9 kDa soluble form. The 9 kDa soluble form would consist only of the EGF-like motif (Brown et al., 1998). The different biological activities and occurrence in the extracellular milieu of these various soluble and membrane forms is unknown. The recent work regarding the biologic activity of AREG exosomes verses soluble ligand sheds some light on the potency of different AREG forms (Higginbotham et al., 2011). However, there is still much more to learn about the

regulation of different forms of AREG and the role they play in normal and disease states.

The work in this chapter focuses on the critical residues present in the cytoplasmic domain of AREG necessary for the proper localization to the BL surface. Previous studies showed that removal of the AREG cytoplasmic domain resulted in a non-polar distribution of AREG on the cell surface, indicating that the cytoplasmic domain contains important BL sorting information (Brown et al., 2001). The extracellular domains of EGFR and EGF are heavily glycosylated; this glycosylation is likely responsible for their predominant apical distribution upon removal of their cytoplasmic domains (Hobert and Carlin, 1995). AREG is also glycosylated, but removal of the AREG cytoplasmic domain results in a non-polar distribution of AREG, suggesting that the glycosylated extracellular domain of AREG does not act as a separate apical sorting determinant (Brown et al., 2001). The data in this chapter demonstrate that the AREG cytoplasmic domain contains dominant-acting BL sorting information that is sufficient to redirect the apically targeted 75-kDa human nerve growth factor receptor (NGFR) to the BL surface. The atypical AREG BL sorting motif consists of a mono-leucine preceded by an acidic cluster (EExxxL). In polarized cells that lack the adaptor protein AP-1B, AREG is inappropriately recycled from the BL surface to the apical surface, distributing AREG in a non-polar fashion at steady state. The AREG BL sorting motif sequence configuration and dependence on AP-1B differentiates AREG from the only other known proteins to contain a mono-

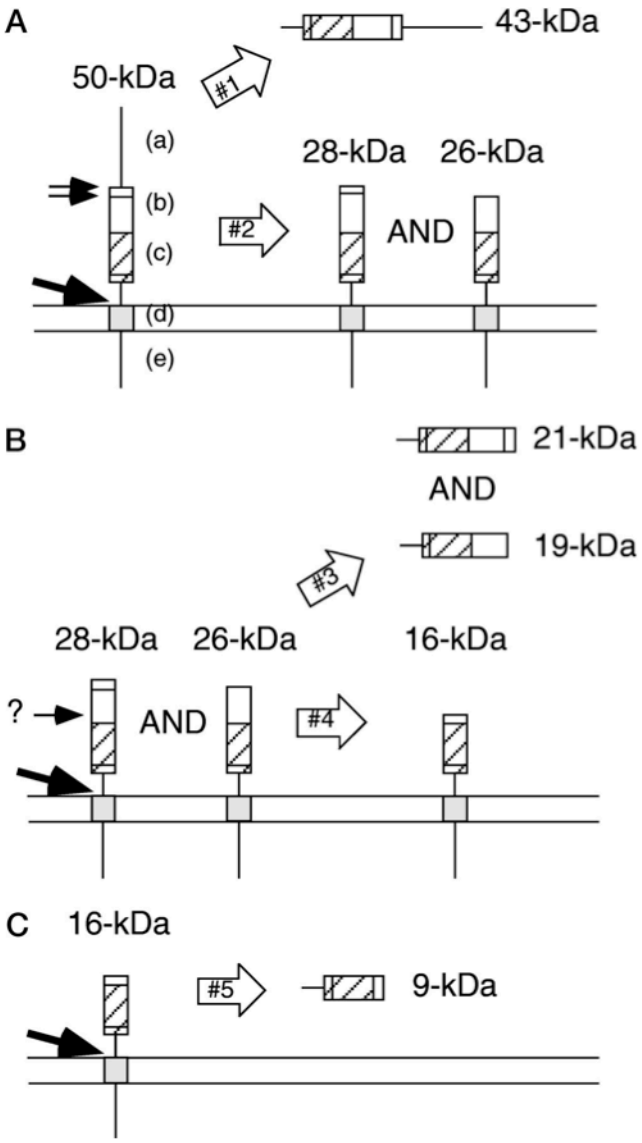

Brown C L et al. J. Biol. Chem. 1998;273:17258-17268

Figure 8. Model proposed by Brown et al. to explain the various membrane and soluble forms of AREG detected in cellular lysates and conditioned media. The indicated domains of the precursor protein are as follows a) pro-peptide b) heparin-binding c) EGF-like motif d) transmembrane e) cytoplasmic. Proposed processing events: #1) release of the soluble 43 kDa form #2) removal of the pro-peptide domain #3) release of the 78- and 84-residue ligands #4) removal of the heparin-binding domain #5) release of the 9 kDa soluble form lacking the heparin-binding domain (Brown et al., 1998).

leucine BL sorting motif, CD147 and stem cell factor (SCF) (Deora et al., 2004; Wehrle-Haller and Imhof, 2001).

Materials and Methods

Reagents and Antibodies

Cell culture media was purchased from Media Tech Inc (Manassas, VA) and fetal bovine serum from Hyclone Laboratories (Logan, UT). All chemicals were purchased from Sigma (St. Louis, MO) unless otherwise stated. Sulfo-NHS-LC-Biotin and micro-BSA protein assay kits were purchased from Pierce Biotechnology (Rockford, IL). All electrophoresis reagents were purchased from Bio-Rad Laboratories (Hercules, CA). Rainbow markers were purchased from Bio-Rad or Fermentas Life Sciences (Glen Burnie, MD). ECL reagents were purchased from Perkin Elmer (Waltham, MA). Nitrocellulose was purchased from Whatman (Dassel, Germany). DNA mini-prep and cleanup kits were purchased from Qiagen Sciences (Hilden, Germany). Protein G agarose beads were purchased from Invitrogen (Carlsbad, CA). All conjugated secondary antibodies were purchased from Jackson ImmunoResearch Laboratories Inc. (West Grove, PA). Labeled phalloidin was purchased from Invitrogen (Eugene, OR). Mouse monoclonal antibody 6R1C2.4 against human AREG was previously described (Brown et al., 2001; Brown et al., 1998; Piepkorn et al., 1995). Anti-NGFR p75 (ME20.4) mouse monoclonal antibody was purchased from Santa Cruz

Biotechnology, Inc (Santa Cruz, CA). IR-Dye680 streptavidin was purchased from LI-COR Biosciences (Lincoln, NE).

Cells and Cell Culture

MDCK II cells were obtained from Enrique Rodriguez-Boulan (Cornell University Medical College, Ithaca, NY). MDCK μ1B KD cells were obtained from Enrique Rodriguez-Boulan and previously described (Gravotta et al., 2007). LLC-PK1::μ1A and LLC-PK1::μ1B cells were previously described (Folsch et al., 1999). Cells were cultured as previously described (Dempsey and Coffey, 1994). Cells were grown on 12 mm Transwells (0.4 μm pores, Corning Inc.) as previously described (Brown et al., 2001).

AREG Constructs

Human AREG cDNA encoding wild-type pro-AREG was obtained from Dr. Greg Plowman (Sugen, Redwood City, CA) (Plowman et al., 1990) and Dr. Gary Shipley (Oregon Health Sciences University, Portland, OR) (Cook et al., 1991) and expressed in pCB6 (Brown et al., 1998). All untagged constructs were expressed in pCB6 (Brewer and Roth, 1991). All EGFP tagged constructs were expressed in the Clontech vector pEGFP-N1 (GenBank Accession #U55762). Human NGFR cDNA was obtained from Dr. Andre Le Bivic (Monlauzeur et al., 1995). A chimera of the extracellular and transmembrane domains of NGFR with the cytoplasmic domain of AREG (NGFR-ACD) was constructed by creating a BsmI site at the transmembrane-cytoplasmic domain junction of NGFR. The

cytoplasmic domain of NGFR was removed with a BsmI/XbaI digest. Using PCR, AREG cytoplasmic domain fragment was ligated to the NGFR to create an NGFR-ACD chimera. AREG cytoplasmic domain truncations and amino acid mutations were obtained by PCR QuikChange® site-directed mutagenesis of wild-type pro-AREG in pCB6 as per manufactures instructions (Stratagene Catalog# 200518). All DNA constructs were confirmed by sequencing prior to use.

Selective Cell Surface Biotinylation

Cells were plated on 12 mm Transwell inserts at a cell density of $1x10^5$ cells/Transwell. Four days after plating, the transepithelial electrical resistance (TEER) for each Transwell was confirmed to be >200 Ω/cm^2. Cells were then treated with 5 mM sodium butyrate overnight. On day five, the cells were washed three times with cold PBS containing 0.1 mM $CaCl_2$ and 1.0 mM $MgCl_2$ (1xPBS-CM) on ice. All subsequent steps were done on ice or at 4^oC. Either the apical or BL cell surface was biotinylated with 0.5 mg/ml biotin in 1xPBS-CM. Cells were incubated with biotin for 20 minutes, then used biotin was removed and replaced with fresh biotin for an additional 20 minutes. The biotin was quenched with five washes of 1xPBS-CM, 0.2% BSA, 100 mM glycine followed by two washes with 1xPBS-CM. Filters were cut from the inserts and placed in 250 µl 1%NP-40 lysis buffer (50 mM Tris-HCl pH 8.0, 150 mM NaCl, 1% NP40, 2 mM EDTA) plus protease inhibitors (Sigma P2714) and rotated for 30 minutes. Cell lysates were transferred to new eppendorf tubes and centrifuged for 15 minutes at 13,000

RPM. Supernatants were transferred to new tubes and rotated for 1 hour with 10 µl 50% slurry recombinant Protein G agarose beads to pre-clear the samples. The protein concentration of each sample was determined using a BCA protein assay. Equal protein concentration of each sample was transferred to a new tube with 1 µg of mouse anti-AREG antibody (6R1C2.4) and rotated overnight. 20 µl of recombinant Protein G agarose bead slurry was added to each sample and rotated for 3 hours. Beads were gently pelleted and washed three times with 1 ml lysis buffer. The final pellet was resuspended in 20 µl 1x sample buffer (2x sample buffer: 125 mM Tris-HCl pH 6.8, 2% Glycerol, 4% SDS (w/v), 0.05% bromophenol blue) and heated at 75^{o}C for 10 minutes. Sample proteins were separated by 12.5% SDS-PAGE and transferred to nitrocellulose membranes. All subsequent steps were performed with filtered PBS. Membranes were blocked overnight with 1xPBS, 3% BSA. Membranes were probed for 30 minutes at room temperature (RT) with IR-Dye680 streptavidin diluted 1:25000 in 1xPBS, 3% BSA, 0.1% Tween20, 0.01% SDS. Membranes were then washed three times with 1xPBS, 0.1% Tween and two times with 1xPBS before imaged on an Odyssey® infrared imaging system (LI-COR Biosciences). Odyssey® software (version 3.0) was used to determine the integrated intensity of each band. The integrated intensities for all the bands in both the apical and BL lanes were added together to obtain a "total cell surface" value [(apical integrated intensity)+(BL integrated intensity)=total]. The integrated intensities of the bands in either the apical or BL lanes were divided by the total cell surface value to give

the percentage of total value [(apical integrated intensity/total)x100= percentage of total on apical surface].

Immunofluorescence and Confocal Microscopy

LLC-PK1 cells were stained as previously described (Folsch et al., 1999). Cells were plated on 12 mm Transwell inserts at a cell density of $1x10^5$ cells/Transwell. Cells were grown on Transwells for four days and reached appropriate TEER (MDCK >200 Ω/cm^2, LLC-PK1 >400 Ω/cm^2) before staining. MDCK cells were washed three times with ice cold PBS-CM then stained for 1 hour on ice with primary antibody diluted in 1xPBS-CM. Cells were washed six times with ice-cold 1xPBS-CM prior to fixation with 4% paraformaldehyde/PBS-CM for 15 minutes on ice then quenched with 50 mM ammonium chloride in 1x PBS-CM for 10 minutes. Cells were washed and blocked in 1x PBS-CM, 1% BSA, 0.2% fish skin gelatin (blocking buffer) three times over 1 hour. Secondary antibodies were diluted 1:200 in blocking buffer and incubated on cells for 1 hour. Cells were washed three times followed by a 10 minute wash with blocking buffer plus 0.1% Triton X-100. Cells were incubated with labeled phalloidin diluted 1:200 in blocking buffer for 30 minutes prior to three washes with blocking buffer and mounting in ProLong® Gold (Invitrogen P36934). Immunofluorescence imaging was acquired on a Zeiss LSM 510 confocal microscope (Zeiss Microscope Imaging, Inc., Thornwood, NY) using a 40x objective with a 2x zoom at 1024x1024 resolution. Contents of image window were exported as Tiff files using LSM Image Browser software (Version 4.2.0.121, Carl Zeiss GmbH Jena

1997-2006; Zeiss Microscope Imaging, Inc., Thornwood, NY). Tiff files were processed and cropped using Adobe Photoshop software (Version 12.0). Levels for each channel were independently modified and include all available data.

Transcytosis Assay

LLC-PK1 cells were plated on 12 mm Transwell inserts at a cell density of $1x10^5$ cells/Transwell. Cells were grown on Transwells for six days and reached appropriate TEER (>400 Ω/cm^2). Integrity of the monolayer was confirmed using 3000 MW dextran Texas Red® (Invitrogen D3328) diluted to 63 µg/ml in phenol red-free complete media. Labeled dextran was added to the apical compartment of the Transwell only and incubated at 37^oC for 30 minutes. 100 µl of media was removed from the BL compartment and replaced with fresh media every five minutes. The diffusion of the dextran across the monolayer was measured using a Synergy 4 BioTek plate reader and Gen5 OLE Automation software (Version 1.06.10) (BioTek Instruments, Inc., Winooski, VT). Once the monolayer was determined to be intact, mouse anti-AREG antibody (6R1C2.4) diluted 4 µg/ml in serum free media was added to the BL compartment only for 30 minutes at 37^oC. Cells were washed three times with RT 1xPBS-CM, 1% BSA to remove unbound antibody. In 1xPBS-CM, 1% BSA, Alexa-488 conjugated anti-mouse secondary antibody (1:200) was added to the BL compartment only and Cy5 conjugated anti-mouse secondary antibody (1:200) was added to the apical compartment only. Cells were incubated with secondary antibodies for 10 minutes at RT, washed three times with 1xPBS-CM, 1% BSA, then fixed with 4%

paraformaldehyde/PBS-CM for 15 minutes at RT. Cells were washed three times with 1xPBS-CM, 1% BSA then one 15 minute wash with 1xPBS-CM, 1% BSA, 0.1% Triton X-100. F-actin was stained with phalloidin- Texas Red® diluted 1:200 in 1xPBS-CM, 1% BSA for 30 minutes followed by three washes with 1xPBS-CM, 1% BSA then mounted with ProLong® Gold. Images were acquired as described above.

Quantitative RT-PCR

Two sets of primers were used to determine the mRNA level of canine μ1B in μ1B knockdown MDCK cells. Primer set 1 (RealTimePrimers.com) (annealing and extension: 61^{o}C, 45 seconds) contained the forward primer 5'-ACA AGA CGG TGG AGG TTT TC -3' and reverse primer 5'-CCT GCT GCG TGA TGT ACT CT -3'. Primer set 2 (Sigma) (annealing and extension: 65^{o}C, 45 seconds) was self-designed and contained the forward primer 5'-CCT GAT CAG CCG CAA CTA CAA GG -3' and reverse primer 5'-GTA CTC AGA GAA AAC CTC CAC CG -3'. Primers for canine beta-actin (RealTimePrimers.com) (annealing and extension: 61^{o}C, 45 seconds) contained the forward primer 5'-CCC AGA TCA TGT TCG AGA CT -3' and reverse primer 5'-CAT GAG GTA GTC GGT CAG GT -3'. Platinum® SYBR® Green qPCR supermix-UDG (Invitrogen Cat # 11733-038) was used as per manufactures instructions. Samples were run and analyzed on a StepOnePlus real-time PCR system with StepOne software version 2.1 (Applied Biosystems).

Statistical Analysis

We used analysis of variance to compare apical distribution of AREG in polarized MDCK cells. Tukey's honestly significant difference was used for pair-wise comparisons. Statistical significance was declared for $p<0.05$.

Results

The cytoplasmic domain of AREG contains a dominant BL sorting motif

The cytoplasmic domain of AREG controls its delivery to the BL surface of polarized epithelial cells using information within the last 27 amino acids of its 31 amino acid cytoplasmic domain, such that deletion of these amino acids results in a non-polar surface distribution of AREG in MDCK cells (Brown et al., 2001). By contrast, NGFR, which contains an extracellular apical sorting determinant consisting of an O-glycosylated region, is normally localized to the apical surface of polarized MDCK cells and removal of the NGFR cytoplasmic domain does not affect apical localization (Le Bivic et al., 1991; Yeaman et al., 1997). To confirm that the cytoplasmic domain of AREG contains BL sorting information, a chimeric protein consisting of the extracellular and transmembrane domains of NGFR and the cytoplasmic domain of AREG (NGFR-ACD) was generated and stably expressed in MDCK cells. Cell surface immunofluorescence for the ectodomain of NGFR showed NGFR on the apical surface while NGFR-ACD was present on the BL surface of polarized MDCK cells (Figure 9A). Selective cell surface biotinylation was used to compare the distribution of NGFR with the NGFR-ACD

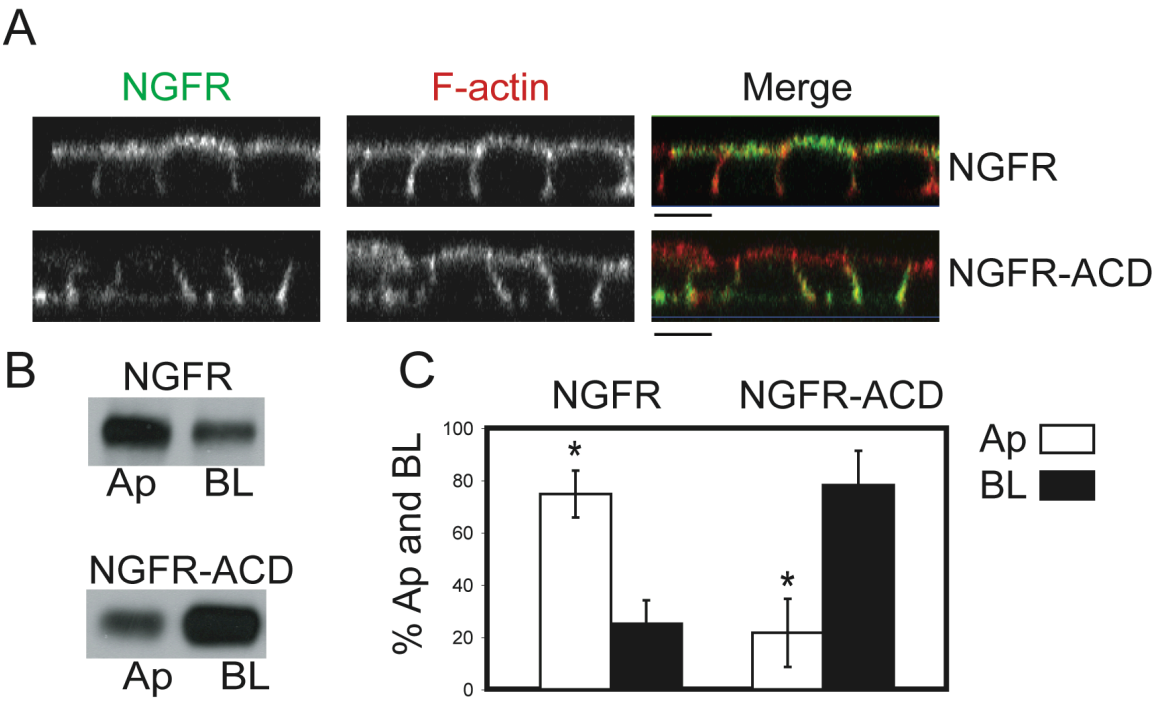

Figure 9. The cytoplasmic domain of AREG redirects NGFR from the apical (Ap) to the basolateral (BL) surface of polarized MDCK cells. MDCK cells stably expressing either full-length NGFR or the NGFR extracellular and transmembrane domains fused to the AREG cytoplasmic domain (NGFR-ACD) were polarized on Transwell filters (TEER>200 Ω/cm^2) and then analyzed for steady state cell surface distribution of NGFR using an NGFR ectodomain-specific antibody (ME20.4). (A) Polarized cells were stained for NGFR (green) under non-permeabilized conditions followed by permeabilization with 0.1% Triton and F-actin (red) staining. Analysis was performed by confocal microscopy. Bar, 10 μm. (B) Polarized cells were selectively biotinylated on the Ap or BL surface, immunoprecipitated with ME20.4, separated by SDS-PAGE, transferred to nitrocellulose and then probed with streptavidin-HRP, or (C) with streptavidin-IRDye680. Results were scanned on an Odyssey scanner and quantitated using Odyssey software (n=3). Columns marked with an * are significantly different ($p<0.05$).

chimera. At steady state, 75% of NGFR was distributed to the apical surface of polarized MDCK cells whereas 78% of the NGFR-ACD chimera was distributed to the BL surface (Figure 9C). The BL redistribution of the NGFR ectodomain via the cytoplasmic domain of AREG demonstrates it contains a dominant BL sorting motif, over-riding the NGFR apical sorting determinant. Interestingly, CD147, which contains a canonical mono-leucine BL sorting motif (EDDXXXXXL) (Deora et al., 2004), was unable to redirect NGFR to the BL surface (Castorino et al., 2010).

Determining the amino acids within the cytoplasmic domain necessary for the BL localization of AREG

Having established the presence of a dominant BL sorting motif within the cytoplasmic domain of AREG, we set out to determine the specific amino acids that contain necessary BL sorting information. Sequential cytoplasmic domain truncation mutants of AREG were constructed using PCR and were C-terminally fused to EGFP (Figure 10A). These chimeras were transfected into MDCK cells, selected for G418 resistance and enriched using flow cytometry to generate a stable population of cells expressing high levels of the mutants. The localization of the truncation mutants was analyzed by cell surface immunofluorescence (Figure 10B) and selective cell surface biotinylation (Figure 10C). Full-length AREG and AREG with 6-amino acids removed from the cytoplasmic domain (25 aa) were 95% and 93% localized to the BL surface, respectively. However, truncating the cytoplasmic domain by 17-amino acids (14 aa) resulted in only

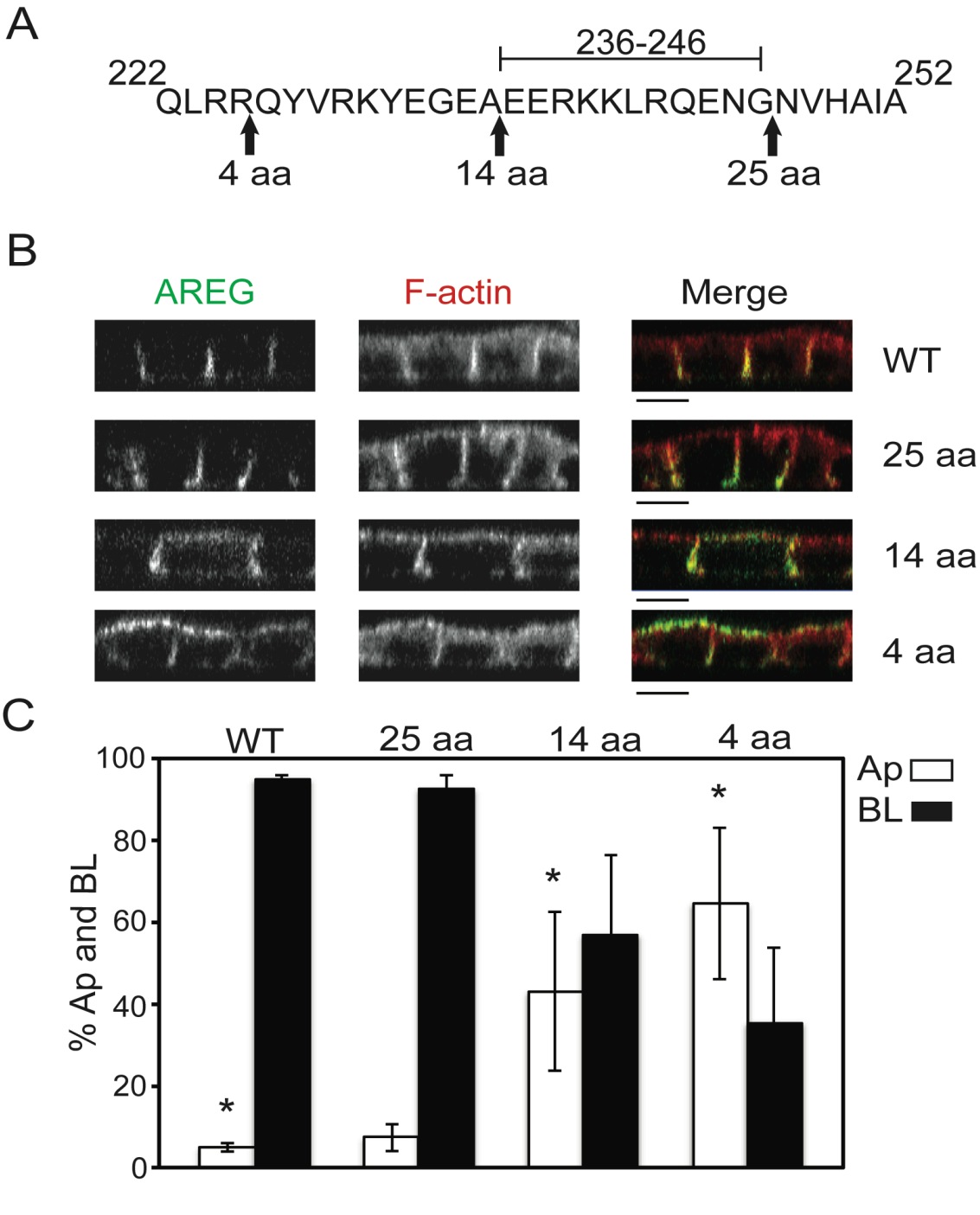
A
236-246
222
252
QLRRQYVRKYEGEAEERKKLRQENGNVHAIA
4 aa
14 aa
25 aa
B
AREG
F-actin
Merge
WT
25 aa
14 aa
4 aa
C
WT
25 aa
14 aa
4 aa
100
80
60
40
20
0
% Ap and BL
Ap
BL
*
*
*

Figure 10. AREG cytoplasmic domain (ACD) truncations reveal that residues 236-246 contain BL sorting information. (A) Amino acid composition of ACD and points of truncation. MDCK cells stably expressing EGFP-tagged ACD truncations were generated and used to determine the region of the tail that contains BL sorting information. Cells were polarized on Transwell filters and (B) surface stained for AREG (green) followed by permeabilization and F-actin (red) staining. Analysis was performed by confocal microscopy. Bars, 10 μm. (C) Polarized cells were selectively biotinylated on the Ap or BL surface, immunoprecipitated with anti-AREG mAb, separated by SDS-PAGE, transferred to nitrocellulose and then probed with IRDye680-streptavidin. Results were scanned on an Odyssey scanner and quantitated using Odyssey software ($n \geq 3$). Columns marked with an * are significantly different from WT ($p<0.05$).

57% of total surface AREG localized to the BL surface. The difference in distribution between full-length and 14 aa AREG is statistically significant, whereas the difference in distribution of 14 aa and a 4-amino acid cytoplasmic domain (4 aa) is not statistically significant. These results indicate that important BL sorting information resides within amino acids 236 (14 aa) thru 246 (25 aa) of AREG within the cytoplasmic domain.

Identification of a mono-leucine-based BL sorting motif

Analysis of amino acids 236 thru 246 (EERKKLRQENG) revealed no obvious canonical BL sorting motifs. Comparison across species showed this region of the domain to be 73% identical and 91% similarly conserved, making this the most highly conserved region of the cytoplasmic domain (Figure 7). This region contains an acidic cluster, a basic cluster and a mono-leucine. Mono-leucine BL sorting motifs consisting of an acidic cluster N-terminal of a mono-leucine (EDDXXXXXL) have been reported for two other BL proteins, SCF and CD147 (Deora et al., 2004; Wehrle-Haller and Imhof, 2001). Although this exact motif is not present in the cytoplasmic domain of AREG, we further analyzed the possibility of AREG containing a variation of the consensus mono-leucine BL sorting motif. Using PCR site-directed mutagenesis, individual amino acids were changed to alanine (A) residues (Figure 11A). When the single leucine (L) residue was changed to alanine (L241A [LA]), AREG polarity was lost with 45% of total surface AREG distributed to the apical surface at steady state (Figure 11B and 11C). When the two conserved acidic glutamine (E) residues were

A


236
246
EERKKLRQENG WT
EERKKARQENG LA
AARKKLRQENG EEAA
AARKKARQENG EEAA/LA
EERAALRQENG KKAA

B

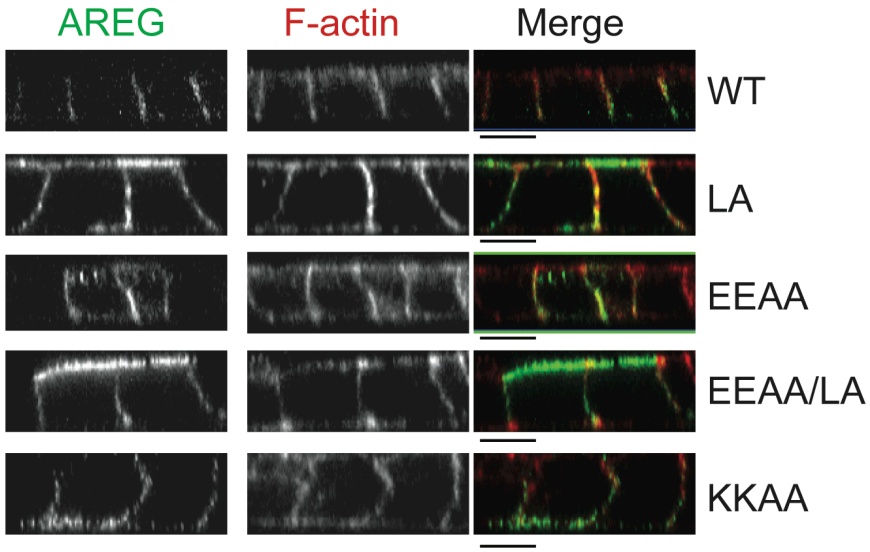
AREG
F-actin
Merge
WT
LA
EEAA
EEAA/LA
KKAA

C

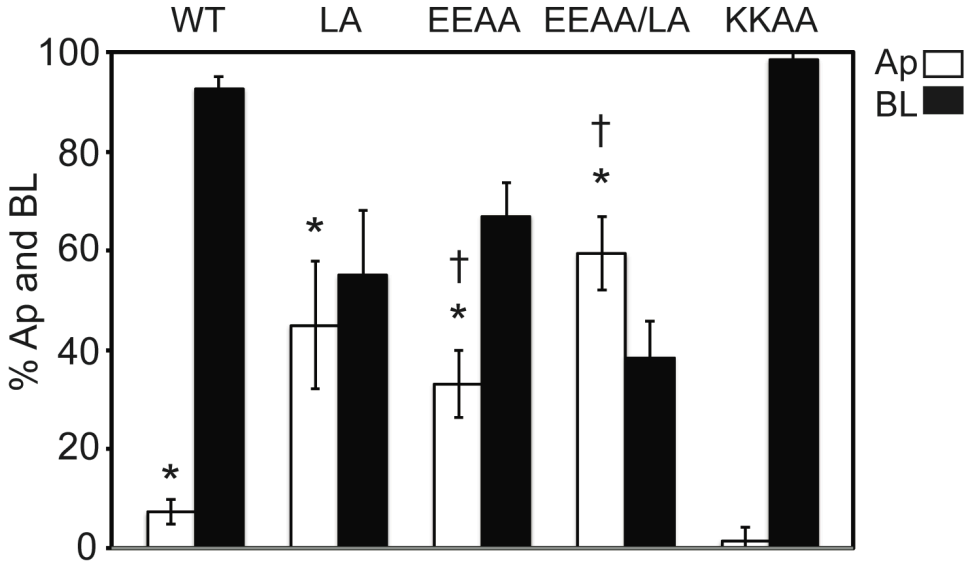
WT
LA
EEAA
EEAA/LA
KKAA
100
80
60
40
20
0
% Ap and BL
Ap
BL
*
*
†
*
†
*

Figure 11. Amino acid substitutions within residues 236-246 identify a mono-leucine-based sorting signal.
(A) Amino acid composition of AREG cytoplasmic domain (ACD) between residues 236 and 246. Specific amino acid mutations are indicated in red. MDCK cells stably expressing the ACD mutants were generated and used to determine the BL sorting motif. Cells were polarized on Transwell filters and (B) surface stained for AREG (green) followed by permeabilization and F-actin (red) staining. Analysis was performed by confocal microscopy. Bars, 10 μm. (C) Polarized cells were selectively biotinylated on the Ap or BL surface, immunoprecipitated with anti-AREG mAb, separated by SDS-PAGE, transferred to nitrocellulose, and then probed with IRDye680-streptavidin. Results were scanned on an Odyssey scanner and quantitated using Odyssey software (n≥3). Columns marked with an * are significantly different from WT. Columns marked with a † are significantly different from each other ($p<0.05$).

Table 2. AREG cytoplasmic domain and mutations. The 31-amino acid cytoplasmic domain of AREG (222-252) is aligned with the different alanine substitution mutants. Residues that are substituted with alanine are highlighted in red. Whether the mutant is delivered to the basolateral (BL) surface or to both surfaces (Ap/BL) of the cell in a non-polarized fashion is indicated on the right.

Domain Mutation	Amino Acid Composition	Localization
WT AREG	QLRRQYVRKYEGEAEERKKLRQENGNVHAIA	BL
25aa AREG	QLRRQYVRKYEGEAEERKKLRQENG	BL
14aa AREG	QLRRQYVRKYEGEA	AP/BL
4aa AREG	QLRR	AP/BL
L241A	QLRRQYVRKYEGEAEERKKARQENGNVHAIA	AP/BL
EE236/237AA	QLRRQYVRKYEGEAAARKKLRQENGNVHAIA	AP/BL
EEL236/237/241A	QLRRQYVRKYEGEAAARKKARQENGNVHAIA	AP/BL
KK239/240AA	QLRRQYVRKYEGEAEERAALRQENGNVHAIA	BL
Y231A	QLRRQYVRKAEGEAEERKKLRQENGNVHAIA	BL
Y227A	QLRRQAVRKYEGEAEERKKLRQENGNVHAIA	BL
Y227/231A	QLRRQAVRKAEGEAEERKKLRQENGNVHAIA	BL

changed to alanine residues (EE236,237AA [EEAA]), the amount of AREG detected on the apical surface at steady state was 33% (Figure 11C). These changes in AREG apical distribution are both significantly different from the 7% of steady state wild-type AREG detected on the apical surface. Combining the two mutations (EEAA/LA) resulted in 59% of total surface AREG to be apical at steady state (Figure 11C). In order to rule out the possibility that the charge of the region played a role in BL sorting (Wolff et al., 2010), we mutated the two positive lysine (K) residues (KK239,240AA [KKAA]) to alanine residues. This mutant exhibited normal BL localization of AREG with 98% present on the BL surface (Figure 11C). These results indicate both the acidic cluster and the mono-leucine, which are both highly conserved across species (Figure 7), are important components to the BL sorting motif in the cytoplasmic domain of AREG.

Loss of AP-1B affects the polarized distribution of AREG at steady state

Heterotetrameric adaptor protein complexes (AP-1A, AP-1B, AP-2, AP-3A, AP-3B, AP-4) selectively incorporate cargo proteins and facilitate vesicle formation (Nakatsu and Ohno, 2003). Of the known AP complexes, only AP-1B and AP-4 have been implicated in BL sorting (Folsch, 2005). AP-1B expression is epithelial cell-specific and only differs from the ubiquitous AP-1A by the medium (μ1B) subunit (Ohno et al., 1999). AP-1B is localized to recycling endosomes and plays a role in biosynthetic delivery and recycling of BL proteins (Cancino et al., 2007; Folsch et al., 2003; Gan et al., 2002; Gravotta et al., 2007). LLC-PK1 cells

are a polarizing epithelial cell line that does not express AP-1B and missorts proteins that are dependent on AP-1B for BL delivery (Folsch et al., 1999). In order to determine the role of AP-1B in AREG BL delivery, clonal lines of LLC-PK1 cells expressing either pCB6::μ1A (LLC-PK1::μ1A) or pCB6::μ1B (LLC-PK1::μ1B) were transiently transfected with AREG and then analyzed by cell surface immunofluorescence (Figure 12A). In the LLC-PK1::μ1A cells, which lack AP-1B, AREG was detected on the apical and BL surface, indicating a role for AP-1B in maintaining the polar distribution of AREG (Figure 12A). In the LLC-PK1::μ1B cells, AREG was restricted to the BL surface and no longer present on the apical surface (Figure 12A). Since AREG was detected on both surfaces in LLC-PK1::μ1A cells at steady state, we wanted to further characterize the AREG distribution using selective cell surface biotinylation. However, LLC-PK1 cells are not suitable for use in selective cell surface biotinylation (Folsch et al., 1999); therefore, we used a clonal line of MDCK cells expressing shRNA against μ1B (Gravotta et al., 2007). This clonal line was transfected with AREG, selected with G418 and enriched by flow cytometry to produce a pool of MDCK μ1B knockdown cells expressing AREG. Knockdown of μ1B in the clonal line has been previously characterized (Gravotta et al., 2007); this was confirmed in these AREG-expressing cells by quantitative RT-PCR, which showed a 93% reduction in μ1B message compared to control MDCK cells (Figure 12C). AREG immunoreactivity was detected on the apical surface of polarized μ1B knockdown MDCK cells (Figure 12A). To quantitate the cell surface distribution of AREG in the μ1B knockdown MDCK cells at steady state, cells were polarized on

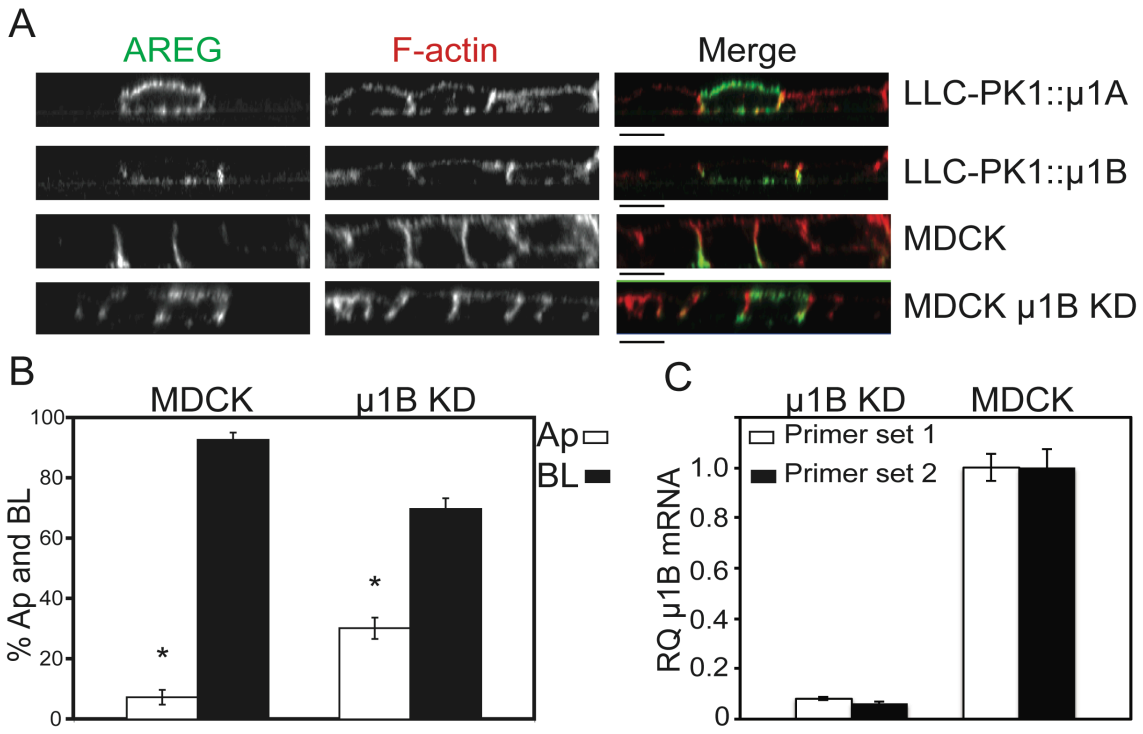

Figure 12. Loss of AP-1B results in apical distribution of AREG. μ1B-deficient LLC-PK1 cells stably expressing either the μ1B or μ1A subunit or MDCK cells stably expressing shRNA against the μ1B subunit of AP-1B were used to demonstrate the role of AP-1B in the cell surface distribution of AREG. The cells were transiently transfected with AREG and then polarized on Transwell filters. (A) The polarized monolayer was surface stained for AREG (green) followed by permeabilization and F-actin (red) staining. Analysis was performed by confocal microscopy. Bars, 10 μm. (B) AREG-expressing parental and μ1B knockdown MDCK cells polarized on Transwell filters were selectively biotinylated on the Ap or BL surface, immunoprecipitated with AREG mAb, separated by SDS-PAGE, transferred to nitrocellulose, and then probed with IRDye680-streptavidin. Results were scanned on an Odyssey scanner and quantitated using Odyssey software ($n \geq 3$). Columns marked with an * are significantly different ($p<0.05$). (C) Knockdown of μ1B was confirmed by quantitative RT-PCR using two different primer sets. Relative quantity= RQ.

Transwell filters and selectively biotinylated on either the apical or BL surface. The μ1B knockdown MDCK cells expressed 30% of the total cell surface AREG on the apical surface at steady state, a two-fold increase over control MDCK cells with μ1B (Figure 12B). This result, along with the presence of AREG on the apical surface of LLC-PK1::μ1A cells, demonstrates a role for AP-1B in the polar distribution of AREG.

Loss of AP-1B results in inappropriate recycling of post-endocytic AREG to the apical surface in fully polarized LLC-PK1 cells

The presence of AREG on the apical and BL surface of polarized epithelial cells lacking AP-1B led us to ask what role AP-1B plays in the polar distribution of AREG. Previous studies have shown that AP-1B is localized to the recycling endosomes and participates in both biosynthetic delivery and recycling of proteins to the BL surface (Cancino et al., 2007; Folsch et al., 2003; Gan et al., 2002; Gravotta et al., 2007). Since the majority of steady state cell surface AREG was detected on the BL surface of polarized MDCK cells with reduced AP-1B, we hypothesized that the AREG biosynthetic route was AP-1B-independent, but recycling of post-endocytic AREG was AP-1B dependent. To test this hypothesis we used LLC-PK1::μ1A and LLC-PK1::μ1B cells transfected with AREG. These cells were polarized on Transwell filters and the integrity of the monolayer was determined by transepithelial electrical resistance (TEER) (>400 Ω/cm^2) and inhibited diffusion of 3000 MW dextran Texas Red across the monolayer. Once the monolayer was determined to be intact, the cells were incubated for 30

minutes at 37^{o}C with a primary mouse antibody against AREG in the BL compartment only. This provided the antibody access to only the AREG on the BL surface and ample time for the antibody bound AREG to be endocytosed and transit through the recycling endosomes back to the cell surface. The cells were then washed and incubated for 10 minutes at room temperature with two separate secondary antibodies, anti-mouse-Cy5 on the apical surface only and anti-mouse-Alexa488 on the BL surface only. The LLC-PK1::μ1A cells, which lack AP-1B, had recycled AREG bound with the primary antibody to the apical surface in 80% of cells with positive BL staining for AREG (Figure 13A). The LLC-PK1::μ1B cells restricted the AREG primary antibody to the BL surface in 65% of AREG positive cells (Figure 13B). These data support our hypothesis that AREG is endocytosed from the BL surface and inappropriately recycled to the apical surface in AP-1B deficient cells.

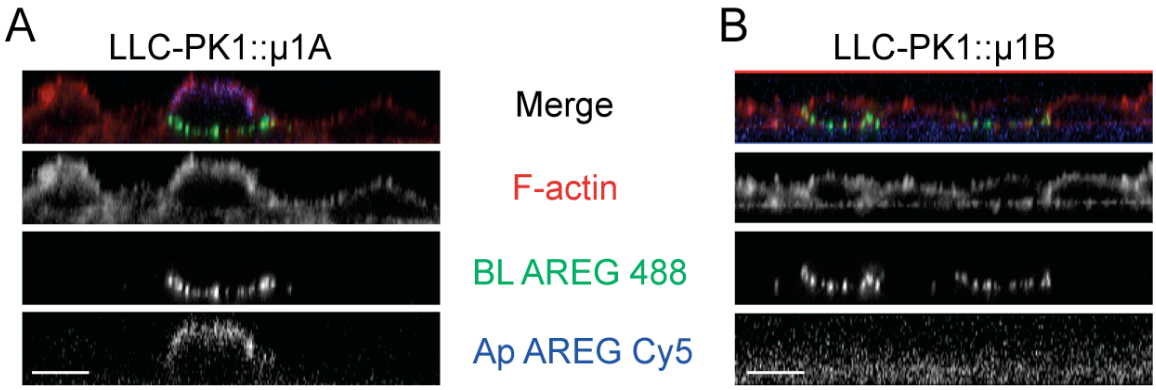

Figure 13. BL labeled AREG appears at Ap surface of μ1B-deficient LLC-PK1 cells. AREG primary antibody was added only to the BL compartment of polarized LLC-PK1 cells stably expressing μ1A or μ1B and incubated at 37°C for 30 minutes. Cells were washed and then selectively incubated with Alexa488-conjugated secondary antibody in the BL compartment and Cy5-conjugated secondary antibody in the Ap compartment for 10 min at RT. (A) BL primary antibody-bound AREG was detected at the Ap surface of LLC-PK1 cells that lack μ1B using a Cy5 secondary antibody. This occurred in 80% of the cells with BL Alexa488 secondary antibody staining (n=100). (B) LLC-PK1 cells that express μ1B retained the primary antibody bound to AREG on the BL surface in 65% of cells with BL Alexa488 secondary antibody staining (n=93). The individual channels of the X-Z axis are displayed. Bar, 10 μm.

Discussion

Our earlier work demonstrated the importance of the cytoplasmic domain for polar distribution of AREG (Brown et al., 2001). The present study extends those observations to show that the AREG cytoplasmic domain contains a dominant-acting BL sorting motif consisting of a mono-leucine preceded by an acidic cluster and show that the adaptor protein, AP-1B, is necessary to maintain the proper polar distribution of AREG.

The 31-amino acid cytoplasmic domain of AREG is 35% identical across species (Figure 7). Using cytoplasmic domain truncation mutants, we identified that amino acids 236-246 contain essential information needed for the polarized distribution of AREG. These amino acids constitute the most conserved region of the cytoplasmic domain that is 73% identical and 91% similar across species (Figure 7). In the 14 aa truncation mutant, the remaining amino acids in this region are only 14% identical across species. Removal of this region (4 aa) did not significantly disrupt the polarized distribution of AREG (Figure 10C). However, we cannot rule out the possibility that additional information within this juxtamembrane region contributes to the steady state BL localization of AREG. We previously reported that the juxtamembrane region of TGFα was sufficient to maintain its BL distribution (Dempsey et al., 2003). There are similarities between the amino acid composition of the AREG (QLRR**Q**Y**VRK**) and TGFα (HCC**QVRK**H) juxtamembrane regions. However, in contrast to TGFα, the presence of this region alone in AREG does not maintain polar distribution (Figure 10) (Dempsey et al., 2003). Also unlike TGFα, AREG BL delivery is not

dependent on NKD2, which, in part, binds the juxtamembrane region of TGFα (Li et al., 2004a). The AREG juxtamembrane region does contain tyrosine residues at positions 227 and 231. Since tyrosine residues are established constituents of BL sorting motifs (Bonifacino and Traub, 2003; Carmosino et al., 2010), we mutated these tyrosine residues individually and together to alanine residues, but no change in AREG polarity was observed (Table 2). In addition, we confirmed that removal of all but 4-amino acids from the cytoplasmic domain still resulted in 35% of total surface AREG being distributed to the BL surface (Brown et al., 2001). We believe this indicates the absence of an apical sorting determinant within the ectodomain of AREG.

Canonical BL sorting motifs (YXXΦ, FXNPXY, [DE]XXXL[LI]) (Bonifacino and Traub, 2003; Rodriguez-Boulan and Musch, 2005) are not present within amino acids 236-246 (EERKKLRQENG) of AREG. However, a less well-characterized BL sorting motif consisting of a mono-leucine is present. The consensus motif for a mono-leucine BL sorting signal consists of a single leucine five residues C-terminal to an acidic cluster (EEDXXXXXL) and is present in the only other two proteins identified to contain mono-leucine BL sorting motifs, CD147 and SCF (Deora et al., 2004; Gonzalez and Rodriguez-Boulan, 2009; Wehrle-Haller and Imhof, 2001). Although AREG does not contain this exact consensus motif, it does contain a mono-leucine C-terminal to an acidic cluster (EEXXXL). The AREG BL sorting motif differs from CD147 not only in the consensus motif, but also in its dominance over the NGFR apical sorting determinant. CD147 and SCF can both redirect the apical reporter Tac to the BL

surface, but CD147 is incapable of redirecting NGFR to the BL surface (Castorino et al., 2010; Deora et al., 2004; Wehrle-Haller and Imhof, 2001). CD147 also has a much more pronounced apical distribution compared to AREG after mutation of the mono-leucine, with 80% of L252A CD147 distributed apically compared to 45% of L241A AREG (Figure 11C) (Deora et al., 2004). This may indicate additional BL sorting information is present in the AREG cytoplasmic domain, although removal of the AREG cytoplasmic domain results in only 65% apical distribution (Figure 10C). Also, removal of the AREG cytoplasmic domain does not result in a statistically significant difference in apical distribution compared to the 59% apical distribution of the complete mono-leucine motif mutant (EEAA/LA) (Figure 11C). Another commonality between SCF and CD147 is their formation of homo- and heterodimers, respectively. SCF homodimerization is necessary for efficient surface expression while CD147 heterodimerization with the proton- coupled monocarboxylate transporter 1 (MCT1) directs the localization of MCT1 (Castorino et al., 2010; Paulhe et al., 2009). It is unknown if AREG dimerizes.

The dependence on AP-1B for proper localization of AREG also differentiates AREG from CD147, which is delivered to the BL surface in both LLC-PK1 cells and μ1B knockdown MDCK cells (Castorino et al., 2010; Deora et al., 2004). We have demonstrated a dependence on AP-1B for the polar distribution of AREG (Figure 12) and future studies will seek to identify the motif recognized by AP-1B. Currently, μ1B is thought to mainly interact with tyrosine-based sorting motifs (Carmosino et al., 2010; Fields et al., 2007; Folsch, 2005).

However, mutation of the only two tyrosine residues in the AREG cytoplasmic domain does not disrupt AREG BL distribution in MDCK cells (Table 2). Since knockdown of μ1B in MDCK cells disrupts AREG polarity, mutation of the sorting motif recognized by AP-1B should also disrupt AREG polarity in MDCK cells. AREG may be interacting with AP-1B through a linker/adaptor protein, as has been recently reported for LDL receptor and the autosomal recessive hypercholesterolemia protein (ARH) (Kang and Folsch, 2011). In the case of LDL receptor, ARH interacts with the proximal FXNPXY motif in the LDL receptor cytoplasmic domain (Traub, 2009). Extensive efforts by our group have yet to identify and confirm an interacting protein for the AREG cytoplasmic domain. An alternative explanation may be that the tyrosine residues are involved in endocytosis of AREG and mutation of these residues prevents post-endocytic AREG from reaching recycling endosomes where missorting to the apical membrane can occur in AP-1B-deficient cells (Figure 13). However, the AREG tyrosine motifs do not resemble the well-characterized NPXY internalization motif or the YXXΦ motif demonstrated to interact with the medium subunit, μ2, of AP-2 (Chen et al., 1990; Matter et al., 1994; Ohno et al., 1995; Owen and Evans, 1998). AREG does contain a YXXXXEE motif, similar to the proximal BL sorting motif in LDL receptor, but mutation of the acidic residues in the LDL receptor motif did not affect endocytosis (Matter et al., 1994). Mutation of the tyrosine in the LDL receptor proximal motif results in apical distribution of truncated LDL receptor (Matter et al., 1992), while the Y231A mutation in AREG did not affect BL delivery. Also, if this YXXXXEE motif in AREG acts as a BL signal, we would

expect the L241A mutant to maintain polar BL distribution, as is the case if only one BL motif in LDLR is mutated (Matter et al., 1992). Future work to determine the critical residues involved in AREG endocytosis and identification of interacting proteins for the cytoplasmic domain of AREG will address these questions.

Although polar distribution of AREG is AP-1B-dependent, some AREG is still delivered to the BL surface in AP-1B-deficient cells and subsequently delivered to the apical membrane after internalization (Figure 12 and Figure 13). This suggests a role for AP-1B in the recycling of AREG and not in the biosynthetic delivery in fully polarized MDCK cells, as previous studies have demonstrated for LDL receptor, transferrin receptor, and CAR (Cancino et al., 2007; Diaz et al., 2009; Gonzalez and Rodriguez-Boulan, 2009; Gravotta et al., 2007). These previous studies demonstrated an AP-1B-independent biosynthetic route for transferrin receptor in fully polarized cells, but also showed an AP-1B-dependent trans-endosomal biosynthetic route in recently confluent MDCK cells (Gravotta et al., 2007). It should be noted that all our experiments were performed on fully polarized cells. To investigate the possibility of AP-1B affecting AREG polar distribution in a recycling capacity, we performed an antibody binding and transcytosis assay in LLC-PK1::μ1A and LLC-PK1::μ1B cells transfected with AREG. Because the integrity of the monolayer is important in this type of assay and LLC-PK1 cells have notoriously incomplete monolayers, we used stringent criteria to validate the monolayer was fully intact, performing the assay only on monolayers that prevented the diffusion of a molecule 50 times

smaller than mouse IgG (3000 MW dextran Texas Red) across the monolayer. Our results support the hypothesis that post-endocytic AREG is missorted to the apical surface in AP-1B-deficient cells (Figure 13), as has been shown for CAR (Diaz et al., 2009). Future work will determine the biosynthetic route taken by AREG to the BL surface and the adaptor protein(s) involved.

The main focus of this study was to identify the components necessary for the polarized distribution of AREG. We have demonstrated the presence of a dominant-acting BL sorting motif in the cytoplasmic domain of AREG that consists of a mono-leucine and an acidic cluster (EEXXXL). This motif differs from previously described mono-leucine motifs. We have also revealed a role for AP-1B in the maintenance of AREG polarity. However, additional studies are needed to identify the AREG biosynthetic route, adaptor proteins in the biosynthetic route, and the motif recognized by AP-1B within the AREG cytoplasmic domain.

CHAPTER III

AREG IN EXOSOMES

Introduction

Exosomes are nano-vesicles (40-100 nm in diameter) produced by intralumenal budding into multivesicular bodies (MVB) and are released from most cell types after fusion of the MVB with the plasma membrane (Simons and Raposo, 2009). Our initial understanding of how cells communicated with each other was via the exchange of individual proteins like neurotransmitters, hormones, or receptor ligands. Exosomes provide an additional method of communication that facilitates the transfer of large amounts of information in one vehicle. The protein composition of exosomes is dependent on the donor cell and can relay “quanta” of information instead of just one piece of information contained in a single protein such as a receptor ligand. The diversity of information in exosomes makes them valuable tools in intercellular communication.

The definition of exosomes is an area of debate because of the variety of vesicles released from the cell into the extracellular milieu. Extracellular vesicles include exosomes and microvesicles (aka microparticles) and are classified by size, method of origin, and protein composition. Microvesicles are heterogeneous cytoplasmic protrusions that shed from the cell surface into the extracellular space and range in size from 100-200 nm in diameter. How proteins are sorted

into these protrusions is unclear, but the process is regulated and can be stimulated by Ca^{2+} and application of phorbol esters (Cocucci et al., 2009). While the content of microvesicles is dependent on the donor cell, integrins and metalloproteases are common constituents of shed microvesicles (Cocucci et al., 2009). The functions of microvesicles indentified to date include important roles in coagulation and inflammation (Ardoin et al., 2007; Falati et al., 2003). The importance of microvesicles will become more apparent as we learn more about how their content and shedding is regulated.

Exosomes are smaller and uniform in size, ranging between 40-100 nm in diameter. Exosomes originate from endosomes through the formation of intralumenal vesicles (ILV) within a late endosome, forming a MVB (Denzer et al., 2000). Exosomes are enriched in ILV proteins, supporting the origin of exosomes from MVBs (Simons and Raposo, 2009). A MVB can take two pathways, fusion with a lysosome and degradation of the lipids and proteins contained within the ILVs, or fusion with the cell surface to release the ILVs as exosomes. The regulation of what causes a MVB to fuse with the lysosome or fuse with the cell surface to release exosomes is unclear.

The mechanism by which an ILV is formed may provide a level of regulation that determines if the ILV is degraded in the lysosome or secreted as an exosome. ILV biogenesis for lysosomal degradation has been shown to involve the ESCRT (endosomal sorting complex required for transport) machinery, which recognizes ubiquitylated proteins and clusters them into ILVs destined for the lysosome (Hurley, 2008). The presence of ESCRT and

ubiquitylated proteins in exosomes suggests a possible role for the ESCRT machinery in exosome biogenesis (Simons and Raposo, 2009). However, more recent studies have demonstrated certain proteins are still present in exosomes in the absence of ESCRT machinery, but instead require the sphingolipid ceramide (Trajkovic et al., 2008). Ceramide is enriched in exosomes and is formed by sphingomyelinases, inhibition of which can reduce the release of exosomes (Trajkovic et al., 2008). A possible ESCRT-independent model for ILV biogenesis involves the formation of lipid microdomains enriched in sphingolipids, which are converted to ceramide by sphingomyelinases. The structure of ceramide, clustered in the microdomain, induces the inward curvature of the endosomal membrane to form ILVs (Trajkovic et al., 2008). Proteins that are not clustered by the ESCRT machinery may cluster within these lipid microdomains and become enriched in exosomes. This would be one level of regulation to generate two populations of ILVs within a single MVB.

Just as there are different endosomes with distinct protein and lipid compositions, the formation of different MVB subpopulations may be another method to regulate the destination of ILVs (Simons and Raposo, 2009). The enrichment of certain lipids within a particular organelle membrane allows for the recruitment of specific proteins, such as phosphatidylinositol 3,4,5-trisphosphate [PI(3,4,5)P3] enrichment at the recycling endosome enhances recruitment of AP-1B (Fields et al., 2010). Enrichment of particular phosphoinositides along with sphingolipids in a population of MVBs may create a distinct population of MVBs that produce exosomes. One membrane component already demonstrated to

differentiate distinct populations of MVBs is cholesterol, which in B lymphocytes is present in one population of MVBs but absent in another (Mobius et al., 2002). Different subpopulations of MVBs have been observed in the tumor cell line HEp2 (White et al., 2006). Analysis of EGF stimulated EGFR and the late endosomal/lysosomal marker lyso-bisphosphatidic acid (LBPA) in HEp2 cells revealed two distinct populations of MVBs. After stimulation with EGF, the EGFR and LBPA were detected in distinct MVBs well past the time in which EGFR is reported to be localized in the lysosome (White et al., 2006). This phenomenon with EGFR and LBPA was observed in numerous cell lines indicating it may be a common occurrence. EGFR is detected in exosomes, and EGF stimulates EGFR positive exosome secretion (Sanderson et al., 2008). It may be possible the EGFR positive, LBPA negative, MVB subpopulation is a distinct MVB population destined for fusion with the cell surface. Comparison of the ILV protein compositions within these two MVB subpopulations with the protein composition of exosomes may provide evidence of an exosomal MVB population.

Ubiquitylation, addition of the 76-amino acid globular protein ubiquitin to a lysine residue, is a reversible post-translational modification that can mark a protein for a variety of purposes, including delivery to a MVB. Ubiquitin can be added to a single lysine residue on a protein for monoubiquitylation or to multiple lysine residues on a single protein for polyubiquitylation. Ubiquitin contains seven lysine residues itself where additional ubiquitins can be added (K11, K28, K48 and K63) to form a multi-ubiquitin chain (Weissman, 2001). The structure of the final ubiquitin tag depends on which lysine on ubiquitin is modified and the

number of ubiquitins added. A multi-ubiquitin chain of four or more ubiquitins on a membrane protein typically results in protein degradation, whereas a monoubiquitylation results in endocytosis (Hicke, 2001).

Monoubiquitylation and K63 multi-ubiquitylation can target a membrane protein to the MVB (Lauwers et al., 2009; Urbanowski and Piper, 2001). The role of ubiquitin in protein delivery to exosomes is unclear, although ubiquitylated proteins are present in exosomes (Buschow et al., 2005). It has been proposed that ubiquitin is removed from proteins targeted for degradation to prevent depletion of ubiquitin from the cell (Swaminathan et al., 1999). Since ubiquitylated proteins are present in exosomes, ubiquitin may function to first mark a protein for delivery to the MVB and secondly mark the protein for sorting into exosomes, while deubiquitylated proteins are sorted for degradation. Another possibility is modification of the ubiquitin chain at the MVB (Raiborg and Stenmark, 2009). In this model one form of ubiquitin could mark the protein for delivery to the MVB and be removed at the MVB. Then a different ubiquitin chain could be added to mark the protein for sorting into an exosome. Further understanding of how an exosome is differentiated from an ILV destined for degradation may reveal a role for ubiquitin.

The role of exosomes in cell signaling is still being unraveled. Our recent publication on exosomal signaling reveals a new mode of EGFR signaling through exosomes (Higginbotham et al., 2011). This study was the first to demonstrate the presence of biologically active EGFR ligands in exosomes. Exosomes containing EGFR ligands stimulate cellular invasion through Matrigel,

with AREG-containing exosomes inducing four fold higher rates of invasion than TGFα or HB-EGF exosomes. Colorectal cancer (CRC) cell lines containing mutant KRAS produce exosomes with increased amounts of AREG and increased invasiveness of recipient cells compared to CRC cell lines with wild-type KRAS. This difference in exosomal composition and function between cells with or without mutant KRAS could contribute to such diverse cancer phenomena as field effect and priming the metastatic niche.

Our analysis of exosomes began with the observation by Ada Braun that full-length HB-EGF was present in cell culture conditioned medium. Isolation of exosomes from conditioned medium and analysis by sucrose gradient fractionation confirmed the presence of HB-EGF in exosome abundant fractions. Using fluorescence-activated vesicle sorting (FAVS), an approach developed for purifying small (<100 nm) vesicles, we confirmed the presence of HB-EGF, TGFα, and AREG in exosomes (Cao et al., 2008b; Higginbotham et al., 2011). FAVS recognizes the extracellular domains of these EGFR ligands, indicating the topology of the ligands was such that the receptor binding domains were present on the outside of the exosome. However, the presence of a heparin-binding domain in AREG and HB-EGF would allow for cleaved soluble ligand to be present on an exosome and detected by FAVs. To determine whether full-length AREG is present in exosomes, I performed western blotting analysis on exosome preparations. Analysis of the western blots revealed the presence of post-translational modified forms of AREG not seen in regular whole cell lysate or immunoprecipitation (IP) western blots. Suspecting this post-translational

modification to be ubiquitin, I demonstrated with HA-tagged ubiquitin that AREG could be ubiquitylated. However, I was unable to detect endogenous ubiquitin on AREG in lysates or exosomes. To determine if ubiquitylation was necessary for delivery of AREG to exosomes, I generated a mutant form of AREG (AREG-K2A) that does not contain any lysine residues within the cytoplasmic domain. Western blotting analysis of exosomes from MDCK cells expressing wild-type AREG or the lysine mutant AREG-K2A showed a reduction of AREG in the AREG-K2A mutant compared to wild-type, suggesting a role for ubiquitylation in AREG delivery to exosomes. These data provide a strong foundation for future work to determine how AREG is delivered to exosomes.

Materials and Methods

Generation of AREG-K2A Mutant

The following quick change primers were designed to change K239 and K240 to alanine residues:

KK to AA fw QC (oligo# 37516386-010)

5'-ggagaagccgaggaacgaGCgGCacttcgacaagagaatgg-3'

KK to AA rv QC (oligo# 37516386-020)

5'-ccattctcttgtcgaagtGCcGCtcgttcctcggcttctcc-3'

QC PCR mixture: AREG-pCB6 template at 15ng/µl = 30ng; 5µl 10x Pfu Turbo Buffer; 1µl 10mM DNTPs; 1.25 µl at 100ng/µl (125ng final) KK to AA fw QC primer; 1.25 µl at 100ng/µl (125ng final) KK to AA rv QC primer; 38.5 µl H2O; 1µl Pfu Turbo enzyme.

PCR Cycles: 95^{o}C 3 min; 95^{o}C 30 sec; 55^{o}C 1 min; 68^{o}C 7 min 30 sec; 17 cycles; 68^{o}C 10 min; 4^{o}C Hold.

1µl of DpnI enzyme was added to the reaction and incubated at 37^{o}C for 45 min. 5µl was transformed into DH5α cells and plated on ampicillin (amp) plates. Two colonies from the transformation were picked and grown in amp medium overnight. The minipreps were sequenced and clone #1 was determined to be correct. 072407 pCB6 KK2AA ART clone #1 is correct.

The following quick change primers were used to change K-230 to alanine.

K230A QC Fw primer: 5' GACAATACGTCAGGgcATATGAAGGAGAAGC 3'

K230A QC Rv primer: 5' GCTTCTCCTTCATATgcCCTGACGTATTGTC 3'

The template used was the pCB6 KK2AA ART mutant. This quick change removes all lysine residues from the AREG cytoplasmic domain.

QC PCR reaction mixture: 3.3µl template = 50ng; 5µl 10x Pfu Buffer; 1µl 25mM DNTPs; 1.25µl Fw primer at 100ng/µl; 1.25µl Rv primer at 100ng/µl; 37.2µl H2O; 1µl Pfu turbo

PCR cycles: 95^{o}C 3min; 95^{o}C 30 sec; 53^{oC} 30 sec; 68^{o}C 8min; 20 cycles; 68^{o}C 10min; 4^{o}C Hold

The entire PCR reaction was digested with 1µl Dpn1 at 37^{o}C for 4 hrs.

Four µl of the digested reaction was transformed into 50µl DH5α competent cells and plated on an amp plate. The following day 6 colonies were collected from the plate and minipreped. All of the minipreps were sequenced. Miniprep #2 was analyzed four ways, pCB6FW, pCB6RV, ARIFW, ARIRV (internal primers for AREG), all indicating it is correct. pCB6 K230A mini #2 082309 is correct**.**

Isolation of Exosomes

Exosomes were isolated by James Higginbotham (Higginbotham et al., 2011). Native and ionomycin elicited exosome pellets were subjected to sucrose gradient fractionation as described previously (Sanderson et al., 2008; Thery et al., 2006).

Fluorescence-Activated Vesicle Sorting (FAVS)

All FAVS was performed by James Higginbotham and previously described (Cao et al., 2008b).

Amphiregulin Western Blot of Cell Lysates and Exosome Preparations.

Cells were resuspended in 1% NP-40 lysis buffer (50mM Tris-HCl pH 8.0, 150mM NaCl, 1% NP40, 2mM EDTA, and protease inhibitor cocktail Sigma P2714) and incubated for 30 min at room temperature (RT). Lysates were centrifuged at 20,000xg for 15 min at 4^{o}C and supernatants were transferred to fresh tubes. Prior to use, protein concentrations of each lysate were determined with a MicroBCA protein reagent kit (Pierce, Rockford, USA). A 12.5% SDS PAGE gel was used to separate cell lysate or exosomal preparations (10µg total) under non-reducing conditions. After separation, samples were transferred at 4^{o}C overnight at 50mA to nitrocellulose membranes (0.2 µm, Whatman Optitran BA-S 83). Membranes were rinsed 3x in PBS-T (1xPBS 0.05% Tween 20) and blocked overnight at 4^{o}C in 5% milk PBS-T. Subsequent steps were performed at RT. Membranes were probed with the anti-AREG mouse monoclonal antibody 6R1C2.4 at 2µg/ml in 5% milk PBS-T for 1.5 hrs and then washed 3x in PBS-T. Membranes were incubated with secondary donkey anti-mouse IgG-HRP 1:2000, in 5% milk PBS-T for 1hr. Membranes were washed 3x in PBS-T. The ECL western blotting kit (Western Lighting plus ECL, Perkin Elmer, Waltham, USA) was used as per manufacturer's instructions to visualize AREG protein bands.

HA-Ubiquitin AREG co-Transfection, AREG IP, anti-HA Western Blot

293T cells were plated at a cell density of 500,000 cells/well in a six well dish and transfected the following day with wild-type AREG alone, HA-ubiquitin alone, wild-type AREG and HA-ubiquitin together, or AREG K2A and HA-ubiquitin

together. Two days following transfection, the cells were washed 3x with cold 1xPBS. The cells were lysed for 1hr on the 4°C shaker in 500µl 1%NP-40 lysis buffer with protease inhibitor (same as above). Lysates were kept cold during the entire protocol. The lysates were centrifuged in the tabletop centrifuge at max speed at 4°C for 15 min. The supernatants were transferred to fresh tubes containing 20µl of a 50% slurry of recombinant protein G agarose beads (Invitrogen Catalog no. 15920-010) to pre-clear the lysates. Lysates were cleared for 1.5hrs. The protein concentration of each sample was determined using the MicroBCA protein reagent kit and equal amounts of protein were transferred to fresh tubes. 20µl of the AREG-K2A + HA-ubiquitin cleared lysate was removed and set aside for a western blot positive control. 50µl of 6R1C2.4 (≈2.5µg) was added to each lysate and rotated in the cold room overnight. 20µl of a 50% slurry of recombinant protein G agarose beads was added and incubated on the cold room rocker for 4 hrs to IP AREG. The beads were gently centrifuged and washed 5x with 1ml lysis buffer. After the last wash as much lysis buffer as possible was removed using a loading tip and 20µl 1x sample buffer without DTT was added (2x sample buffer = 125mMTris-HCl pH6.8, 2%Glycerol, 4%SDS (w/v), 0.05% bromophenol blue). The positive control sample had equal volume 2x sample buffer without DTT added. The samples were heated for 5min at 72°C then stored at RT until ready to run gel. The proteins were separated by a 7.5% SDS PAGE gel at 80v until the dye front reached the bottom of the gel. The samples were transferred to a nitrocellulose membrane at 18v overnight in the cold room. After removing the membrane from the transfer apparatus, the top

was immediately cut off at the 130 kDa mark to remove any antibody at the top of the membrane. The membrane was washed with 1xTBS 0.05% Tween then blocked with 1xTBS pH8 0.05% Tween 5% milk (TBS blocking buffer) overnight in the cold room. The next day, the membrane was blotted with mouse anti-HA antibody (Clone HA-7 Sigma H 9658) diluted 1:1000 in TBS blocking buffer for 2 hrs at RT. The membrane was washed for 1.5 hrs with multiple changes of 1xTBS 0.05% Tween. The membrane was blotted with Mouse TrueBlot® ULTRA: Anti-Mouse Ig HRP (eBiosciences 18-8817) diluted 1:1000 in TBS blocking buffer for 1.5 hrs at RT. Subsequently, the membrane was washed for 1 hr with multiple changes of 1xTBS 0.05% Tween. The ECL chemiluminescent reagent was added for 1 min and the blot was exposed to film for 1 min, 3 min and overnight (max).

HA Blot of Exosome Preparations

Exosomes were collected from MDCK cells expressing either HB-EGF or AREG-HA. 30µg of each exosome preparation was diluted 1:1 with 2x sample buffer, without DTT, and heated at 95^{o}C for 5 min. The samples remained at RT for a few days before being run. Half of each exosome preparartion (15µg) was run on a 4-20% gradient gel until the dye front reached the bottom of the gel. The samples were transferred to a nitrocellulose membrane overnight. The PBS used in this protocol was a premade bottle purchased from Sigma. The membrane was blocked overnight in the cold room with 5% milk in 1xPBS. The remaining steps were all performed at RT. The membrane was washed 3x 5 min with

1xPBS 0.05% Tween then blocked for 10 min with 1xPBS 1% BSA. The membrane was blotted with the primary anti-HA antibody (Clone HA-7 Sigma H 9658) diluted 1:1000 in 1xPBS 1%BSA 0.05% Tween for 2.5 hrs. Our antibody stocks are already diluted 1:10; therefore, I diluted 1:100 to get a final 1:1000 dilution. The membrane was washed 3x 15 min with 1xPBS 0.05% Tween. The membrane was blotted with secondary donkey anti-mouse HRP-conjugated antibody diluted 1:2000 in 1xPBS 0.05% Tween for 1 hr. The membrane was washed 3x 5 min with 1xPBS 0.05% Tween. ECL chemiluminescent reagent was added for 1 min and film was exposed for 1 min, 5 min, and overnight (max).

Results

AREG is present in exosomes with the extracellular domain on the outside of the exosome.

The observation by Ada Braun that full-length HB-EGF is present in the conditioned medium of MDA-MB-231 breast cancer cells raised the possibility that EGFR ligands are present in exosomes. To address this possibility, exosomes were isolated from the conditioned medium of MDA-MB-231 cells and the CRC cell line HCA-7 cells. FAVS revealed the presence of HB-EGF and TGFα in MDA-MB-231 and HCA-7 exosomes, while AREG was detected only in HCA-7 exosomes (Higginbotham et al., 2011). It should be noted that HCA-7 cells endogenously express very high amounts of AREG (Damstrup et al., 1999). Detection of these ligands by FAVS indicates the topology of the ligand displays the extracellular domain on the outside of the exosome. To confirm this is the only topology of AREG in exosomes we used an MDCK cell line expressing AREG fused to a HA-tag on the cytoplasmic domain (AREG-HA) as a negative control. Analysis by FAVS revealed the exosomes were positive for the extracellular domain of AREG but negative for HA on the cytoplasmic domain. Western blot analysis for HA confirmed the HA-tag was present; demonstrating the HA-tagged cytoplasmic domain of AREG is inside of the exosome (Figure 14). These experiments established the presence of AREG in exosomes with a topology displaying the receptor-binding domain on the outside of the exosome.

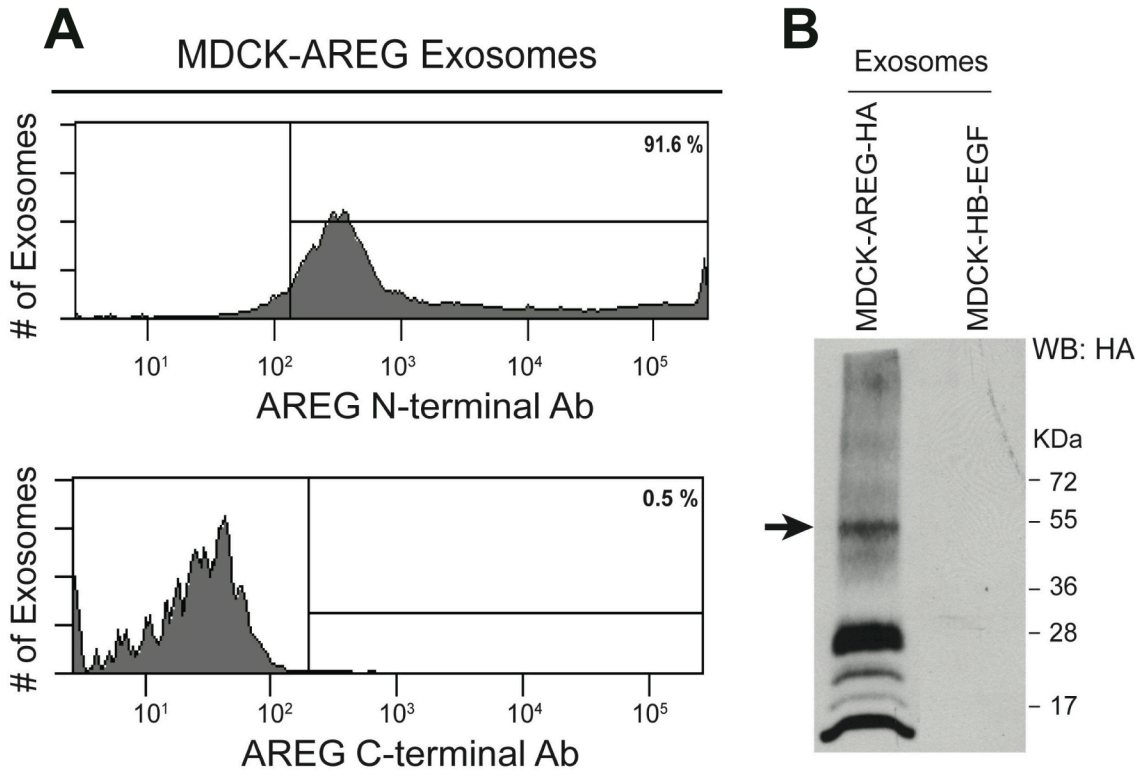

Figure 14. **AREG is present in exosomes with a signaling competent topology.**
To confirm the presence of AREG in exosomes we used FAVS to detect and quantitate AREG-containing exosomes. Exosomes were isolated from MDCK cells expressing AREG-HA. A) Mouse anti-AREG, 6R1C2.4 (AREG N-terminal Ab), which recognizes the EGF-like motif in AREG was used to detect the extracellular domain on the outside of the exosomes. Mouse anti-HA (AREG C-terminal Ab) was used to detect the HA-tag on the cytoplasmic domain of AREG. The histograms demonstrate the N-terminal extracellular domain is present on the outside of the exosome while the C-terminal cytoplasmic domain is inside the exosome, inaccessible to the anti-HA antibody. B) Western blot analysis for HA confirms the presence of membrane-bound AREG-HA within exosomes. The arrow marks full-length AREG-HA while the lower bands are processed forms of AREG that are still integrated into the membrane. The smear suggests some form of post-translational modification, which is detected with the anti-HA antibody and the anti-AREG antibody. HB-EGF exosomes were used as a negative control for the anti-HA blot.

AREG is enriched in exosomes derived from donor cells containing mutant forms of KRAS.

Having established the presence of signaling competent AREG in exosomes we contemplated the clinical relevance of this discovery. If EGFR ligands are present in exosomes released from transformed cancer cells, do non-transformed cells also release exosomes? To address this question, we used isogenically matched cell lines, DLD-1, DKO-1, and DKs-8 cells (Shirasawa et al., 1993). These three lines were derived from the transformed CRC line DLD-1, which contains one copy of wild-type KRAS and one copy of mutant active KRAS. Using homologous recombination, the wild-type copy was removed to generate DKO-1 cells or the mutant copy was removed to generate DKs-8 cells. The resulting cell lines are isogenic for all other genes except KRAS for which DLD-1 cells contain one wild-type copy and one mutant copy, DKO-1 cells only contain a mutant copy, and DKs-8 cells only contain a wild-type copy (Shirasawa et al., 1993). Having lost the mutant copy, DKs-8 cells are no longer transformed and do not grow in soft agar or nude mice. DLD-1 and DKO-1 cells are transformed and grow in both soft agar and nude mice (Shirasawa et al., 1993).

Exosomes were isolated from the conditioned medium of the isogenic cell lines and compared with lysates of each line by ELISA and western blot. ELISA was used to quantitate the amount of AREG present in the lysates and exosomes. The results revealed AREG was enriched in the exosomes of all three lines compared to the matched lysates. AREG was enriched in DKO-1 exosomes 4-fold compared to lysate, while DLD-1 and DKs-8 cells had 3-fold more AREG in

exosomes compared to lysates (Figure 15C). The cells with mutant KRAS had considerably more AREG present than DKs-8 cells that only express wild-type KRAS. These results suggests mutant KRAS not only increases the overall expression of AREG, but also increases the amount of AREG loaded into exosomes to be released into the surrounding extracellular space.

ELISA is an excellent quantitative technique that uses the anti-AREG antibody 6R1C2.4, which recognizes an epitope in the EGF-like domain within the mature ligand. This is why the antibody does not recognize the reduced forms of AREG; the di-cysteine bonds that make up the EGF-like motif are necessary for the structure of the epitope. This also allows the antibody to recognize all the membrane and soluble forms of AREG. Because the antibody recognizes all forms of AREG that contain the EGF-like motif, quantitative techniques like FAVS and ELISA that use this antibody provide solid data for quantification of total AREG, but not valuable information on which forms of AREG are present. Only western blotting analysis provides data on the relative abundance of different soluble or membrane forms of AREG.

In order to confirm the presence of membrane AREG and not soluble AREG in exosomes a western blotting analysis was performed on exosomes isolated from the conditioned medium of DLD-1, DKO-1, and DKs-8 cells (Figure 15B). Western blotting analysis confirmed the presence of membrane-bound forms of AREG, and not soluble AREG in the exosomes. The western blots also supported the ELISA data demonstrating increasing amounts of AREG in exosomes derived from cells with mutant KRAS. Interestingly, the most

prominent forms of AREG in the exosomes are the 26 kDa and 28 kDa processed forms. While the lysates appear to have similar levels of the full-length 50 kDa and 26-28 kDa forms (Figure 15A), exosomes have considerably more 26-28 kDa AREG (Figure 15B). (Forms referred to as 26 kDa and 28 kDa were initially described by Brown et al. as 26 kDa and 28 kDa, but run as a doublet below 25 kDa in my blots. This may be the result of running the samples under non-reduced conditions compared to reduced as done by Brown (Brown et al., 1998). These forms run below 25 kDa in lysates as well and I have confirmed them to be membrane forms. See Appendix B for a detailed explaination).

Even more interesting is the presence of the smear detected in exosomes and not in lysates. A smear pattern in western blots results from various sizes of the protein being created by some sort of post-translational modification and detected by the antibody. This smear increases in size, indicating it is not a result of degradation but from the addition of something to the AREG. The same smear was also detected in the HA blot in Figure 14, suggesting it is not an artifact of the AREG antibody. Since the smear is not present in lysates, it may result from the modification responsible for delivery of AREG to exosomes, possibly ubiquitin.

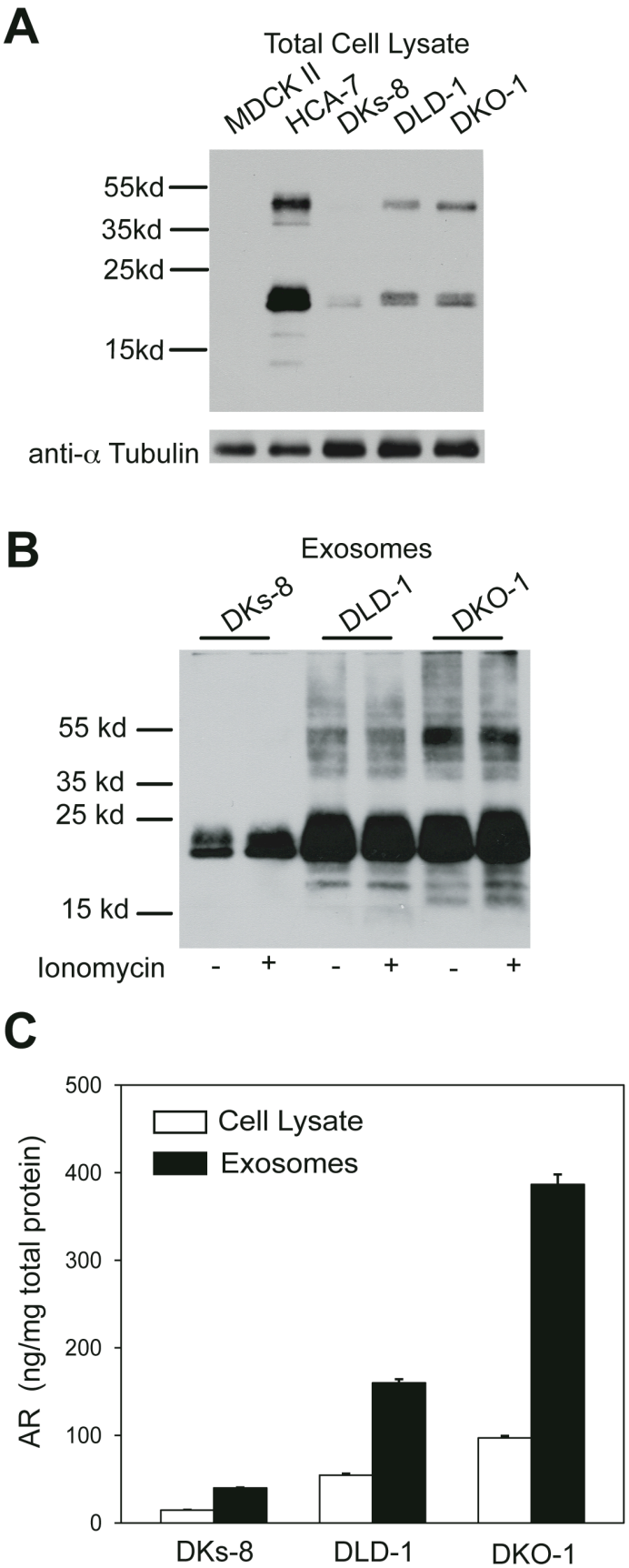
A
Total Cell Lysate
MDCK II
HCA-7
DKs-8
DLD-1
DKO-1
55kd
35kd
25kd
15kd
anti-α Tubulin
B
Exosomes
DKs-8
DLD-1
DKO-1
55 kd
35 kd
25 kd
15 kd
Ionomycin - + - + - +
C
AR (ng/mg total protein)
Cell Lysate
Exosomes
500
400
300
200
100
0
DKs-8
DLD-1
DKO-1

Figure 15. **AREG is enriched in exosomes compared to lysates, with the 26 kDa and 28 kDa processed forms being most prominent in exosomes.**
A) AREG western blot of the indicated cell lysates. 10μg of each lysate was run on a 12.5% SDS-PAGE gel, transferred to nitrocellulose and blotted for AREG using the mouse anti-AREG antibody 6R1C2.4. MDCK II cells were used as a negative control because 6R1C2.4 cannot detect canine AREG. The positive control is HCA-7 cells, a human CRC cell line that expresses high levels of endogenous AREG. DKs-8, DLD-1, and DKO-1 cells are isogenic, with the exception of their KRAS gene. B) AREG western blot of exosomes isolated from the isogenic cell lines DKs-8, DLD-1, and DKO-1. 10μg of exosomes were run on a 12.5% SDS-PAGE gel, transferred to nitrocellulose, and blotted for AREG with 6R1C2.4. These exosome preparations were collected from cells treated with or without ionomycin, which does not appear to affect the amount of AREG or the forms of AREG loaded into exosomes. C) Results from an ELISA assay quantitating the amount of AREG in cell lysates or exosomes collected from the isogenic cell lines DKs-8, DLD-1, and DKO-1 (n=3).

AREG can be ubiquitylated *in vitro*.

Analysis of the exosome AREG western blots revealed a smearing pattern not seen in previous AREG blots of total cell lysates or AREG IP samples (Figure 15B). Since the smear pattern increases in size compared to the defined sizes of AREG, I speculated that the AREG in exosomes contains a post-translational modification. Others have already demonstrated monoubiquitylation and K63 multi-ubiquitylation can target a membrane protein to the MVB (Lauwers et al., 2009; Urbanowski and Piper, 2001). It has also been shown that ubiquitylated proteins are present in exosomes (Buschow et al., 2005). This led me to investigate if the AREG contained within exosomes is ubiquitylated.

Since the smear pattern suggesting ubiquitylation is only seen in exosomes and not in cell lysates, the modified AREG appears to be enriched in exosomes. This would make exosomes a good source of material to isolate and characterize this post-translational modification. However, I was unable to IP AREG from the exosomes due to technical difficulties. I suspect due to the small size of the exosomes the detergent in my lysis buffer (1% NP-40) was unable to integrate into the exosomal lipid membrane and dissociate the proteins from the exosomes. Another possibility is that the lipid composition of the exosome may make the exosomes insoluble in 1% NP-40 lysis buffer; similar to the way different membrane lipid domains are Triton-soluble or Triton-insoluble. While I could effectively detect AREG in a total exosome preparation, I could not isolate AREG from the exosomes in order to determine if it is ubiquitylated.

I can IP AREG from cell lysates, so as an alternative approach to detect ubiquitylated AREG I attempted to detect endogenous ubiquitin on AREG isolated from cell lysates. However, detection of ubiquitin on a protein is technically challenging because ubiquitylation is such a dynamic process. Once a protein is ubiquitylated by an ubiquitin ligase, the ubiquitin can be immediately removed by a de-ubiquitylating enzyme (DUB). This requires the use of DUB inhibitors to allow for the ubiquitylated protein to be modified long enough for isolation and detection. However, inhibition of DUBs will cause the protein to be degraded more quickly, so protease inhibitors must be used as well. The protease inhibitor pepstatin A can inhibit the cathepsin proteases in the lysosome, however the protease inhibitor cocktail used in my experiments did not contain pepstatin A and may not have effectively inhibited protein degradation by the lysosome. The ubiquitin antibody is another technical challenge because it is not very robust and provides considerable background. In addition to the challenges of detecting ubiquitin, because the vast majority of AREG in the lysate is not ubiquitylated, the AREG IP protocol would need to be close to 100% efficient to isolate enough of the ubiquitylated AREG to be detected by the anti-ubiquitin antibody. Due to time constraints and all the technical difficulties needed to be overcome I was not able to detect endogenous ubiquitin on AREG.

An alternative approach to detecting endogenous ubiquitin is to use a HA-tagged form of ubiquitin. HA-tagged ubiquitin has a couple of advantages: it is not as easily removed by DUBs, and it can be detected by a robust anti-HA antibody with less background. The disadvantage of using the HA-tagged

ubiquitin is that it is an artificial system. However, HA-tagged ubiquitin is an accepted tool to demonstrate a protein can be ubiquitylated.

I used HA-tagged ubiquitin to demonstrate AREG can be ubiquitylated. Wild-type AREG contains three lysine residues within the cytoplasmic domain that can be ubiquitylated (Figure 16A). I generated a lysine-free AREG mutant (AREG-K2A) by changing all three lysine residues to alanine (Figure 16A). 293-T cells were transiently co-transfected with HA-ubiquitin and either wild-type AREG or AREG-K2A. Two days after transfection the cells were lysed, AREG was isolated by IP, run on a 7.5% SDS-PAGE gel, and transferred to nitrocellulose. The nitrocellulose membrane was blotted for HA. The anti-HA antibody did not detect the AREG-K2A mutant but did detect the wild-type AREG in a smearing pattern similar to the exosomes (Figure 16B). However, the wild-type AREG sizes were larger. The prominent bands detected below 25 kDa in exosomes were above the 25 kDa marker in the anti-HA blot. Full-length AREG runs around 50 kDa but a prominent band around 68 kDa was present in the anti-HA blot. Addition of a mono-ubiquitin to a protein results in a 9 kDa increase in size on a gel. Detection of these larger bands by the anti-HA antibody could represent the ubiquitylated AREG. These results clearly demonstrate AREG can be ubiquitylated.

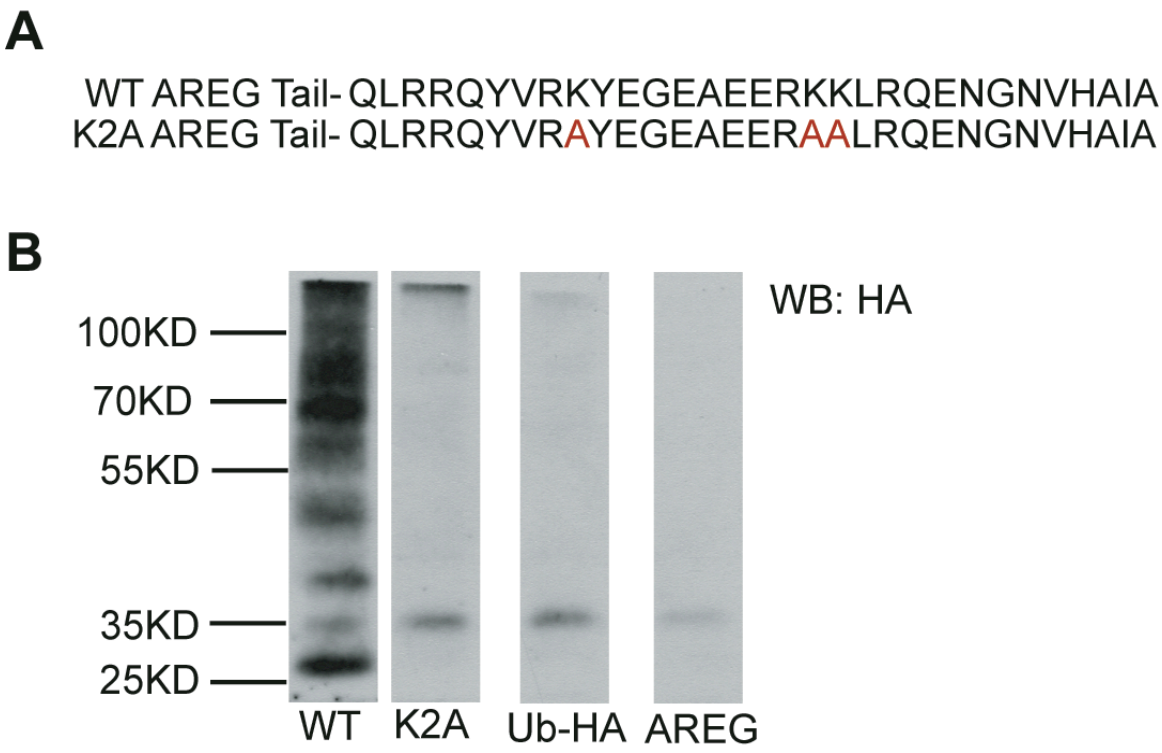

Figure 16. **AREG can be ubiquitylated by HA-tagged ubiquitin.**
A) Amino acid composition of wild-type AREG (WT) and the lysine-free AREG mutant (K2A). The alanine residues highlighted in red represent the lysine residues changed to alanine to generate the mutant. B) Western blotting analysis of 293-T cells co-transfected with HA-ubiquitin and either WT or K2A AREG. AREG was isolated by IP, run on a 7.5% SDS-PAGE gel, transferred to nitrocellulose, and blotted for HA. The Ub-HA lane represents cells transfected only with HA-ubiquitin. The AREG lane represents cells transfected only with AREG. These two controls demonstrate the anti-HA antibody is not detecting significant background. There is one 36 kDa background band present in all lanes.

Ubiquitylation is necessary for efficient delivery of AREG to exosomes.

Having established that AREG can be ubiquitylated, I next wanted to determine the role ubiquitylation plays in delivery of AREG to exosomes. Exosomes were isolated from MDCK cells expressing either wild-type AREG or the AREG-K2A mutant. An equal amount of exosomes, as determined by BCA protein concentration, was run on a 12.5% SDS-PAGE gel and transferred to nitrocellulose. The membrane was blotted for AREG to determine any differences between wild-type and K2A in the amount and forms of AREG present in exosomes. The results clearly demonstrate there is much less of the AREG-K2A present in the exosomes (Figure 17). There is a small amount of the 26-28 kDa doublet detected in the AREG-K2A sample, but not nearly as much as in the wild-type AREG exosomes. This experiment was conducted only one time but was later confirmed by Michelle Demory Beckler. Future studies will determine the overall AREG levels between the two lines to demonstrate the difference in exosomal AREG is really due to the lack of lysine residues and not because the AREG-K2A line expresses less AREG. While these results should be regarded as preliminary, they provide some foundation to the hypothesis that AREG ubiquitylation may be involved in delivery of AREG to exosomes.

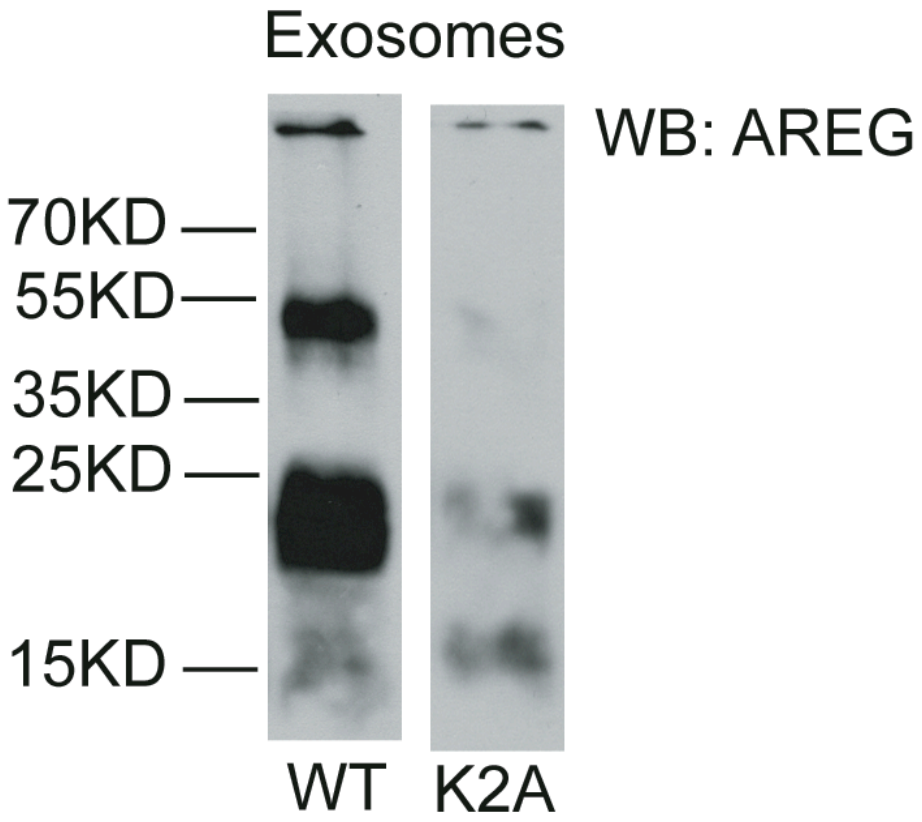

Figure 17. **AREG must be ubiquitylated to be efficiently loaded into exosomes.**
Western blotting analysis of exosomes isolated from MDCK cells expressing wild-type AREG (WT) or mutant AREG-K2A (K2A). 10μg of exosomes, as determined by BCA assay, were run on a 12.5% SDS-PAGE gel, transferred to nitrocellulose, and blotted for AREG. The AREG-K2A mutant does not contain any lysine residues within the cytoplasmic domain and cannot be ubiquitylated, possibly inhibiting its loading into exosomes.

Discussion

The data I have produced provide a solid foundation on which to build our understanding of AREG in exosomes. It is clear that full-length AREG is present in a signaling competent topology within exosomes. The most prominent forms of AREG present in exosomes are the 26-28 kDa forms. Exosomal AREG appears to contain a post-translational modification not detected on AREG isolated from total cell lysate. AREG containing this modification is enriched in exosomes indicating a role for this modification in delivery of AREG to exosomes. While I was unable to identify the modification, AREG can be ubiquitylated and lysine-free AREG is not efficiently loaded into exosomes. These data provide clues on how AREG delivery to exosomes might be regulated.

One of the questions still remaining is the route taken to the exosome by AREG. One clue to the answer of this question is the forms of AREG most prominent in exosomes. Our current understanding of AREG is that full-length glycosylated AREG runs around 50 kDa on a SDS-PAGE gel. Proper secretion of AREG from the cell requires the N-terminal pro-protein domain to shield the heparin-binding domain of AREG during exocytosis (Thorne and Plowman, 1994). Once at the cell surface, there are multiple forms of AREG present, including the full-length 50 kDa form as well as 28 kDa and 26 kDa processed forms (Brown et al., 1998). The 28 kDa and 26 kDa forms do not contain the N-terminal pro-protein domain, which if required for secretion must be removed post arrival at the cell surface. The 26 kDa and 28 kDa AREG forms are the most prominent exosomal forms of AREG. If removal of the pro-protein domain takes

place at the cell surface, then the majority of exosomal AREG must have been at the cell surface prior to arrival in the exosome. These data suggest the route to the exosome is via the cell surface.

Assuming AREG transits the cell surface prior to delivery to exosomes, what distinguishes an AREG molecule for delivery to the exosome verses cleavage or recycling back to the cell surface? Western blot analysis indicates AREG has some form of post-translational modification that could mark AREG for delivery to the exosomes. Using HA-tagged ubiquitin, I have demonstrated AREG can be ubiquitylated. However, the size of the HA-ubiquitylated AREG was larger then exosomal AREG. The size difference may result from removal of the ubiquitin prior to invagination of the ILV, while the remaining smear pattern in exosomal AREG western blots that indicates a post-translational modification may simply result from inefficient removal of the modification. Identification of the actual modification causing the smear would provide clarity on how AREG delivery to exosomes is regulated.

An alternative explanation to ubiquitin modification of AREG is sumoylation. Sumo (small ubiquitin-related modifier) proteins are added to proteins in a similar fashion as ubiquitin and can form multi-sumo chains (Geiss-Friedlander and Melchior, 2007). The smear pattern in the exosomal AREG western blots indicates addition of a protein chain and the function of multi-sumoylation chains is unknown. AREG does not contain a classical consensus sumoylation acceptor site, but does contain a similar sequence. The consensus sumoylation site is ΨKxE, where Ψ is an aliphatic branched amino acid and x is

any amino acid (Geiss-Friedlander and Melchior, 2007). The site in AREG that closely matches the consensus sumoylation site is RKYE, where the aliphatic amino acid is replaced with the basic arginine residue. If the amino acid sequence of AREG were extended it would include an acidic patch C-terminal to the possible sumoylation site (RKYEGEAEE). In addition to the classical consensus sumoylation site, acidic clusters C-terminal to the accepting lysine residue have been shown to enhance sumoylation (Yang et al., 2006). The presence of a tyrosine residue in this site is interesting because it adds an additional level of possible regulation. Analysis of this region of the AREG cytoplasmic domain may reveal critical residues in the regulation of AREG in exosomes and beyond.

The observation that mutant active KRAS increases the amount of AREG expressed in cell lysate and loaded into exosomes has clinical relevance. KRAS is downstream of EGFR activation in the EGFR signaling cascade, so cancer treatment directed against the EGFR is only effective in patients with wild-type KRAS (Peeters et al., 2009). If KRAS is active regardless of EGFR activation, blocking EGFR activation is ineffective. However, the results of mutant KRAS on increasing exosomal AREG composition may increase EGFR signaling in surrounding cells, which could affect the tumor microenvironment. The increase in exosomal AREG within the tumor microenvironment could increase inflammation and disrupt tissue homeostasis (Nishimura et al., 2008). It is possible that EGFR targeted treatment early in cancer progression could block the effect of AREG exosomes on the tumor microenvironment, possibly

preventing metastasis and increasing a patients overall survival. Unfortunately, since clinical trials are only conducted on patients who have failed to respond to standard care and have progressed disease, the effects of EGFR targeted treatment in early cancer progression cannot be observed under the current clinical trial methodology.

The role of exosomes in cancer is still to be determined. The potency of exosomal AREG on cancer cell invasion *in vitro* provides us with clues to the importance of this signaling vehicle in disease (Higginbothem J, et. al. 2011). Understanding the regulation of AREG delivery to exosomes could provide a point of attack from which to prevent aberrant EGFR signaling via exosomes. Future work on how exosomes and their cargo are regulated is critical to understanding this important cell signaling process.

CHAPTER IV

IDENTIFICATION OF AREG INTERACTING PROTEINS

Introduction

Prior to my joining the Coffey laboratory, studies were already underway to identify interacting proteins for the EGFR ligands TGFα and AREG. The goal of these studies was to identify proteins involved in the delivery of these ligands to the basolateral (BL) cell surface. Two proteins were identified to interact with TGFα: Naked2 (NKD2) and membrane associated guanylate kinase inverted-3 (MAGI-3) (Franklin et al., 2005; Li et al., 2004a). Similar studies did not elucidate AREG interacting proteins. As a consequence, a major aspect of my dissertation proposal was to identify interacting proteins for AREG.

TGFα is delivered to the BL surface of polarized epithelial cells where it is rapidly cleaved by the metalloprotease TACE and avidly bound by the EGFR (Dempsey and Coffey, 1994; Peschon et al., 1998). The cleavage of TGFα at the cell surface is so rapid that expression of a membrane-fixed form is necessary to detect the ligand on the lateral membrane by indirect immunofluorescence (Dempsey and Coffey, 1994). The released ligand is efficiently consumed by the EGFR such that soluble TGFα cannot be detected in the conditioned media without using an EGFR blocking antibody (Dempsey and Coffey, 1994). Combined, these results strongly suggest the rate-limiting step in TGFα activation of the EGFR is the delivery to the cell surface.

A yeast two-hybrid screen was performed to identify proteins that regulate the rate-limiting cell surface delivery of TGFα through interaction with the cytoplasmic domain of TGFα. The 39-amino acid TGFα cytoplasmic domain was screened against a cDNA library generated from polarized HCA-7 cells, a polarizing human CRC cell line. This screen identified the myristoylated protein NKD2, a mammalian homolog of Drosophila Naked Cuticle (Li et al., 2004a). In Drosophila, others have shown Naked Cuticle to antagonize the Wnt pathway via interaction with Dishevelled (Rousset et al., 2001). Our laboratory demonstrated in zebra fish and mammalian HEK293 cells that NKD2 can also antagonize Wnt signaling, in a myristoylation-dependent manner, through mutual ubiquitin-mediated proteasomal degradation of Dishevelled at the cell surface (Hu et al., 2010). TGFα plays an important role in NKD2 antagonism of Wnt signaling by stabilizing NKD2 and ensuring its delivery to the cell surface where it can interact with Dishevelled (Ding et al., 2008). In turn, NKD2 coats TGFα containing vesicles and escorts them to the BL surface of polarized epithelial cells as previously described in Chapter 1 (Li et al., 2004a) (Li et al., 2007). Increased expression of NKD2 in MDCK cells accelerates the cell surface delivery of TGFα, revealing NKD2 as an important regulator of TGFα activation of the EGFR (Li et al., 2004a).

The identification of NKD2 and its role in TGFα cell surface delivery provided the foundation for the idea that AREG must also interact with a protein during delivery to the cell surface. Just as the cytoplasmic domain of TGFα was used as bait to identify NKD2, the 31-amino acid cytoplasmic domain of AREG

was used to screen the same HCA-7 library. However, no proteins were identified to interact with the AREG cytoplasmic domain.

I hypothesized that the traditional yeast two-hybrid screen was inappropriate to identify interacting proteins for AREG because the screen did not express the cytoplasmic domain in its native location within the cell. The traditional yeast two-hybrid screen utilizes the GAL4 transcriptional activator that consists of two essential domains for proper function, a DNA binding domain and activating domain (Fields and Song, 1989). In a yeast two-hybrid screen the bait protein is tagged with one of these domains while the prey protein is tagged with the other. When the two proteins interact they bring the two GAL4 domains together to form a functional transcriptional activator that activates transcription of a reporter gene (Fields and Song, 1989). However, the two interacting proteins are tethered to the transcriptional activator and must be able to translocate to the nucleus in order to activate transcription. In the case of transmembrane proteins such as AREG and TGFα this allows for only the expression of the cytoplasmic domain and does not allow for the full-length protein to be integrated into the membrane where it would normally be expressed. This was not a problem for identifying TGFα interacting proteins, but may have inhibited identification of AREG interacting proteins.

An alternative to the traditional yeast two-hybrid screen that allows for full-length proteins to be expressed in their native location is the split ubiquitin yeast two-hybrid screen. This screen utilizes the protein ubiquitin, which is endogenously expressed as a single domain protein. Ubiquitin can form fusions

with itself on the last glycine residue (Gly-76), which are rapidly cleaved by ubiquitin specific proteases (UBP) (Baker et al., 1992). While ubiquitin is a monomer protein, it can be divided into N-terminal (NUB) and C-terminal (CUB) portions that will fuse to reconstitute a complete ubiquitin protein (Johnsson and Varshavsky, 1994). NUB and CUB fused to interacting proteins will reconstitute during protein interactions to form a complete ubiquitin protein that will be recognized by UBPs. If a reporter protein is fused to the CUB at Gly-76, reconstitution of a complete ubiquitin will result in cleavage of the reporter protein, which can then be detected on a SDS-PAGE gel by radiolabeling or western blotting (Johnsson and Varshavsky, 1994). This split ubiquitin phenomenon can be used to detect protein interactions between integral membrane proteins expressed in their native localizations in the cell.

A split ubiquitin membrane yeast two-hybrid screen uses the reconstitution of ubiquitin to indentify interacting proteins for transmembrane proteins (Figure 18) (Iyer et al., 2005). Instead of using a reporter protein separated on a SDS-PAGE gel, this screen works by fusing a transcription factor for a reporter gene to Gly-76 of CUB. The CUB is fused to the bait protein and the NUB is fused to the prey protein. When the bait and prey proteins interact the NUB and CUB reconstitute a complete ubiquitin that is then recognized by a UBP. The UBP will cleave the transcription factor from the CUB allowing it to translocate to the nucleus and activate the reporter gene. The bait and prey proteins stay integrated into the membrane and do not need to translocate to the nucleus to

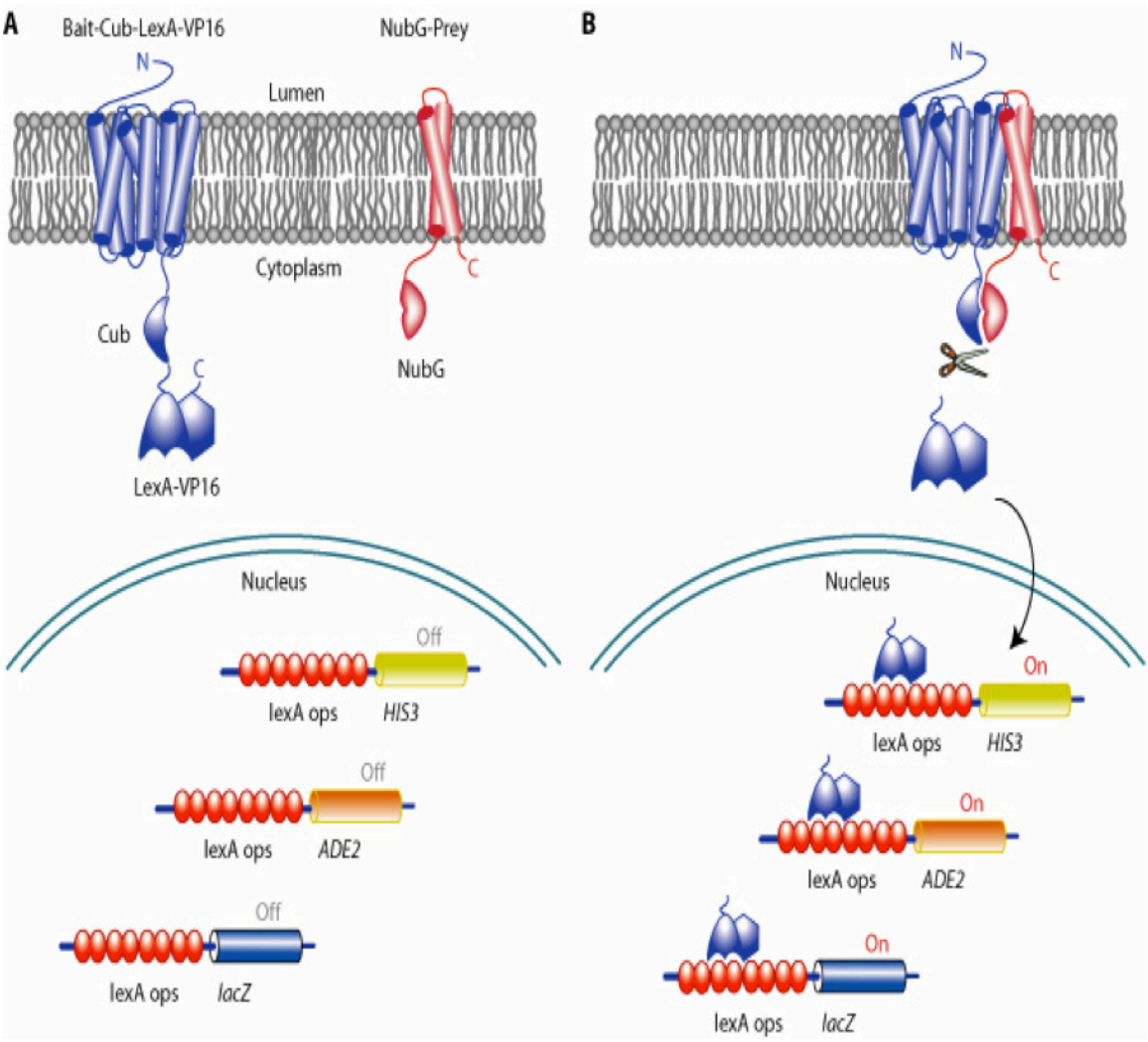

Iyer et al Sci STKE. 2005 Mar 15;2005(275):pl3

Figure 18. Illustration of a split ubiquitin membrane yeast two-hybrid screen. Illustration of how the split ubiquitin yeast two-hybrid screen used to identify AREG interacting proteins works. A) AREG would be tagged with the CUB-LexA-VP16 transcription factor and the prey library would be tagged with the NUB. B) Upon interaction of AREG with a tagged prey protein the ubiquitin would reconstitute and be recognized by the UBP, releasing the LexA-VP16 transcription factor from AREG. The transcription factor can then translocate to the nucleus and activate the HIS3, ADE2, and LacZ reporter genes (Iyer et al., 2005).

activate transcription. Removing the requirement for interacting proteins to translocate to the nucleus to activate the reporter gene allows for the proteins to be expressed in their proper location and increases the chances of identifying interacting proteins.

Yeast two-hybrid screens are good tools for identifying interacting proteins, but these screens do not always produce results. A yeast two-hybrid screen relies on expression of the interacting proteins in the prey library. If the library does not express an interacting protein then it cannot be identified in a yeast two-hybrid screen. During construction of the prey library a protein may not be included or the cDNA may not translate a full-length protein. Many things may go wrong that cause an important protein to be absent from a prey library.

One approach to the problems caused by use of a prey library is to look for interactions with endogenously expressed proteins. This can be accomplished through immunoprecipitation (IP) of the protein of interest followed by mass spectral analysis. If two proteins have a strong interaction that is stable over time then the interaction could be maintained during an IP at 4^{o}C. However, most protein interactions are transient and do not fall under this criteria, particularly interactions involved in protein trafficking. To maintain the interaction through the IP process crosslinking reagents can be used. These reagents will covalently link the interacting proteins and prevent them from separating during the IP procedure. The resulting pellet from a crosslinked IP can then be digested into small peptides with trypsin and analyzed by mass spectrometry.

Just as a yeast two-hybrid screen is not perfect, neither is a crosslinked IP. The main problem resulting from crosslinking is background. The crosslinking reagent has a 12-angstrom spacer arm and will crosslink proteins that come within that distance of each other. While this is a very small distance, in a densely packed cytoplasm non-interacting proteins may come this close to each other, leading to a false-positive result. The large amount of background noise created by crosslinking may drown out genuine signals from interacting proteins during the mass spectral analysis. The problem of background is amplified by the lack of sensitivity of mass spectrometry. While mass spectrometry is generally accepted to be extremely sensitive, my own experience with the procedure has revealed it to be rather insensitive. For example, detection of AREG in exosomes by mass spectrometry has been elusive, even though AREG has been confirmed in exosomes by three other methods: western blotting, ELISA, and FAVs. The inability to detect an abundant protein in exosomes by mass spectrometry raises questions about the number of other proteins not detected in a mass spectrometry analysis.

To identify interacting proteins for AREG, I employed both the split ubiquitin yeast two-hybrid screen and a crosslinked AREG IP. The split-ubiquitin yeast two-hybrid screen was more successful then the traditional yeast two-hybrid screen in identifying a number of possible interacting proteins. However, none of the identified proteins are reported to be involved in protein trafficking. Efforts to verify these interacting proteins outside of the yeast two-hybrid system also proved difficult, leading me to attempt the crosslinked AREG IP. The

crosslinked AREG IP was successful in identifying one interesting protein possibly involved in protein trafficking, but was not pursued due to the time frame of my graduate studies and the lack a publishable story. While the proteins identified by these two screens did not advance my graduate work, they may shed light on future studies of AREG.

Material and Methods

Isolation of the RNA Used to Generate the Split Ubiquitin Prey cDNA Library.

Total RNA was isolated from polarized HCA-7 cells. The cells were plated in 24mm Transwell filters at a cell density of 500,000 cells per Transwell. The cells were determined to be polarized on day six after plating with a TEER between 350-420 Ω/cm^2. The RNA was isolated using the Qiagen RNA easy kit. The protocol in the manual was followed, using 350µl of collection buffer for each Transwell. Each Transwell (total of 3) was treated as a separate sample. Two 30µl elution steps were performed and all samples were combined at the end. The final concentration was determined to be 500 ng/µl in a total volume of 180µl. This RNA was sent to Dualsystems Biotech for generation of the prey library. The generated prey library was an N-terminally tagged library, meaning the NUB is on the N-terminus. It was suggested by the company to use an N-terminally tagged library to ensure the NUB was present on each protein. If the NUB is placed on the C-terminus, there is a chance it would not be included due to incomplete translation of the cDNA during library expression. If the NUB is absent, there is no chance of detecting an interaction, however, if the NUB is present but the protein is truncated, there is still a chance the portion of the protein fused to the NUB can mediate an interaction.

Split Ubiquitin Yeast Two-Hybrid Screen.

The split ubiquitin yeast two-hybrid screen was performed following the Dualsystems DUALmembrane kit 2 protocols. In order to obtain a high transformation efficiency of the library, high quality bottled water was used.

To create the signal sequence minus AREG for the screen, AREG was cloned into the pCCW-SUC vector using the following primers:

Forward Primer 2: 5' aaaaaaatggccattacggcctcaggccattatgctgctg 3'

Reverse Primer 2: 3' cctttacatgtacgatatcgtttccggcggagccggaaaaaaaaa 5'

The following PCR reaction was used to generate the signal sequence minus AREG PCR fragment:

1µl diluted hAREG = 25ng, 5µl 10x buffer w/ MgCl, 1µl Forward primer 2 at 100ng/µl, 1µl Reverse primer 2 at 100ng/µl, 2.5µl 10mM DNTPs = 500uM final, 38.5µl H2O, 1µl Pfu turbo enzyme

PCR Program used:

94^0C for 2 min, 94^0C for 1 min, 58^0C for 1 min, 72^0C for 1.5 min, cycle 20 times, 72^0C for 10 min, 4^0C hold.

The PCR product was digested with SfiI then ligated into pCCW-SUC also digested with SfiI. The pCCW-SUC-AREG Clone#3 was determined to be correct and was transformed into the yeast strain NMY32 for screening of the prey library. Following protocol 4 in the DUALmembrane kit 2 user manual, the expression of the AREG-CUB-LexA-VP16 construct was confirmed in the AREG-SUC yeast clone#4 by western blotting for LexA (Figure 19F). The positive

control in this blot was yeast transformed with pCCW-Alg5 and the negative control was non-transformed NYM32 yeast.

After concluding that AREG was being expressed in the AREG-SUC yeast clone 4, I went forward with clone 4 because it had the highest protein concentration in the lysate. The next step was to determine the correct topology of the protein in the membrane by co-transforming clone 4 with a positive and negative control. The positive control is pAI-Alg5 which is Alg5 fused to the wild-type NUB protein. This wild-type NUB should spontaneously reconstitute with the CUB on AREG. The negative control is pDL2-Alg5 which is Alg5 fused to the NUBG which will not reconstitute with CUB unless a protein-protein interaction brings them together. The results of the co-transformations were growth with pAI-Alg5 and no growth with pDL2-Alg5 (Figure 19A-E). The growth with pAI-Alg5 demonstrates the CUB is correctly oriented in the cytoplasm. The lack of growth with pDL2-Alg5 demonstrates the AREG-CUB-LexA-VP16 protein is integrated into the membrane and is not self-activating. There was very little growth on the SD-LWHA plates indicating the level of stringency with the SD-LWH is enough. The total lack of growth on SD-LWH plates with pDL2-Alg5 indicates no background and no need for 3-AT.

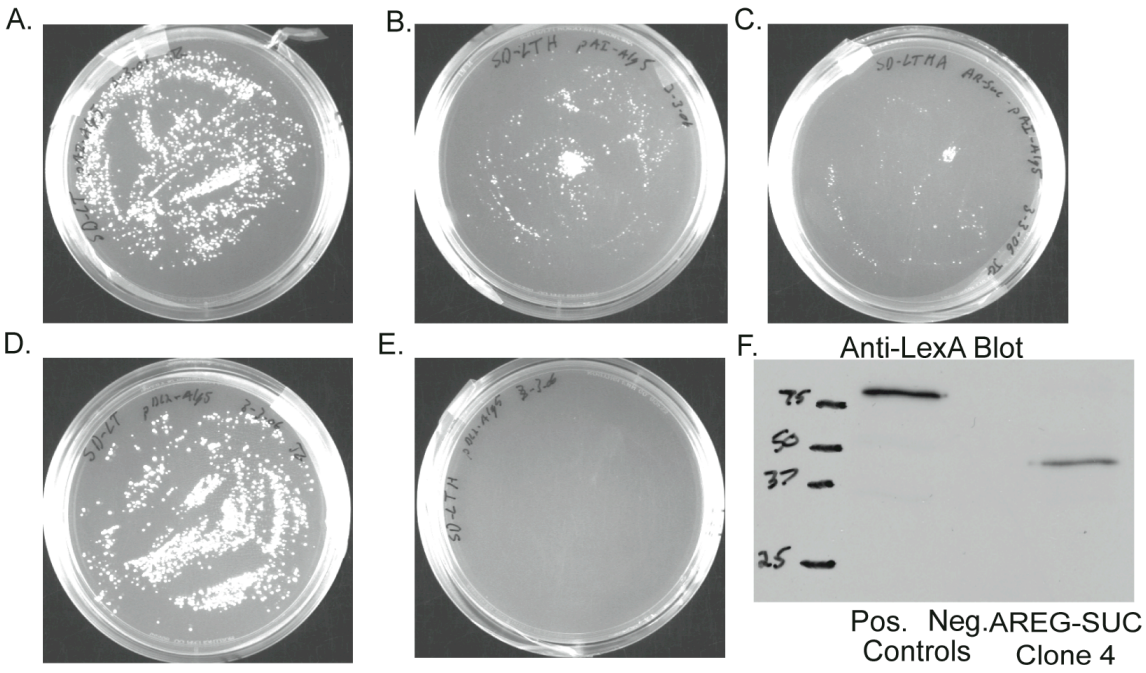

Figure 19. Split ubiquitin yeast two-hybrid screen controls for expression, topology and self-activation of AREG-CUB-LexA-VP16 clone 4.
Positive controls for the correct topology of the AREG-CUB-LexA-VP16 clone 4 (A-C). A) Growth on the SD-LW plate shows the transformation of Clone 4 with pAI-Alg5 was successful. B) Growth on the SD-LWH plate shows the CUB-LexA-VP16 is in the cytoplasm and available to interact with the NUB. This demonstrates AREG is in the proper topology. C) The reduced growth seen on the SD-LWHA plate shows the stringency of the SD-LWH plate is best for screening the library. Negative controls for self-activation of CUB-LexA-VP16 (D-E). D) Growth on the SD-LW plate shows the transformation of Clone 4 with pDL2-Alg5 was successful. E) Lack of growth on the SD-LWH plate demonstrates the AREG-CUB-LexA-VP16 is not self-activating and is properly integrated into the membrane and unable to translocate to the nucleus. F) Western blot for LexA to demonstrate the expression of the AREG-CUB-LexA-VP16 protein in the AREG-SUC yeast clone 4. This clone was used for transformation and screening of the prey library. The positive control in this blot was yeast transformed with pCCW-Alg5 and the negative control was non-transformed NYM32 yeast.

Crosslinked AREG Immunoprecipitation and Mass Spectrometry Analysis.

Bead Preparation

The beads used for the IP were protein G Dynal beads (Invitrogen) prepared as follows:

1350µl of beads were removed from the stock solution ($6x10^8$ beads/ml) and washed 3x with 1xPBS 0.1%BSA. These beads have a binding capacity of 1µg IgG/10^7 beads (1350µl beads = $8.1x10^8$ beads which can bind 81µg IgG). The mouse anti-AREG 6R1C2.4 stock is at 40ng/µl (2025µl x 40ng/µl = 81µg IgG). 2025µl of 6R1C2.4 stock was added to the 1350µl of beads. The beads were incubated with IgG antibody overnight in the cold room rotator. The IgG bound beads were washed 3x with 1xPBS 0.1% BSA followed by two washes with 1ml 0.2M triethanolamine pH 8.2. To crosslink the antibody to the beads, 1ml 20mM DMP (0.0054g/ml) in 0.2M triethanolamine pH 8.2 was used. The beads were incubated with this crosslinking reagent for 40min at RT in the rotator. The crosslinking reaction was quenched with 1ml 50mM Tris pH 7.5 for 15min in the rotator at RT then washed 3x with 1xPBS 0.1% BSA. In order to elude any un-crosslinked antibody, the beads were washed 2x 2min with 1ml 0.1M Citrate pH 3.1 in the rotator at RT, then washed 3x with 1xPBS 0.1% BSA. The final product was resuspended in 1350µl 1xPBS 0.1% BSA plus 13µl 2% Sodium Azide and stored at 4^{o}C.

Crosslinking of Cells and Preparation of Cell Lysates for IP

Fresh DSP was prepared immediately prior to use. The protocol is as follows:

Stock solution of 10mM: 0.0142g DSP + 3.5ml DMSO = 10mM stock

1.0mM working solution: 1.0mM -> 3ml 10mM stock + 27ml 1xPBS

The cells used in this experiment were CC3 cells (a derivative of HCA-7 cells) grown in seven 150x25mm dishes. Four of these dishes were treated with DSP, while three were not treated. The cells were washed 3x with ice cold 1x PBS. The PBS was removed and 7ml 1.0mM DSP was added to each of the four treated dishes. The cells were incubated with the crosslinking reagent for 30min at RT. The crosslinking reaction was quenched with 7ml 20mM Tris pH7.5 for 15min at RT then washed 3x with 1xTBS. At this point the three dishes that were not treated were washed with cold 1xTBS. From this point on the crosslinked and non-crosslinked cells were treated equally. The cells were scraped from the dish using a cell lifter in 1xTBS. Cells were then transferred to a 50ml conical and centrifuged at 1000 rpm for 5min. Cells were lysed with 4ml 1%NP-40 (50mM Tris-HCl pH 8.0, 150mM NaCl, 1% NP40, 2mM EDTA) plus protease inhibitor cocktail (Sigma) for 20min on the RT rocker. The lysates was divided evenly between eppendorf tubes and centrifuged at 16000g for 15min at 4^{o}C. Pellets were saved and 25µl 1x sample buffer (2x sample buffer = 125mM Tris-HCl pH6.8, 2% Glycerol, 4% SDS (w/v), 0.05% bromophenol blue) added to each. The supernatant was transferred to fresh tubes and a BCA assay was used to determine protein concentration. 12.5µl of each sample was reserved as a Total Lysate (TL) sample. The protein concentration for each sample was determined:

The DSP treated lysate had a protein concentration of 2µg/µl. The untreated lysate had a protein concentration of 3µg/µl. I transferred 2ml of each sample to fresh tubes for the IP.

Immunoprecipitation

For the untreated lysate: 3µg/µl x 2000µl = 6000µg so added 600µl anti-AREG conjugated dynabeads.

For the DSP treated lysate: 2µg/µl x 2000µl = 4000µg so added 400µl anti-AREG conjugated dynabeads.

The lysates were incubated with the dynabeads for 1hr 25min in the coldroom. The tubes were put on the magnet and 12.5µl from each sample was removed for a cleared lysate (CL) sample.

The samples were transferred to eppendorf tubes to make working with the magnet easier. Each sample was consolidated in one eppendorf tube and washed 6x with 1000µl lysis buffer. The antigens were eluted off the beads with 25µl 1x sample buffer without DTT and heated at 95^{o}C for 5min. 5µl from each elution (E) was removed for analysis. All samples were stored at –80^{o}C until delivered to mass spectrometry core for analysis.

Eluted proteins were briefly run by SDS-PAGE (~ 1cm) using a 10% NuPAGE gel. After staining with colloidal coomassie blue, the area corresponding to the proteins was excised and subjected to in-gel trypsin digestion. The resulting peptides were analyzed by a 90min data dependent LC-MS/MS analysis. Briefly, peptides were resolved using an Eksigent 1D+ ultraHPLC equipped with an AS1 autosampler on an 18cm Jupiter (3 micron,

300A) 100 µm internal diameter, self-packed analytical column coupled directly to an LTQ-orbitrap (ThermoFisher) via a nanoelectrospray source. A full scan mass spectrum followed by 5 data-dependent tandem mass spectra (MS/MS) were collected throughout the run using dynamic exclusion to minimize acquisition of redundant spectra. MS/MS spectra were searched against a human protein database (IPI) using SEQUEST (http://www.ncbi.nlm.nih.gov/pubmed/7741214) and results filtered and collated using IDPicker (http://www.ncbi.nlm.nih.gov/pubmed/19522537). Dr. Hayes McDonald, Associate Director in the Vanderbilt Proteomics Laboratory and Mass Spectrometry Research Center performed the LC-MS/MS.

Western Blot Analysis

Western blot analysis was performed on the different samples before sending to the MS core. I wanted to load equal percentages of the total sample on the gel so the samples would be comparable. For the TL and CL I removed 12.5µl from 2000µl or 0.6%. For the elution samples, 0.6% of 25µl = 0.15µl. Since 0.15µl would be impossible to remove I did 0.3µl, which would make it 2x compared to the TL and CL. However pipetting accuracy of 0.3µl is still very poor. The samples were loaded on a 12.5% SDS-PAGE gel in the following order:

M/TL(+)/TL(-)/CL(+)/CL(-)/E(+)/E(-)

(+=with DSP, -=without DSP) The gel was run until the dye front reached the bottom of the gel then transferred to nitrocellulose overnight. When I came in the next morning the power supply had been shut off and since I did not know when

this happened I increased the amps to 0.1 and transferred for an additional 5hrs. The membrane was washed with 1x PBS 0.05% Tween then blocked in 5% milk 1xPBS 0.05% Tween overnight. The membrane was blotted with mouse anti-AREG 6R1C2.4 primary antibody diluted 1:50 in blocking buffer for 1hr at RT then washed 3x with 1xPBS 0.05% Tween. The membrane was blotted with TrueBlot anti-mouse HRP secondary antibody diluted 1:1000 in blocking buffer for 1hr at RT then washed 3x with 1xPBS 0.05% Tween. The chemiluminescence reagent was added for 1min then exposed film to the membrane for 30sec and 1min 30sec.

AREG-Kinectin Co-Immunoprecipitation.

One confluent 100mm dish of HCA-7 cells was used. The dish was washed 3x with cold 1xPBS, and the cells were scrapped from dish and spun into a pellet. The pellet was resuspended in 2ml 1%NP40 lysis buffer plus protease inhibitor. The lysate was divided between two eppendorf tubes. The cells were incubated in lysis buffer for 1hr in the cold room. The lysates were centrifuged for 15min at max speed then the supernatant was transferred to new tubes. Each lysate was cleared with 25µl of a 50% slurry of recombinant protein G agarose beads (Invitrogen Catalog no. 15920-010) for 1hr in cold room followed by a 5min centrifugation at max speed. The supernatants were transferred to fresh tubes. 25µl was removed from one tube for a total lysate (TL) sample. 7.5µg of either goat anti-kinectin antibody(Santa Cruz sc-19909) or mouse anti-AREG antibody (6R1C2.4) was added to one of the lysates then incubated for 1hr in the cold

room. 25µl of a 50% slurry of recombinant protein G agarose beads was added to each IP and incubated in the cold room for 1hr. The beads were centrifuged and 25µl removed for a cleared lysate (CL) sample. The supernatant was removed and the beads washed 4x with 1ml lysis buffer. 40µl of 1x sample buffer without DTT was added to each pellet. Equal volume 2x sample buffer was added to the TL and CL samples and all samples heated at 70^{o}C for 5min. The samples were loaded onto two 10% SDS-PAGE gels with the gel for the anti-kinectin blot run out much further to provide greater separation of the higher molecular weight proteins. The samples were transferred to nitrocellulose and blotted as described above. The anti-kinectin antibody was used at 1:200 and the anti-AREG was used at 1:50. The secondary rabbit anti-goat HRP antibody was diluted 1:10000.

Results

Split ubiquitin yeast two-hybrid screen

The screening of the split ubiquitin library generated from polarized HCA-7 cells using full-length AREG tagged with CUB-LexA-VP16 produced 37 unique hits (Table 3). These hits were confirmed by binary transformations and a LacZ assay. Unfortunately, none of the identified proteins are reported to be involved in protein trafficking to the cell surface and many of the proteins have no indentified functions whatsoever.

Because there was not a clear candidate to investigate, immunofluorescence co-localization was used to further verify which of the identified proteins would be most promising to pursue. At this point the cDNA for each of the hits was in the prey library vector. The prey library was generated using SfiI restriction sites within the multiple cloning site (MCS) to easily clone the cDNA into the prey vector. This SfiI cloning strategy was utilized to release each of the cDNAs from the prey vectors and clone into pCMV-Myc. The pCMV-Myc vector contains a single Myc tag N-terminal to the MCS. Because the prey library was also N-terminally tagged, I was able to modify pCMV-Myc using quick change PCR to introduce SfiI sites that would keep the cDNA in frame with the N-terminal Myc tag. Using the SfiI sites, each of the positive hits from the yeast two-hybrid screen was released from the prey vector and inserted into the pCMV-Myc vector.

Table 3. List of confirmed hits from the split ubiquitin yeast two-hybrid screen of AREG. The protein IDs and pubmed nucleotide identifier numbers are listing in the protein ID column. The number of hits column is the number of times the protein was identified in the screen. All hits listed were confirmed by binary transformations and lac Z assays. The cellular localization column indicates where the protein is reported or predicted to localize in the cell.

Protein ID	# Hits	Cellular Localization
claudin domain containing 1 NM_001040181.1	8	Membrane
solute carrier family 6 NM_001044.2	8	Membrane
PERP, TP53 apoptosis effector NM_022121	5	Desmosmes
stress-associated ER protein 1 NP_055260	4	ER
ADP-ribosylation-like factor 6 interacting protein 5 NM_006407	2	ER, Cytoplasm, Golgi
B-cell receptor-associated protein 31 NM_005745	2	ER
HCV F-transactivated protein 1 NM_001001701	2	
protein disulfide isomerase A6 NM_005742.2	2	ER
ubiquitin C (UBC) NM_021009.3	2	Cytoplasm, Nucleus
cytochrome c oxidase subunit II ABB78341	2	Mitochondria
ATP synthase F0 subunit 6 AAX53794	2	Mitochondrial membrane
serine palmitoyltransferase NM_006415.2	1	ER
surfeit 4 (SURF4) NM_033161	1	COP2 vesicles
ATPase, H+ transporting, lysosomal accessory protein NM_005765.2	1	Membrane
thioredoxin domain cont. 14 NM_015959.1	1	Cytoplasm, Nucleus
CKLF-like MARVEL TM domain 6 NM_017801.2	1	
NAD(P) dependent steroid dehydrogenase-like NM_015922.1	1	ER, Lipid droplets
signal sequence receptor NM_007107.2	1	ER
farnesyl-diphosphate farnesyltransferase 1 NM_004462.3	1	ER
Solute Carrier copper transporter NM_001860	1	Membrane
Disulfide isomerase related P5 AK026926	1	ER
Fanconi anemia, comp group F NM_022725	1	Nucleus
ELOVL family NM_021814.3	1	Membrane
CD163 molecule-like 1 NM_174941.4	1	Membrane
transmembrane protein 45B NM_138788	1	Membrane
transmembrane protein 165 NM_018475.2	1	Membrane
transmembrane protein 14A NM_014051.2	1	Membrane
ribosomal protein S5 NM_001009.3	1	Cytoplasm
interferon induced TM protein 3 NM_021034.1	1	Membrane
COX15 homolog NM_004376.3	1	Mitochondrial membrane
cytochrome c oxidase subunit I AAZ00451	1	Mitochondria
similar to DNA seg. Chr 11 NM_001004333.1	1	
chromosome 2 genomic contig NT_022184.14|Hs2_22340	1	
chromosome 6 open reading frame 55 NM_016485.3	1	
seq similarity 18, member B NM_016078.3	1	Membrane
unnamed protein product BAC85662	1	
unknown protein 1 AY513722	1	

Once the cDNAs were successfully cloned into pCMV-Myc, they were transiently transfected into MDCK cells stably expressing AREG-GFP, which was used to simplify the staining procedure. Using indirect immunofluorescence and confocal microscopy each of the Myc-tagged constructs was screened for co-localization with AREG-GFP. The most promising hit was transmembrane protein 165 (TM165), which appears to co-localize with AREG in a Golgi-like structure (Figure 20A). However, Golgi markers were not used to confirm the structure, but the co-localization appears to be perinuclear. Because TM165 is a multi-pass transmembrane protein, there was concern that placement of the tag on the N-terminus could result in false positive co-localization. Therefore, TM165 was cloned into a pCherry-N1 vector to fuse a cherry fluorescent protein on the C-terminus of TM165. The C-terminally tagged version of TM165 co-localized with AREG-GFP in a similar perinuclear region as the N-terminal Myc-tag, demonstrating the co-localization to be genuine (Figure 20B).

The final criterion for establishing a true interacting protein was the ability to co- immunoprecipitate (co-IP) the protein with AREG. Attempts to co-IP AREG and Myc-tagged TM165 through an AREG IP and an anti-Myc blot could not be interpreted due to background issues with the anti-Myc blot. Using the Cherry-tagged TM165 instead to IP AREG and blot for cherry produced negative results, with the cherry tag detected in the total lysate samples, but not in the AREG IP samples. I concluded after multiple attempts that I could not co-IP AREG and TM165, either due to the technical difficulty of immunoprecipitating a multi-pass transmembrane protein or because they do not physically interact.

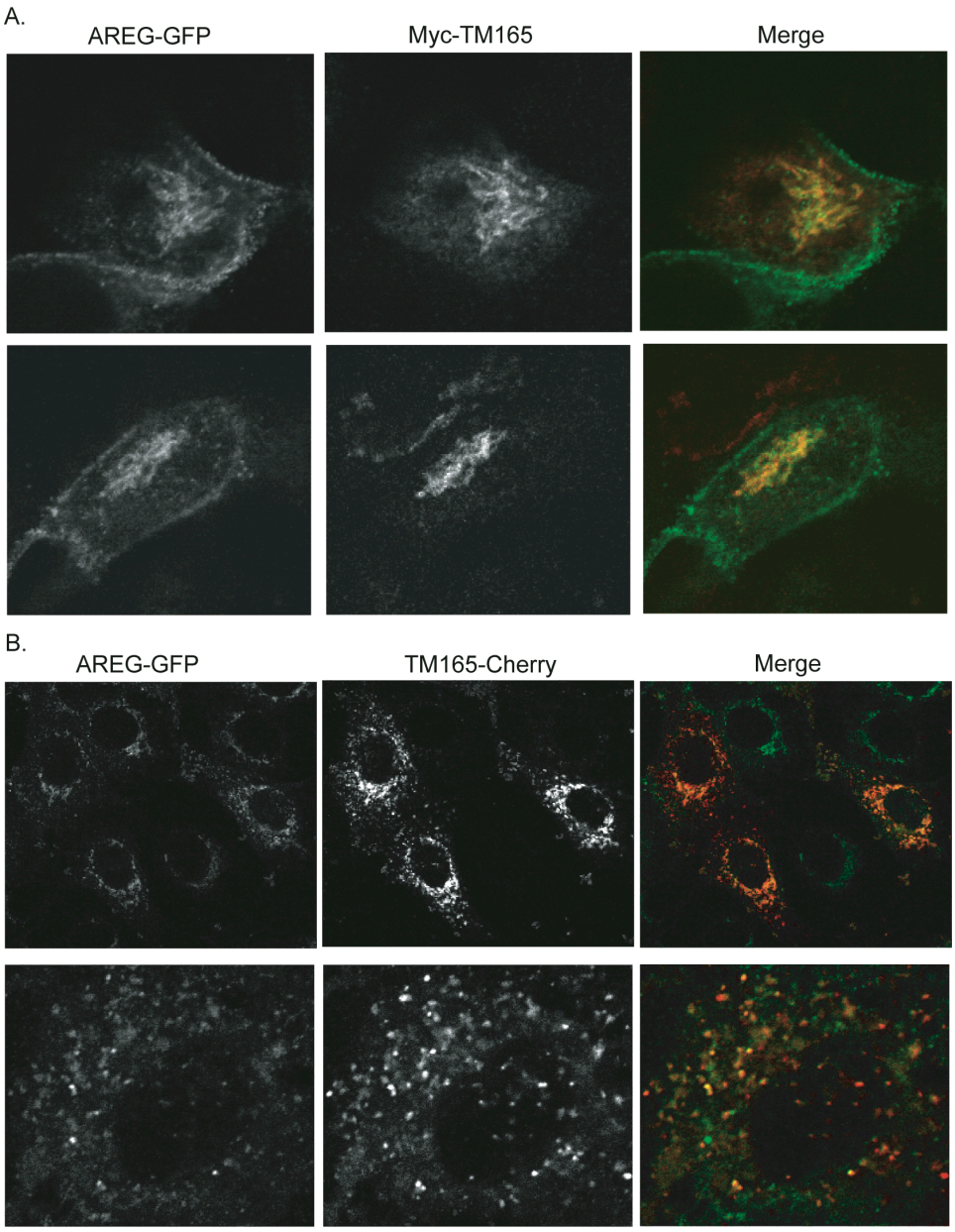

Figure 20. Co-localization of AREG and TM165. A) N-terminally Myc-tagged TM165 was transiently transfected into MDCK cells expressing AREG-GFP. Indirect immunofluorescence for the Myc tag (Red) suggests co-localization with AREG-GFP (Green) in a perinuclear region of two different cells. B) C-terminally Cherry-tagged TM165 (Red) was transiently transfected into MDCK cells expressing AREG-GFP (Green). Detection of the two proteins by confocal microscopy demonstrates co-localization in a perinuclear region. The upper image shows a field image while the lower image is a magnification of the perinuclear region of one cell and shows puncta of co-localization.

Table 4. Condensed list of proteins identified from the crosslinked AREG IP mass spectral analysis. Protein identification numbers and descriptions are listed in descending order of peptide coverage. See appendix A for the full list.

Protein	Description	Coverage
IPI:IPI00026272.2	Histone H2A	42
IPI:IPI00008530.1	60S ribosomal protein	40
IPI:IPI00453473.6	Histone H4	39
IPI:IPI00009865.2	Keratin	35
Cntm_Q65ZC0|Q65ZC0	Kappa light chain C_region - Mus musculus	34
IPI:IPI00217030.10	40S ribosomal protein	31
IPI:IPI00783060.1	Ubiquitin	30
IPI:IPI00012023.1	Amphiregulin precursor	29
IPI:IPI00470657.1	Anti-colorectal carcinoma heavy chain	28
IPI:IPI00220740.1	Nucleophosmin	27
IPI:IPI00069693.4	Uncharacterized protein ENSP00000350479	25
IPI:IPI00031812.3	Nuclease sensitive element-binding protein 1	24
IPI:IPI00827674.1	Nucleolin	22
Cntm_P00761|TRYP	Trypsin - Sus scrofa	21
IPI:IPI00023048.4	Elongation factor 1	20
IPI:IPI00550766.1	RRP1-like protein	20
IPI:IPI00477179.1	Nucleolar RNA helicase 2	19
IPI:IPI00218592.5	Splicing factor	19
IPI:IPI00007188.5	ADP/ATP translocase 2	18
IPI:IPI00295992.4	ATPase family AAA domain-containing protein 3A	18
IPI:IPI00014230.1	Complement component 1 Q subcomponent-binding protein	17
IPI:IPI00003881.5	Heterogeneous nuclear ribonucleoprotein	17
IPI:IPI00328753.1	Kinectin	16
IPI:IPI00795040.1	Heat shock 70kDa protein 8	15
IPI:IPI00037070.2	Heat shock cognate 71 kDa protein	15
IPI:IPI00217467.3	Histone H1	15
IPI:IPI00515047.1	Actin	14
IPI:IPI00815690.1	Leucocyte antigen A	14
IPI:IPI00745955.2	Probable rRNA-processing protein EBP2	13
IPI:IPI00328840.9	THO complex subunit 4	12
IPI:IPI00844578.1	ATP-dependent RNA helicase	11
IPI:IPI00644631.3	HLA class I histocompatibility antigen	11
IPI:IPI00005198.2	Interleukin enhancer-binding factor	11
IPI:IPI00396321.1	Leucine-rich repeat-containing protein 59	11
IPI:IPI00410017.1	Polyadenylate-binding protein	11
IPI:IPI00015838.3	Cell growth-regulating nucleolar protein	10
IPI:IPI00024684.1	Interferon-induced GTP-binding protein Mx2	10
IPI:IPI00008708.5	Ribosomal L1 domain-containing protein 1	10
IPI:IPI00413611.1	DNA topoisomerase 1	9
IPI:IPI00641873.1	Staufen	9
IPI:IPI00003362.2	HSPA5 protein	8
IPI:IPI00005416.3	NICE-4 protein	8
IPI:IPI00328715.4	Protein LYRIC	8
IPI:IPI00513959.3	RNA binding motif protein 39	8
IPI:IPI00027107.5	Tu translation elongation factor	8
IPI:IPI00005492.2	WD repeat-containing protein 5	8
IPI:IPI00555602.1	CD68 antigen variant	7
IPI:IPI00009328.4	Eukaryotic initiation factor	7
IPI:IPI00027831.1	Glutamate-rich WD repeat-containing protein 1	7
IPI:IPI00102815.1	Nucleolar complex protein 3	7
IPI:IPI00556297.1	Arginine/serine-rich splicing factor 6	6
IPI:IPI00220834.8	ATP-dependent DNA helicase	6
IPI:IPI00554715.2	Fragile X mental retardation syndrome-related protein 1	6
IPI:IPI00607584.1	Myb-binding protein	6
IPI:IPI00018971.7	52 kDa Ro protein	5
IPI:IPI00414676.6	Heat shock protein HSP 90	5
IPI:IPI00328293.2	Serine/arginine repetitive matrix 1	5
IPI:IPI00025874.2	Dolichyl-diphosphooligosaccharide--protein glycosyltransferase	4
IPI:IPI00797590.2	NOL1 protein	4
IPI:IPI00015808.3	Nucleolar GTP-binding protein 2	4
IPI:IPI00644127.1	Isoleucyl-tRNA synthetase	2
IPI:IPI00177817.4	Sarcoplasmic/endoplasmic reticulum calcium ATPase 2	2

Crosslinked AREG immunoprecipitation, mass spectral analysis, and kinectin co-immunoprecipitation.

The second approach taken to identify interacting proteins for AREG was a technique developed by Andrew Smith (Smith et al., 2011). This technique uses crosslinking reagents to stabilize transient protein interactions and increase the chances of isolating interacting proteins during an IP of the protein of interest. Using this approach a number of proteins were identified by mass spectral analysis, including the protein kinectin as a possible interacting protein for AREG (Table 4).

Kinectin was first identified as a kinesin-binding protein of motile vesicles that localized to the endoplasmic reticulum (ER) (Toyoshima et al., 1992). Kinesin, the binding partner for kinectin, is a molecular motor involved in anterograde movement along microtubules and plays a role in delivery of endocytic vesicles from the cell surface to endosomes (Bomsel et al., 1990; Schroer et al., 1988). The association between kinectin and the molecular motor kinesin prompted me to further investigate the possible interaction between AREG and kinectin.

To determine if AREG and kinectin interact, two co-IP experiments were performed, an IP of AREG followed by a western blot for kinectin and an IP of kinectin followed by a western blot for AREG. The kinectin blot of the AREG IP produced a band at 160 kDa, the same size detected in the TL sample and the predicted size for kinectin (Figure 21A). The AREG blot of the kinectin IP resulted in a 25 kDa doublet and a band at approximately 45 kDa (Figure 21B).

The 25 kDa doublet ran at the same size in the TL sample and corresponds to what was previously described as a 26-28 kDa doublet (Brown et al., 1998). However, the 45 kDa band was clearly smaller then the predominant 50 kDa band in the TL sample indicative of full-length, mature AREG (Figure 21B). The 45 kDa band was previously characterized as an immature ER form of AREG that is endo H-sensitive and is not fully processed by the Golgi (Brown et al., 1998). It is interesting that the 45 kDa band, not the predominant post-Golgi 50 kDa band, co-IPs with kinectin (Figure 21B). These results demonstrate that AREG and kinectin do interact and suggest this happens in the ER.

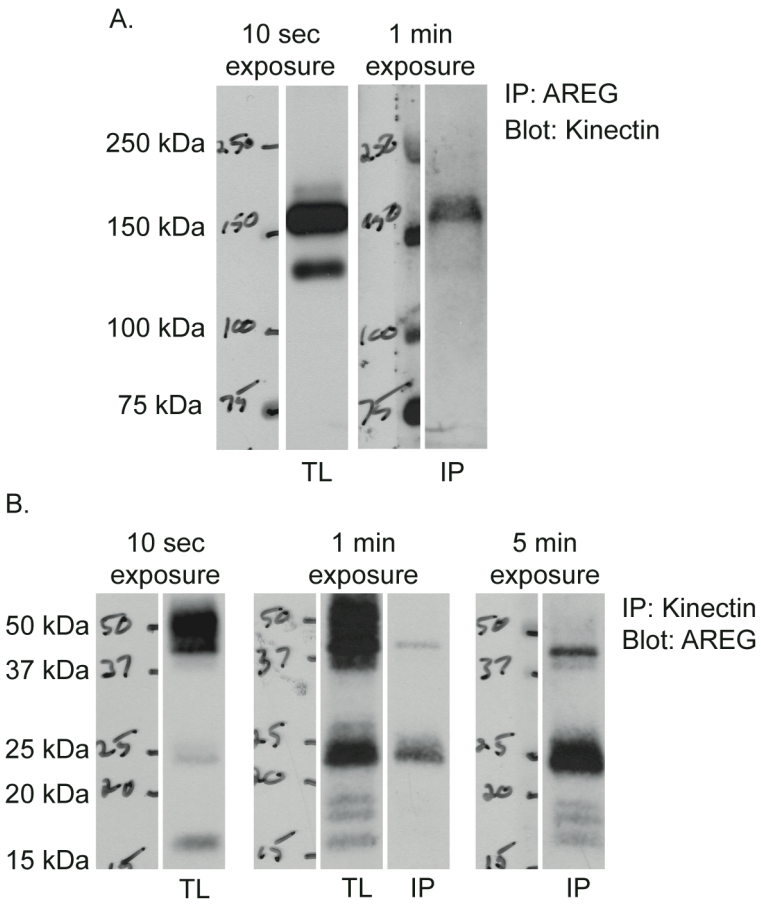

Figure 21. Co-immunoprecipitation of AREG and kinectin. Because of the varying intensities of the IP verse the TL samples, different exposure times are shown side by side for size comparison. The actual size marker marks are shown for an accurate indication of size. A) An IP of AREG followed by an anti-kinectin blot detects a band at 160 kDa in the TL and IP samples. B) An IP of kinectin followed by an anti-AREG blot detects a band at 45 kDa and a doublet at 25 kDa. The 25 kDa doublet is the same size in both the IP and TL sample. The 45 kDa band in the IP sample represents an immature ER form of AREG.

Discussion

While I was unsuccessful in conclusively determining interacting proteins for AREG, the data produced by this work may be beneficial to future members of the Coffey lab. Two areas of study that could benefit from these screens are the exosome and trafficking projects. The mechanism of how proteins are delivered and sorted into exosomes is unclear and may involve proteins indentified in these screens that currently have no known function. The identification of TM165 and localization to the perinuclear region could reveal an unknown role in protein trafficking. As the science progresses and we gain a better understanding of how receptor ligands are trafficked within and between cells, some of the proteins identified in these two screens may become relevant.

TM165, a protein identified in the split ubiquitin yeast two-hybrid screen and verified by co-localization, should be followed up with further experiments. As a nascent and naive graduate student I set strict criteria for confirming an authentic interacting protein, including the ability to co-IP. Now at the end of my graduate education, I understand the difficulties of a co-IP and the inability to co-IP two proteins should not rule out the possibility of an interaction. If given the chance I would pursue different methods to confirm an interaction between TM165 and AREG.

Small interference RNA (siRNA) is one method I would use to investigate the possible role of TM165 in the trafficking of AREG. The co-localization of AREG and TM165 in the perinuclear region and the punctate co-localization pattern could indicate these two proteins are co-localizing in an endosomal

compartment (Figure 20). Since identifying TM165, I have demonstrated the dependence on AP-1B for the proper recycling of AREG, a function that would take place in the recycling endosome. Knockdown of TM165 in polarized cells may have dramatic effects on the recycling or biosynthetic delivery of AREG.

Additionally, I would use organelle markers to identify where AREG and TM165 are co-localizing. While perinuclear staining can specify Golgi localization, AREG and TM165 were never confirmed to be co-localizing in the Golgi. Staining for golgin 97 is commonly used as a Golgi marker and could be used to determine whether TM165 is localized in this organelle. As mentioned earlier, the puncta revealed by immunofluorescence (Figure 20B) could be recycling endosomes, which could be identified with labeled transferrin. The presence of AREG in exosomes is another discovery since the identification of TM165 as a possible AREG interacting protein, making MVBs a possible localization. Identifying the organelle where AREG and TM165 co-localize could reveal the consequences of their possible interaction.

In addition to TM165, the interaction between AREG and kinectin is another avenue of study I would devote further work. The identification of kinectin as a possible AREG interacting protein was a late discovery in my graduate education and the development of a publishable story with kinectin and AREG was not possible within the timeframe for my graduation. However, if I were to continue in the Coffey lab I would pursue this interaction.

A role for kinectin in vesicle and organelle delivery to the cell surface has already been established. In pancreatic islet β-cells, kinectin has been shown to

participate in the delivery of hormone containing vesicles to the cell periphery for secretion (Bai et al., 2006). In COS-7 cells, overexpression of kinectin facilitates the microtubule-dependent transport of lysosomes to the cell periphery, while overexpression of kinectin-kinesin interacting domain fragments inhibited lysosomal redistribution (Ong et al., 2000; Vignal et al., 2001). Given these recent reports, further investigation of the kinectin-AREG interaction would be of interest.

The role kinectin plays in lysosomal delivery to the cell periphery is particularly interesting considering our recent findings regarding AREG and exosomes (Higginbotham et al., 2011). It is unclear what regulatory mechanisms determine if a MVB fuses with a lysosome for degradation or the cell membrane to release exosomes. The connection between kinectin and lysosomal transport begs the question, could kinectin be involved in MVB transport to the cell periphery? Kinectin associates with two forms of AREG, the 45 kDa immature ER form and the 25 kDa doublet forms (Figure 21B). The 45 kDa ER form may associate with kinectin during the elongation step of protein synthesis while kinectin anchors elongation factor-1δ to the ER membrane (Ong et al., 2003). Interestingly, elongation factor-1 was identified in the crosslinked AREG IP screen for interacting proteins (Table 4 and Appendix A). The 25 kDa AREG doublet that associates with kinectin is also the most abundant form of AREG detected in exosomes, an observation that could shed light on how AREG is delivered to exosomes. Could the processing event that generates the 25 kDa AREG forms take place in the ER instead of the cell surface? Could the 25 kDa

forms originate from the 45 kDa immature ER form of AREG that may be improperly folded and processed in the ER before being delivered to a MVB for degradation or exosome release? These are just a few questions that arise from the observed association of AREG and kinectin that should be pursued in the future.

Hopefully the data generated from the AREG split ubiquitin yeast two-hybrid screen and the crosslinked AREG IP screen will be useful in future studies by the Coffey lab. Expansion from a protein trafficking focus to other areas of interest, such as exosome generation, could make the data more relevant. As more is learned about AREG, this data could provide a missing piece of information to complete future work.

CHAPTER V

DISCUSSION AND FUTURE DIRECTIONS

Polar Distribution of AREG

AREG delivery to the BL surface of polarized epithelial cells is dependent on a novel mono-leucine-based BL sorting motif. Only one mono-leucine BL sorting motif has been previously described and has been identified in only two other proteins, SCF and CD147, both of which contain the canonical motif EEDXXXXXL (Deora et al., 2004; Gonzalez and Rodriguez-Boulan, 2009; Wehrle-Haller and Imhof, 2001). The AREG motif is different and consists of EEXXXL (Figure 11). Identification of a novel sorting motif increases the opportunities for identifying other proteins that also use this motif for BL distribution. One such protein may be HB-EGF, which contains an EEXXXL sequence with a similar amino acid composition to the AREG motif (Table 1). Both proteins contain the amino acid sequence EEbXbL, where “b” represents a basic residue, within a similar distance from the membrane. The similarity in charged residues associated with a mono-leucine, located in a region of the HB-EGF cytoplasmic domain similar to the location of the AREG motif, suggests this sequence could be the HB-EGF BL sorting motif. This is a future line of investigation that has been opened by the discovery of the novel AREG BL motif.

The steady state polarized distribution of AREG is dependent on the epithelial specific adaptor protein AP-1B (Figure 12). My data suggest AREG

biosynthetic delivery to the BL surface is independent of AP-1B because of the amount of AREG present on the BL surface in LLC-PK1 cells and μ1B KD MDCK cells. However, I demonstrated AREG is dependent on AP-1B after endocytosis for proper recycling back to the BL surface in LLC-PK1 cells (Figure 13). Interestingly, AREG is the most rapidly endocytosed of the EGFR ligands, suggesting the proper recycling of AREG is important for its function (personal communication with Steve Wiley, unpublished data). AREG is the only EGFR ligand known to date to be dependent on AP-1B for polarized distribution. TGFα is delivered to the BL surface by the CaRT protein NKD2 and is independent of AP-1B for polarized distribution (Li et al., 2007). EGF is delivered to both the apical and BL surface and selectively cleaved from the BL surface (Dempsey et al., 1997). EGF does contain a BL sorting motif, which if mutated impairs BL delivery (Groenestege et al., 2007). The role AP-1B plays in BL delivery of EGF has not been investigated. EREG is the most recent EGFR ligand to be investigated in the Coffey laboratory and has been shown to contain a tyrosine-based BL sorting motif that is AP-1B-independent (unpublished data). Future studies will discern if other EGFR ligands rely on AP-1B for polarized distribution.

The EGFR is dependent on AP-1B for polarized distribution in a similar manner as AREG. In LLC-PK1 cells, the EGFR is present on both the apical and BL surface (Ryan et al., 2010). The EGFR was shown to bind AP-1B via a non-canonical di-leucine motif in an *in vitro* peptide pulldown assay. Interestingly, when an acidic residue was introduced to create a canonical di-leucine motif, the EGFR was still delivered on the BL surface but absent from the apical surface in

LLC-PK1 cells. The authors concluded the EGFR is delivered to the BL surface via multiple routes, both AP-1B-depenent and independent (Ryan et al., 2010). I draw a different conclusion; the EGFR is delivered to the BL surface via an AP-1B-independent route but is recycled via an AP-1B-dependent route, just like AREG. Introduction of the canonical di-leucine motif created a lysosomal targeting signal that may have diverted the EGFR from the recycling endosome and prevented mis-recycling to the apical surface (Letourneur and Klausner, 1992). If I am correct, AREG and the EGFR are both delivered to the BL surface via AP-1B-independent routes but are both dependent on AP-1B for proper recycling back to the BL surface.

Future studies of the signal recognized by AP-1B in AREG could shed light on how the EGFR is recycled by AP-1B. Analysis for similarities between the EGFR non-canonical di-leucine signal demonstrated to bind AP-1B and the AREG mono-leucine motif reveals some commonalities. The EGFR di-leucine and AREG mono-leucine motifs are surrounded by similarly charged residues (RRLLQE vs KKLRQE). Comparisons of the AREG cytoplasmic domain structure with the previously described EGFR structure of this region my reveal similarities between the AREG and EGFR cytoplasmic domains (Hobert et al., 1997). It would also be interesting to know if both of the leucine residues in the EGFR di-leucine motif are necessary for binding to AP-1B. While mutation of the two basic lysine residues in the AREG cytoplasmic domain did not affect BL distribution, mutation of the single leucine did and may have disrupted the AP-1B interaction.

This recent report on EGFR interaction with AP-1B via leucine residues may provide important clues into how AREG interacts with AP-1B (Ryan et al., 2010).

Post-Translational Modification of AREG

Analysis of AREG in exosomes revealed a possible post-translational modification of AREG not previously observed in AREG IP or cellular lysate samples. AREG is known to be N-glycosylated during its transit through the Golgi to the cell surface (Brown et al., 1998). However, the modifications detected in the exosome preparations were much more extensive and created a smearing pattern more indicative of ubiquitylation than glycosylation (Figure 15). The enrichment of the modified AREG in exosomes suggests the modification could be important for delivery to exosomes, a process that is currently poorly understood.

I could not identify the modification on the exosomal AREG due to the technical difficulties of isolating the transmembrane AREG from the exosomes. However, I was able to identify ubiquitin as a possible modification of AREG using HA-tagged ubiquitin (Figure 16). While ubiquitin may not be the modification seen in the exosomes, it is still interesting to know AREG does contain sites suitable for ubiquitylation. This information could be useful in future studies of how AREG is regulated at the cell surface, especially considering AREG is the most rapidly endocytosed EGFR ligand and is recycled in an AP-1B-dependent process (Figure 13 and personal communication with Steve Wiley, unpublished data). Analysis of the AREG cytoplasmic domain, which only

contains three lysine residues, may reveal an unknown consensus ubiquitylation site present in other proteins important in disease.

I was able to support the hypothesis that ubiquitylation regulates exosomal AREG without directly demonstrating ubiquitylation is the modification seen in exosomes. This was accomplished analyzing exosome preparations from MDCK cells expressing wild-type AREG and lysine-free AREG-K2A. The data suggest AREG-K2A was not incorporated into the exosomes as efficiently as wild-type AREG (Figure 17). These preliminary data provide a foundation for future investigations into the role ubiquitylation may play in regulating exosomal AREG.

Ubiquitylated proteins are present in exosomes (Buschow et al., 2005). However, the data suggest the majority of AREG in exosomes is not ubiquitylated. Addition of one ubiquitin monomer to a protein increases the molecular weight of that protein by approximately 9 kDa, but the prominent AREG bands detected in exosomes do not represent an increased molecular weight. My hypothesis is ubiquitylation regulates delivery to exosomes followed by deubiquitylation prior to ILV formation, a hypothesis supported by the literature (Hurley, 2008; Swaminathan et al., 1999). The smear seen in exosomes could result from inefficient deubiquitylation prior to ILV formation. Future studies will clarify the role ubiquitin plays in regulating AREG.

AREG Interacting Proteins

Two proteins, TM165 and kinectin, were identified as possible interacting proteins for AREG and both have the potential to play important roles in AREG

trafficking. Kinectin interacts with the molecular motor kinesin and has been demonstrated to play a role in vesicular secretion and organelle trafficking to the cell periphery (Bai et al., 2006; Ong et al., 2000). There is no reported function for TM165, but it co-localizes with AREG in a region of the cell possibly involved in proteins sorting and trafficking (Figure 20). While these two proteins cleared the most hurdles of all the proteins identified in the two screens for AREG interacting proteins, the remaining identified proteins should not be completely ignored. The complete list of all the proteins identified in these screens is included in this thesis for future reference, as they may become relevant in future studies of AREG (Table 3, Table 4, and Appendix A).

My graduate studies have focused on the EGFR ligand AREG and how it is trafficked within polarized epithelial cells. The EGFR signaling pathway is often dysregulated in cancer, so understanding each aspect of this pathway provides us with additional knowledge to develop effective treatments. My work has expanded this knowledge by revealing the critical elements involved in delivery of AREG to the BL surface of polarized epithelial cells. I have demonstrated that AREG contains a mono-leucine-based BL sorting motif and depends on AP-1B for steady state polar distribution. Ubiquitylation has been revealed as a possible level of AREG regulation. Kinecitn and TM165 have been uncovered as potential interacting proteins for AREG. Additional studies are needed, but our understanding of how AREG is trafficked and regulated has been expanded.

APPENDIX A

Complete list of proteins identified in the crosslinked AREG co-IP screen for AREG interacting proteins. Protein identification numbers are listed in the left column, protein descriptions in the center column and peptide coverage in the right column. Proteins are listed in descending order of peptide coverage.

Protein	Description	Coverage
IPI:IPI00026272.2	Histone H2A type 1-B	42
IPI:IPI00031562.3	Histone H2A type 3	42
IPI:IPI00081836.3	Histone H2A type 1-H	42
IPI:IPI00216456.5	Histone H2A type 1-C	42
IPI:IPI00220855.3	H2A histone family	42
IPI:IPI00255316.5	Histone H2A type 1-D	42
IPI:IPI00291764.5	Histone H2A type 1	42
IPI:IPI00552873.2	Histone H2A type 1-J	42
IPI:IPI00008530.1	60S acidic ribosomal protein P0	40
IPI:IPI00453473.6	Histone H4	39
IPI:IPI00794746.1	24 kDa protein	38
IPI:IPI00008529.1	60S acidic ribosomal protein P2	37
Cntm_P13645|K1C10_HUMAN	Keratin	35
IPI:IPI00009865.2	Keratin	35
IPI:IPI00102165.3	H2A histone family member J	35
Cntm_Q65ZC0|Q65ZC0_MOUSE	Kappa light chain C_region (Fragment) - Mus musculus (Mouse).	34
IPI:IPI00030179.3	60S ribosomal protein L7	32
IPI:IPI00141938.4	H2A histone family	32
IPI:IPI00219156.7	60S ribosomal protein L30	32
IPI:IPI00217030.10	40S ribosomal protein S4	31
IPI:IPI00013415.1	40S ribosomal protein S7	31
IPI:IPI00215719.6	60S ribosomal protein L18	30
IPI:IPI00216587.9	40S ribosomal protein S8	30
IPI:IPI00413324.6	60S ribosomal protein L17	30
IPI:IPI00478208.2	hypothetical protein LOC645296	30
IPI:IPI00514874.1	hypothetical protein LOC645441	30
IPI:IPI00644171.1	hypothetical protein LOC642250	30
IPI:IPI00010153.5	60S ribosomal protein L23	30
IPI:IPI00742805.1	15 kDa protein	30
IPI:IPI00795408.1	15 kDa protein	30
IPI:IPI00783060.1	Ubiquitin	30

IPI:IPI00003918.6	60S ribosomal protein L4	29
IPI:IPI00012023.1	Amphiregulin precursor	29
IPI:IPI00470657.1	Anti-colorectal carcinoma heavy chain	28
IPI:IPI00470528.5	60S ribosomal protein L15	28
IPI:IPI00550032.1	Ribosomal protein L15 pseudogene 3	28
IPI:IPI00847986.1	Isoform 2 of 40S ribosomal protein S24	28
IPI:IPI00018278.3	Histone H2AV	28
IPI:IPI00218448.4	Histone H2A.Z	28
IPI:IPI00651660.1	ribosomal protein L3 isoform b	27
IPI:IPI00220740.1	Isoform 2 of Nucleophosmin	27
IPI:IPI00029750.1	Isoform 1 of 40S ribosomal protein S24	27
IPI:IPI00008527.3	60S acidic ribosomal protein P1	27
IPI:IPI00026271.5	40S ribosomal protein S14	27
IPI:IPI00221092.8	40S ribosomal protein S16	27
IPI:IPI00640929.1	Ribosomal protein S6	27
IPI:IPI00795465.1	Protein	27
IPI:IPI00796075.1	20 kDa protein	27
IPI:IPI00414860.6	60S ribosomal protein L37a	27
IPI:IPI00554723.5	60S ribosomal protein L10	26
IPI:IPI00853161.1	ribosomal protein L10	26
IPI:IPI00247583.5	60S ribosomal protein L21	26
IPI:IPI00788010.1	similar to 60S ribosomal protein L21	26
IPI:IPI00444262.3	CDNA FLJ45706 fis	25
IPI:IPI00472171.2	RPL7 protein	25
IPI:IPI00412579.6	60S ribosomal protein L10a	25
IPI:IPI00827508.1	Ribosomal protein L1	25
IPI:IPI00069693.4	Uncharacterized protein ENSP00000350479	25
IPI:IPI00219486.2	40S ribosomal protein S24. Isoform 2	25
IPI:IPI00845507.1	Ribosomal protein L21 variant (Fragment)	25
IPI:IPI00024933.3	60S ribosomal protein L12	25
IPI:IPI00550021.4	60S ribosomal protein L3	24
IPI:IPI00013485.3	40S ribosomal protein S2	24
IPI:IPI00479366.1	Uncharacterized protein ENSP00000351543	24
IPI:IPI00549248.4	Isoform 1 of Nucleophosmin	24
IPI:IPI00031812.3	Nuclease sensitive element-binding protein 1	24
IPI:IPI00385699.3	Uncharacterized protein YBX1	24
IPI:IPI00450235.1	Nuclease sensitive element binding protein-1	24
IPI:IPI00646899.1	Ribosomal protein L10	24
IPI:IPI00555841.2	15 kDa protein	24

IPI:IPI00329389.8	60S ribosomal protein L6	23
IPI:IPI00790342.1	60S ribosomal protein L6	23
IPI:IPI00419880.6	40S ribosomal protein S3a	23
IPI:IPI00472119.2	Uncharacterized protein ENSP00000343748	23
IPI:IPI00221089.5	40S ribosomal protein S13	23
IPI:IPI00216153.7	40S ribosomal protein S15	23
IPI:IPI00827674.1	Isoform 2 of Nucleolin	22
IPI:IPI00794734.1	13 kDa protein	22
IPI:IPI00219155.5	60S ribosomal protein L27	22
IPI:IPI00550247.2	11 kDa protein	22
IPI:IPI00221093.7	40S ribosomal protein S17	22
IPI:IPI00414603.3	similar to 40S ribosomal protein S17 isoform 1	22
IPI:IPI00604620.3	Isoform 1 of Nucleolin	21
IPI:IPI00299573.12	60S ribosomal protein L7a	21
IPI:IPI00479315.2	Uncharacterized protein ENSP00000351738	21
Cntm_P00761|TRYP_PIG	Trypsin - Sus scrofa (Pig).	21
IPI:IPI00382885.1	60S ribosomal protein L27	21
IPI:IPI00550766.1	RRP1-like protein	20
IPI:IPI00021266.1	60S ribosomal protein L23a	20
IPI:IPI00793523.1	18 kDa protein	20
IPI:IPI00794894.1	Protein	20
IPI:IPI00023048.4	Elongation factor 1-delta	20
IPI:IPI00398135.2	hypothetical protein LOC389435	20
IPI:IPI00456758.4	60S ribosomal protein L27a	20
IPI:IPI00827619.1	16 kDa protein	20
IPI:IPI00477179.1	Isoform 2 of Nucleolar RNA helicase 2	19
IPI:IPI00218592.5	Isoform ASF-3 of Splicing factor	19
IPI:IPI00186712.5	OTTHUMP00000018641	19
IPI:IPI00401819.2	Putative uncharacterized protein RPS26	19
IPI:IPI00655650.2	40S ribosomal protein S26	19
IPI:IPI00295992.4	Isoform 2 of ATPase family AAA domain-containing protein 3A	18
IPI:IPI00007188.5	ADP/ATP translocase 2	18
IPI:IPI00005589.1	Uncharacterized protein ENSP00000275524	18
IPI:IPI00395998.5	60S ribosomal protein L32	18
IPI:IPI00456429.3	ubiquitin and ribosomal protein L40 precursor	18
IPI:IPI00012493.1	40S ribosomal protein S20	18
IPI:IPI00015953.3	Isoform 1 of Nucleolar RNA helicase 2	17
IPI:IPI00003881.5	Heterogeneous nuclear ribonucleoprotein F	17

IPI:IPI00012772.8	60S ribosomal protein L8	17
IPI:IPI00412607.6	60S ribosomal protein L35	17
IPI:IPI00014230.1	Complement component 1 Q subcomponent-binding protein	17
IPI:IPI00791426.1	13 kDa protein	17
IPI:IPI00026302.3	60S ribosomal protein L31	17
IPI:IPI00856058.1	ribosomal protein L31 isoform 3	17
IPI:IPI00025091.3	40S ribosomal protein S11	17
IPI:IPI00328753.1	Isoform 1 of Kinectin	16
IPI:IPI00789159.1	22 kDa protein	16
IPI:IPI00215884.4	Isoform ASF-1 of Splicing factor	16
IPI:IPI00021924.1	Histone H1x	16
IPI:IPI00848331.1	ribosomal protein L31 isoform 2	16
IPI:IPI00795717.1	19 kDa protein	16
IPI:IPI00037070.2	Isoform 2 of Heat shock cognate 71 kDa protein	15
IPI:IPI00795040.1	Heat shock 70kDa protein 8 isoform 2 variant (Fragment)	15
IPI:IPI00217465.5	Histone H1.2	15
IPI:IPI00217467.3	Histone H1.4	15
IPI:IPI00465361.4	60S ribosomal protein L13	15
IPI:IPI00797230.1	32 kDa protein	15
IPI:IPI00218606.7	40S ribosomal protein S23	15
IPI:IPI00787131.1	similar to 60S ribosomal protein L35	15
IPI:IPI00179330.6	ubiquitin and ribosomal protein S27a precursor	15
IPI:IPI00784990.2	Ubiquitin C splice variant	15
IPI:IPI00794659.1	16 kDa protein	15
IPI:IPI00217466.3	Histone H1.3	14
IPI:IPI00515047.1	Actin	14
IPI:IPI00815690.1	Leucocyte antigen A precursor	14
IPI:IPI00221088.5	40S ribosomal protein S9	14
IPI:IPI00739952.2	similar to ribosomal protein S23	14
IPI:IPI00793102.1	11 kDa protein	14
IPI:IPI00031691.1	60S ribosomal protein L9	14
IPI:IPI00218591.2	Isoform ASF-2 of Splicing factor	13
IPI:IPI00745955.2	Probable rRNA-processing protein EBP2	13
IPI:IPI00003865.1	Isoform 1 of Heat shock cognate 71 kDa protein	12
IPI:IPI00816229.1	ACTA2 protein (Fragment)	12
IPI:IPI00306332.4	60S ribosomal protein L24	12
IPI:IPI00025329.1	60S ribosomal protein L19	12
IPI:IPI00029731.8	60S ribosomal protein L35a	12
IPI:IPI00735961.2	similar to ribosomal protein L35a	12

IPI:IPI00005978.8	Splicing factor	12
IPI:IPI00796848.1	24 kDa protein	12
IPI:IPI00328840.9	THO complex subunit 4	12
IPI:IPI00742905.1	146 kDa protein	11
IPI:IPI00844578.1	ATP-dependent RNA helicase A	11
IPI:IPI00410017.1	Isoform 2 of Polyadenylate-binding protein 1	11
IPI:IPI00478522.1	61 kDa protein	11
IPI:IPI00216237.5	60S ribosomal protein L36	11
IPI:IPI00644631.3	HLA class I histocompatibility antigen	11
IPI:IPI00005198.2	Interleukin enhancer-binding factor 2	11
IPI:IPI00793696.1	19 kDa protein	11
IPI:IPI00396321.1	Leucine-rich repeat-containing protein 59	11
IPI:IPI00550239.4	Histone H1.0	11
IPI:IPI00024684.1	Interferon-induced GTP-binding protein Mx2	10
IPI:IPI00402391.3	Isoform 3 of Heterogeneous nuclear ribonucleoprotein U-like protein 1	10
IPI:IPI00736859.1	Isoform 4 of Heterogeneous nuclear ribonucleoprotein U-like protein 1	10
IPI:IPI00021840.1	40S ribosomal protein S6	10
IPI:IPI00008708.5	Ribosomal L1 domain-containing protein 1	10
IPI:IPI00642046.1	Putative uncharacterized protein	10
IPI:IPI00735318.1	similar to ribosomal protein L13a isoform 2	10
IPI:IPI00418813.2	CDNA FLJ46113 fis	10
IPI:IPI00719280.2	ubiquitin B precursor	10
IPI:IPI00798155.3	Ubiquitin C splice variant	10
IPI:IPI00015838.3	Cell growth-regulating nucleolar protein	10
IPI:IPI00413611.1	DNA topoisomerase 1	9
IPI:IPI00644079.2	heterogeneous nuclear ribonucleoprotein U isoform a	9
IPI:IPI00008524.1	Isoform 1 of Polyadenylate-binding protein 1	9
IPI:IPI00796945.1	70 kDa protein	9
IPI:IPI00013070.2	Isoform 1 of Heterogeneous nuclear ribonucleoprotein U-like protein 1	9
IPI:IPI00167147.1	Isoform 2 of Heterogeneous nuclear ribonucleoprotein U-like protein 1	9
IPI:IPI00218609.2	Isoform Short of Double-stranded RNA-binding protein Staufen homolog 1	9
IPI:IPI00641873.1	Staufen	9
IPI:IPI00643664.1	staufen isoform c	9
IPI:IPI00000875.6	Elongation factor 1-gamma	9
IPI:IPI00747497.1	50 kDa protein	9
IPI:IPI00642971.3	eukaryotic translation elongation factor 1 delta isoform 1	9
IPI:IPI00304612.9	60S ribosomal protein L13a	9

IPI:IPI00398949.1	Uncharacterized protein ENSP00000349505	9
IPI:IPI00398964.2	similar to ribosomal protein L13a	9
IPI:IPI00398983.3	OTTHUMP00000018470	9
IPI:IPI00003362.2	HSPA5 protein	8
IPI:IPI00215637.5	ATP-dependent RNA helicase DDX3X	8
IPI:IPI00000001.2	Isoform Long of Double-stranded RNA-binding protein Staufen homolog 1	8
IPI:IPI00328715.4	Protein LYRIC	8
IPI:IPI00793729.1	UBC protein	8
IPI:IPI00000494.6	60S ribosomal protein L5	8
IPI:IPI00513959.3	RNA binding motif protein 39	8
IPI:IPI00843773.1	Putative uncharacterized protein DKFZp686A11192	8
IPI:IPI00027107.5	Tu translation elongation factor	8
IPI:IPI00011253.3	40S ribosomal protein S3	8
IPI:IPI00005416.3	NICE-4 protein (Fragment)	8
IPI:IPI00005492.2	WD repeat-containing protein 5	8
IPI:IPI00102815.1	Nucleolar complex protein 3 homolog	7
IPI:IPI00843861.1	Uncharacterized protein NOC3L	7
IPI:IPI00012341.1	Isoform SRP40-1 of Splicing factor	7
IPI:IPI00009328.4	Eukaryotic initiation factor 4A-III	7
IPI:IPI00555602.1	CD68 antigen variant (Fragment)	7
IPI:IPI00746554.2	48 kDa protein	7
IPI:IPI00027831.1	Glutamate-rich WD repeat-containing protein 1	7
IPI:IPI00005024.3	Isoform 1 of Myb-binding protein 1A	6
IPI:IPI00607584.1	Isoform 2 of Myb-binding protein 1A	6
IPI:IPI00383296.5	Isoform 2 of Heterogeneous nuclear ribonucleoprotein M	6
IPI:IPI00555857.1	CS0DF038YO05 variant (Fragment)	6
IPI:IPI00556297.1	Arginine/serine-rich splicing factor 6 variant (Fragment)	6
IPI:IPI00025491.1	Eukaryotic initiation factor 4A-I	6
IPI:IPI00032374.3	Isoform 2 of RRP1-like protein B	6
IPI:IPI00290952.6	Isoform 1 of RRP1-like protein B	6
IPI:IPI00220834.8	ATP-dependent DNA helicase 2 subunit 2	6
IPI:IPI00479630.3	Isoform 3 of Fragile X mental retardation syndrome-related protein 1	6
IPI:IPI00554715.2	Isoform 2 of Fragile X mental retardation syndrome-related protein 1	6
IPI:IPI00163505.2	Isoform 1 of RNA-binding protein 39	6
IPI:IPI00215801.1	Isoform 2 of RNA-binding protein 39	6
IPI:IPI00556364.1	Interleukin enhancer binding factor 3 isoform c variant (Fragment)	6

IPI:IPI00017617.1	Probable ATP-dependent RNA helicase DDX5	5
IPI:IPI00023785.6	DEAD box polypeptide 17 isoform 1	5
IPI:IPI00651653.1	Isoform 3 of Probable ATP-dependent RNA helicase DDX17	5
IPI:IPI00651677.1	Isoform 2 of Probable ATP-dependent RNA helicase DDX17	5
IPI:IPI00012726.4	Isoform 1 of Polyadenylate-binding protein 4	5
IPI:IPI00555747.1	Isoform 2 of Polyadenylate-binding protein 4	5
IPI:IPI00642944.1	Poly	5
IPI:IPI00414676.6	Heat shock protein HSP 90-beta	5
IPI:IPI00796844.1	Full-length cDNA clone CS0CAP007YF18 of Thymus of Homo sapiens	5
IPI:IPI00171903.2	Isoform 1 of Heterogeneous nuclear ribonucleoprotein M	5
IPI:IPI00328293.2	Serine/arginine repetitive matrix 1	5
IPI:IPI00647720.1	Isoform 1 of Serine/arginine repetitive matrix protein 1	5
IPI:IPI00012345.2	Isoform SRP55-1 of Splicing factor	5
IPI:IPI00215879.1	Isoform SRP55-3 of Splicing factor	5
IPI:IPI00016249.2	Isoform 1 of Fragile X mental retardation syndrome-related protein 1	5
IPI:IPI00018971.7	52 kDa Ro protein	5
IPI:IPI00025447.8	Elongation factor 1-alpha	5
IPI:IPI00396485.3	Elongation factor 1-alpha 1	5
IPI:IPI00472724.1	Elongation factor 1-alpha	5
IPI:IPI00847435.1	EEF1A1 protein	5
IPI:IPI00642904.1	Poly	4
IPI:IPI00334775.6	85 kDa protein	4
IPI:IPI00604607.2	Hsp89-alpha-delta-N	4
IPI:IPI00797482.1	CDNA FLJ32377 fis	4
IPI:IPI00219330.2	Isoform 5 of Interleukin enhancer-binding factor 3	4
IPI:IPI00298789.2	Isoform 2 of Interleukin enhancer-binding factor 3	4
IPI:IPI00414335.1	Isoform 3 of Interleukin enhancer-binding factor 3	4
IPI:IPI00556173.1	Isoform 6 of Interleukin enhancer-binding factor 3	4
IPI:IPI00015808.3	Nucleolar GTP-binding protein 2	4
IPI:IPI00797590.2	NOL1 protein	4
IPI:IPI00025874.2	Dolichyl-diphosphooligosaccharide--protein glycosyltransferase 67 kDa subunit precursor	4
IPI:IPI00382470.3	heat shock protein 90kDa alpha (cytosolic)	3
IPI:IPI00784295.2	Isoform 1 of Heat shock protein HSP 90-alpha	3
IPI:IPI00789847.1	Protein	3

IPI:IPI00798127.1	ubiquitin C	3
IPI:IPI00298788.4	Isoform 1 of Interleukin enhancer-binding factor 3	3
IPI:IPI00418313.3	Isoform 4 of Interleukin enhancer-binding factor 3	3
IPI:IPI00029019.5	Isoform 2 of Ubiquitin-associated protein 2-like	3
IPI:IPI00181306.3	Isoform 3 of Ubiquitin-associated protein 2-like	3
IPI:IPI00412535.2	115 kDa protein	3
IPI:IPI00514856.4	Isoform 1 of Ubiquitin-associated protein 2-like	3
IPI:IPI00294891.4	Isoform 2 of Putative RNA methyltransferase NOL1	3
IPI:IPI00654555.2	Isoform 1 of Putative RNA methyltransferase NOL1	3
IPI:IPI00177817.4	Isoform SERCA2A of Sarcoplasmic/endoplasmic reticulum calcium ATPase 2	2
IPI:IPI00219078.5	Isoform SERCA2B of Sarcoplasmic/endoplasmic reticulum calcium ATPase 2	2
IPI:IPI00747443.1	Uncharacterized protein ATP2A2	2
IPI:IPI00792389.1	115 kDa protein	2
IPI:IPI00794296.1	110 kDa protein	2
IPI:IPI00644127.1	Isoleucyl-tRNA synthetase	2

APPENDIX B

This figure demonstrates the accuracy of the 6R1C2.4 anti-AREG mouse monoclonal antibody used throughout my work. Previous work published by the Coffey lab described the main AREG bands detected on SDS-PAGE gels to be 50 kDa, a 28-26 kDa doublet, and 16 kDa (Figure 8) (Brown et al., 1998). These bands were detected from samples metabolically labeled with Tran^{35}S-label and run under reduced conditions. In order to use the 6R1C2.4 antibody for western blotting, I determined the samples must be run under non-reduced conditions in order to preserve the epitope in the extracellular domain recognized by the antibody. The 6R1C2.4 antibody cannot detect reduced AREG. The main bands detected on AREG western blots using 6R1C2.4 are 50 kDa, a doublet below 25 kDa, and a16 kDa band. The size of this doublet is different from the previously described size, so therefore, I set out to confirm I was indeed detecting the membrane forms of AREG in my western blots.

The AREG western blot below is of four different cell lines (from left to right): MDCK II cells, which contain no detectible AREG and act as a negative control; HCA-7 cells, which express high levels of endogenous AREG and act as a positive control for wild-type endogenous AREG; MDCK-ARTL, which express a truncated form of AREG lacking all but four residues of the cytoplasmic domain; MDCK-AR, which over express full-length wild-type AREG. TL is the total lysate sample and IP is an immunoprecipitation of AREG using the 6R1C2.4 antibody. The samples were separated on a 12.5% SDS-PAGE gel and transferred to a nitrocellulose membrane. The membrane was blotted with 6R1C2.4 and an anti-mouse TrueBlot secondary HRP-conjugated antibody.

This blot demonstrates the accuracy of the antibody and confirms the detection of membrane AREG because of the shift seen in the ARTL lanes. The ARTL form of AREG does not contain the cytoplasmic domain so it should run slightly smaller then the wild-type membrane AREG. Slightly smaller forms of all the wild-type AREG forms can be seen in the ARTL samples, confirming these bands to be actual membrane forms of wild-type AREG. If these were not membrane forms, but instead soluble forms, the ARTL bands would be the same size as the wild-type bands. The absence of signal in the MDCK II negative control demonstrates the lack of background. The wild-type AREG bands detected in the MDCK-AR samples are the same size as the AREG bands detected in the HCA-7 samples, which are endogenously produced AREG. Combined, the results in this blot demonstrate the accuracy of the 6R1C2.4 mouse anti-AREG antibody in detecting membrane AREG in total cell lysate and IP samples.

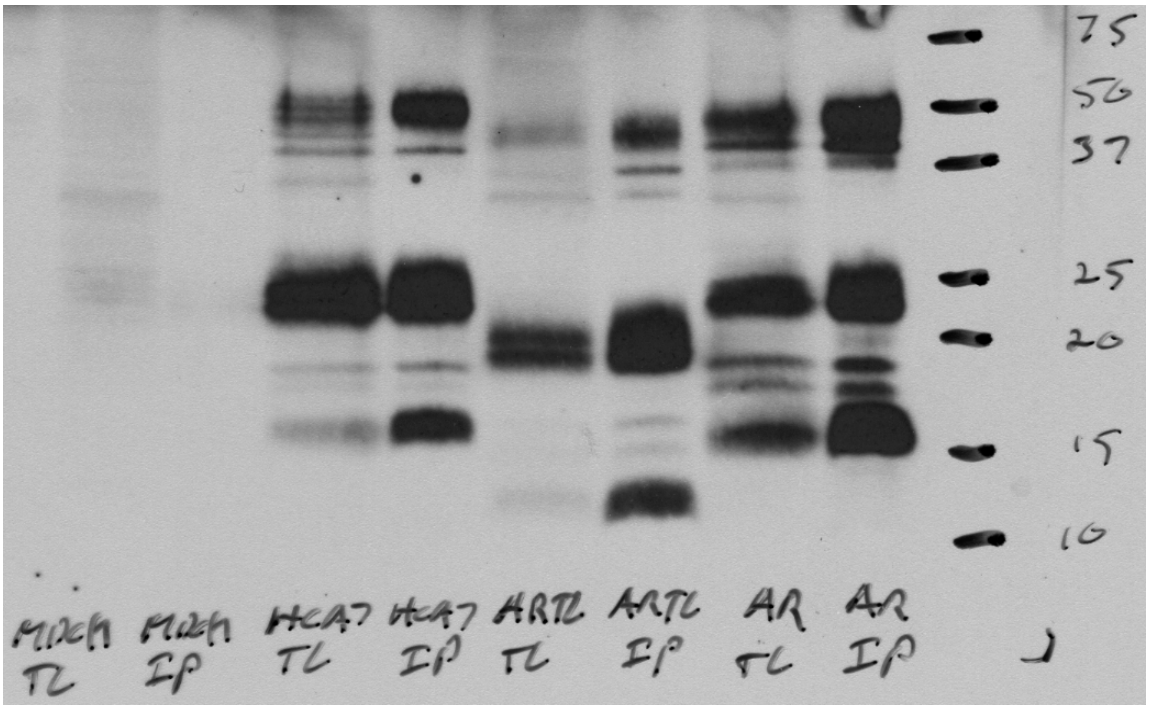
75
50
37
25
20
15
10
TL
IP
TL
IP
TL
IP
TL
IP

REFERENCES

Aberle, H., S. Butz, J. Stappert, H. Weissig, R. Kemler, and H. Hoschuetzky. 1994. Assembly of the cadherin-catenin complex in vitro with recombinant proteins. *J Cell Sci*. 107 (Pt 12):3655-3663.

Aguilar, R.C., M. Boehm, I. Gorshkova, R.J. Crouch, K. Tomita, T. Saito, H. Ohno, and J.S. Bonifacino. 2001. Signal-binding specificity of the mu4 subunit of the adaptor protein complex AP-4. *The Journal of biological chemistry*. 276:13145-13152.

Aijaz, S., M.S. Balda, and K. Matter. 2006. Tight junctions: molecular architecture and function. *Int Rev Cytol*. 248:261-298.

Angelow, S., R. Ahlstrom, and A.S. Yu. 2008. Biology of claudins. *Am J Physiol Renal Physiol*. 295:F867-876.

Ardoin, S.P., J.C. Shanahan, and D.S. Pisetsky. 2007. The role of microparticles in inflammation and thrombosis. *Scand J Immunol*. 66:159-165.

Bachmann, A., M. Schneider, E. Theilenberg, F. Grawe, and E. Knust. 2001. Drosophila Stardust is a partner of Crumbs in the control of epithelial cell polarity. *Nature*. 414:638-643.

Bai, J.Z., Y. Mon, and G.W. Krissansen. 2006. Kinectin participates in microtubule-dependent hormone secretion in pancreatic islet beta-cells. *Cell Biol Int*. 30:885-894.

Baker, R.T., J.W. Tobias, and A. Varshavsky. 1992. Ubiquitin-specific proteases of Saccharomyces cerevisiae. Cloning of UBP2 and UBP3, and functional analysis of the UBP gene family. *The Journal of biological chemistry*. 267:23364-23375.

Balda, M.S., and K. Matter. 2008. Tight junctions at a glance. *J Cell Sci*. 121:3677-3682.

Balda, M.S., J.A. Whitney, C. Flores, S. Gonzalez, M. Cereijido, and K. Matter. 1996. Functional dissociation of paracellular permeability and transepithelial electrical resistance and disruption of the apical-basolateral intramembrane diffusion barrier by expression of a mutant tight junction membrane protein. *The Journal of cell biology*. 134:1031-1049.

Bilder, D., and N. Perrimon. 2000. Localization of apical epithelial determinants by the basolateral PDZ protein Scribble. *Nature*. 403:676-680.

Boehm, M., R.C. Aguilar, and J.S. Bonifacino. 2001. Functional and physical interactions of the adaptor protein complex AP-4 with ADP-ribosylation factors (ARFs). *EMBO J*. 20:6265-6276.

Boman, A.L., C. Zhang, X. Zhu, and R.A. Kahn. 2000. A family of ADP-ribosylation factor effectors that can alter membrane transport through the trans-Golgi. *Molecular biology of the cell*. 11:1241-1255.

Bomsel, M., R. Parton, S.A. Kuznetsov, T.A. Schroer, and J. Gruenberg. 1990. Microtubule- and motor-dependent fusion in vitro between apical and basolateral endocytic vesicles from MDCK cells. *Cell*. 62:719-731.

Bonifacino, J.S. 2004. The GGA proteins: adaptors on the move. *Nat Rev Mol Cell Biol*. 5:23-32.

Bonifacino, J.S., and L.M. Traub. 2003. Signals for sorting of transmembrane proteins to endosomes and lysosomes. *Annu Rev Biochem*. 72:395-447.

Braulke, T., and J.S. Bonifacino. 2009. Sorting of lysosomal proteins. *Biochim Biophys Acta*. 1793:605-614.

Brewer, C.B., and M.G. Roth. 1991. A single amino acid change in the cytoplasmic domain alters the polarized delivery of influenza virus hemagglutinin. *The Journal of cell biology*. 114:413-421.

Bringman, T.S., P.B. Lindquist, and R. Derynck. 1987. Different transforming growth factor-alpha species are derived from a glycosylated and palmitoylated transmembrane precursor. *Cell*. 48:429-440.

Brown, C.L., R.J. Coffey, and P.J. Dempsey. 2001. The proamphiregulin cytoplasmic domain is required for basolateral sorting, but is not essential for constitutive or stimulus-induced processing in polarized Madin-Darby canine kidney cells. *The Journal of biological chemistry*. 276:29538-29549.

Brown, C.L., K.S. Meise, G.D. Plowman, R.J. Coffey, and P.J. Dempsey. 1998. Cell surface ectodomain cleavage of human amphiregulin precursor is sensitive to a metalloprotease inhibitor. Release of a predominant N-glycosylated 43-kDa soluble form. *The Journal of biological chemistry*. 273:17258-17268.

Burgos, P.V., G.A. Mardones, A.L. Rojas, L.L. daSilva, Y. Prabhu, J.H. Hurley, and J.S. Bonifacino. 2010. Sorting of the Alzheimer's disease amyloid precursor protein mediated by the AP-4 complex. *Dev Cell*. 18:425-436.

Buschow, S.I., J.M. Liefhebber, R. Wubbolts, and W. Stoorvogel. 2005. Exosomes contain ubiquitinated proteins. *Blood Cells Mol Dis*. 35:398-403.

Cancino, J., C. Torrealba, A. Soza, M.I. Yuseff, D. Gravotta, P. Henklein, E. Rodriguez-Boulan, and A. Gonzalez. 2007. Antibody to AP1B adaptor blocks biosynthetic and recycling routes of basolateral proteins at recycling endosomes. *Molecular biology of the cell*. 18:4872-4884.

Cao, G., J.G. Hoenderop, and R.J. Bindels. 2008a. Insight into the molecular regulation of the epithelial magnesium channel TRPM6. *Curr Opin Nephrol Hypertens*. 17:373-378.

Cao, Z., C. Li, J.N. Higginbotham, J.L. Franklin, D.L. Tabb, R. Graves-Deal, S. Hill, K. Cheek, W.G. Jerome, L.A. Lapierre, J.R. Goldenring, A.J. Ham, and R.J. Coffey. 2008b. Use of fluorescence-activated vesicle sorting for isolation of Naked2-associated, basolaterally targeted exocytic vesicles for proteomics analysis. *Mol Cell Proteomics*. 7:1651-1667.

Carmosino, M., G. Valenti, M. Caplan, and M. Svelto. 2010. Polarized traffic towards the cell surface: how to find the route. *Biol Cell*. 102:75-91.

Carpenter, G. 1987. Receptors for epidermal growth factor and other polypeptide mitogens. *Annu Rev Biochem*. 56:881-914.

Castorino, J.J., S. Deborde, A. Deora, R. Schreiner, S.M. Gallagher-Colombo, E. Rodriguez-Boulan, and N.J. Philp. 2010. Basolateral sorting signals regulating tissue-specific polarity of heteromeric monocarboxylate transporters in epithelia. *Traffic*.

Chalmers, A.D., M. Pambos, J. Mason, S. Lang, C. Wylie, and N. Papalopulu. 2005. aPKC, Crumbs3 and Lgl2 control apicobasal polarity in early vertebrate development. *Development (Cambridge, England)*. 132:977-986.

Chen, H.J., J. Yuan, and P. Lobel. 1997. Systematic mutational analysis of the cation-independent mannose 6-phosphate/insulin-like growth factor II receptor cytoplasmic domain. An acidic cluster containing a key aspartate is important for function in lysosomal enzyme sorting. *The Journal of biological chemistry*. 272:7003-7012.

Chen, W.J., J.L. Goldstein, and M.S. Brown. 1990. NPXY, a sequence often found in cytoplasmic tails, is required for coated pit-mediated internalization of the low density lipoprotein receptor. *The Journal of biological chemistry*. 265:3116-3123.

Chen, X., and I.G. Macara. 2005. Par-3 controls tight junction assembly through the Rac exchange factor Tiam1. *Nat Cell Biol*. 7:262-269.

Chung, E., R. Graves-Deal, J.L. Franklin, and R.J. Coffey. 2005. Differential effects of amphiregulin and TGF-alpha on the morphology of MDCK cells. *Exp Cell Res*. 309:149-160.

Cocucci, E., G. Racchetti, and J. Meldolesi. 2009. Shedding microvesicles: artefacts no more. *Trends Cell Biol*. 19:43-51.

Cohen, C.J., J.T. Shieh, R.J. Pickles, T. Okegawa, J.T. Hsieh, and J.M. Bergelson. 2001. The coxsackievirus and adenovirus receptor is a transmembrane component of the tight junction. *Proceedings of the National Academy of Sciences of the United States of America*. 98:15191-15196.

Collawn, J.F., L.A. Kuhn, L.F. Liu, J.A. Tainer, and I.S. Trowbridge. 1991. Transplanted LDL and mannose-6-phosphate receptor internalization signals promote high-efficiency endocytosis of the transferrin receptor. *EMBO J*. 10:3247-3253.

Cook, P.W., P.A. Mattox, W.W. Keeble, M.R. Pittelkow, G.D. Plowman, M. Shoyab, J.P. Adelman, and G.D. Shipley. 1991. A heparin sulfate-regulated human keratinocyte autocrine factor is similar or identical to amphiregulin. *Molecular and cellular biology*. 11:2547-2557.

Coradini, D., C. Casarsa, and S. Oriana. 2011. Epithelial cell polarity and tumorigenesis: new perspectives for cancer detection and treatment. *Acta Pharmacol Sin*. 32:552-564.

Coyne, C.B., and J.M. Bergelson. 2005. CAR: a virus receptor within the tight junction. *Adv Drug Deliv Rev*. 57:869-882.

D'Souza-Schorey, C., and P. Chavrier. 2006. ARF proteins: roles in membrane traffic and beyond. *Nat Rev Mol Cell Biol*. 7:347-358.

Damstrup, L., S.K. Kuwada, P.J. Dempsey, C.L. Brown, C.J. Hawkey, H.S. Poulsen, H.S. Wiley, and R.J. Coffey, Jr. 1999. Amphiregulin acts as an autocrine growth factor in two human polarizing colon cancer lines that exhibit domain selective EGF receptor mitogenesis. *British journal of cancer*. 80:1012-1019.

Davis, M.A., R.C. Ireton, and A.B. Reynolds. 2003. A core function for p120-catenin in cadherin turnover. *The Journal of cell biology*. 163:525-534.

Dell'Angelica, E.C., J. Klumperman, W. Stoorvogel, and J.S. Bonifacino. 1998. Association of the AP-3 adaptor complex with clathrin. *Science*. 280:431-434.

Dell'Angelica, E.C., C. Mullins, and J.S. Bonifacino. 1999a. AP-4, a novel protein complex related to clathrin adaptors. *The Journal of biological chemistry*. 274:7278-7285.

Dell'Angelica, E.C., R. Puertollano, C. Mullins, R.C. Aguilar, J.D. Vargas, L.M. Hartnell, and J.S. Bonifacino. 2000. GGAs: a family of ADP ribosylation factor-binding proteins related to adaptors and associated with the Golgi complex. *The Journal of cell biology*. 149:81-94.

Dell'Angelica, E.C., V. Shotelersuk, R.C. Aguilar, W.A. Gahl, and J.S. Bonifacino. 1999b. Altered trafficking of lysosomal proteins in Hermansky-Pudlak syndrome due to mutations in the beta 3A subunit of the AP-3 adaptor. *Mol Cell*. 3:11-21.

Dempsey, P.J., and R.J. Coffey. 1994. Basolateral targeting and efficient consumption of transforming growth factor-alpha when expressed in Madin-Darby canine kidney cells. *The Journal of biological chemistry*. 269:16878-16889.

Dempsey, P.J., K.S. Meise, and R.J. Coffey. 2003. Basolateral sorting of transforming growth factor-alpha precursor in polarized epithelial cells: characterization of cytoplasmic domain determinants. *Exp Cell Res*. 285:159-174.

Dempsey, P.J., K.S. Meise, Y. Yoshitake, K. Nishikawa, and R.J. Coffey. 1997. Apical enrichment of human EGF precursor in Madin-Darby canine kidney cells involves preferential basolateral ectodomain cleavage sensitive to a metalloprotease inhibitor. *The Journal of cell biology*. 138:747-758.

Denker, B.M., and S.K. Nigam. 1998. Molecular structure and assembly of the tight junction. *Am J Physiol*. 274:F1-9.

Denzer, K., M.J. Kleijmeer, H.F. Heijnen, W. Stoorvogel, and H.J. Geuze. 2000. Exosome: from internal vesicle of the multivesicular body to intercellular signaling device. *J Cell Sci*. 113 Pt 19:3365-3374.

Deora, A.A., D. Gravotta, G. Kreitzer, J. Hu, D. Bok, and E. Rodriguez-Boulan. 2004. The basolateral targeting signal of CD147 (EMMPRIN) consists of a single leucine and is not recognized by retinal pigment epithelium. *Molecular biology of the cell*. 15:4148-4165.

Diaz, F., D. Gravotta, A. Deora, R. Schreiner, J. Schoggins, E. Falck-Pedersen, and E. Rodriguez-Boulan. 2009. Clathrin adaptor AP1B controls adenovirus infectivity of epithelial cells. *Proceedings of the National Academy of Sciences of the United States of America*. 106:11143-11148.

Dietrich, J., X. Hou, A.M. Wegener, and C. Geisler. 1994. CD3 gamma contains a phosphoserine-dependent di-leucine motif involved in down-regulation of the T cell receptor. *EMBO J*. 13:2156-2166.

Ding, W., C. Li, T. Hu, R. Graves-Deal, A.B. Fotia, A.M. Weissman, and R.J. Coffey. 2008. EGF receptor-independent action of TGF-alpha protects Naked2 from AO7-mediated ubiquitylation and proteasomal degradation. *Proceedings of the National Academy of Sciences of the United States of America*. 105:13433-13438.

Doray, B., K. Bruns, P. Ghosh, and S.A. Kornfeld. 2002a. Autoinhibition of the ligand-binding site of GGA1/3 VHS domains by an internal acidic cluster-dileucine motif. *Proceedings of the National Academy of Sciences of the United States of America*. 99:8072-8077.

Doray, B., P. Ghosh, J. Griffith, H.J. Geuze, and S. Kornfeld. 2002b. Cooperation of GGAs and AP-1 in packaging MPRs at the trans-Golgi network. *Science*. 297:1700-1703.

Dotti, C.G., and K. Simons. 1990. Polarized sorting of viral glycoproteins to the axon and dendrites of hippocampal neurons in culture. *Cell*. 62:63-72.

Drees, F., S. Pokutta, S. Yamada, W.J. Nelson, and W.I. Weis. 2005. Alpha-catenin is a molecular switch that binds E-cadherin-beta-catenin and regulates actin-filament assembly. *Cell*. 123:903-915.

Dubash, A.D., M.M. Menold, T. Samson, E. Boulter, R. Garcia-Mata, R. Doughman, and K. Burridge. 2009. Chapter 1. Focal adhesions: new angles on an old structure. *Int Rev Cell Mol Biol*. 277:1-65.

Ebnet, K., A. Suzuki, S. Ohno, and D. Vestweber. 2004. Junctional adhesion molecules (JAMs): more molecules with dual functions? *J Cell Sci*. 117:19-29.

Falati, S., Q. Liu, P. Gross, G. Merrill-Skoloff, J. Chou, E. Vandendries, A. Celi, K. Croce, B.C. Furie, and B. Furie. 2003. Accumulation of tissue factor into developing thrombi in vivo is dependent upon microparticle P-selectin glycoprotein ligand 1 and platelet P-selectin. *J Exp Med*. 197:1585-1598.

Fernandez-Larrea, J., A. Merlos-Suarez, J.M. Urena, J. Baselga, and J. Arribas. 1999. A role for a PDZ protein in the early secretory pathway for the targeting of proTGF-alpha to the cell surface. *Mol Cell*. 3:423-433.

Fields, I.C., S.M. King, E. Shteyn, R.S. Kang, and H. Folsch. 2010. Phosphatidylinositol 3,4,5-trisphosphate localization in recycling endosomes is necessary for AP-1B-dependent sorting in polarized epithelial cells. *Molecular biology of the cell*. 21:95-105.

Fields, I.C., E. Shteyn, M. Pypaert, V. Proux-Gillardeaux, R.S. Kang, T. Galli, and H. Folsch. 2007. v-SNARE cellubrevin is required for basolateral sorting of AP-1B-dependent cargo in polarized epithelial cells. *The Journal of cell biology*. 177:477-488.

Fields, S., and O. Song. 1989. A novel genetic system to detect protein-protein interactions. *Nature*. 340:245-246.

Fogg, V.C., C.J. Liu, and B. Margolis. 2005. Multiple regions of Crumbs3 are required for tight junction formation in MCF10A cells. *J Cell Sci*. 118:2859-2869.

Folsch, H. 2005. The building blocks for basolateral vesicles in polarized epithelial cells. *Trends Cell Biol*. 15:222-228.

Folsch, H., H. Ohno, J.S. Bonifacino, and I. Mellman. 1999. A novel clathrin adaptor complex mediates basolateral targeting in polarized epithelial cells. *Cell*. 99:189-198.

Folsch, H., M. Pypaert, S. Maday, L. Pelletier, and I. Mellman. 2003. The AP-1A and AP-1B clathrin adaptor complexes define biochemically and functionally distinct membrane domains. *The Journal of cell biology*. 163:351-362.

Franklin, J.L., K. Yoshiura, P.J. Dempsey, G. Bogatcheva, L. Jeyakumar, K.S. Meise, R.S. Pearsall, D. Threadgill, and R.J. Coffey. 2005. Identification of MAGI-3 as a transforming growth factor-alpha tail binding protein. *Exp Cell Res*. 303:457-470.

Furuse, M., H. Sasaki, K. Fujimoto, and S. Tsukita. 1998. A single gene product, claudin-1 or -2, reconstitutes tight junction strands and recruits occludin in fibroblasts. *The Journal of cell biology*. 143:391-401.

Gaidarov, I., and J.H. Keen. 1999. Phosphoinositide-AP-2 interactions required for targeting to plasma membrane clathrin-coated pits. *The Journal of cell biology*. 146:755-764.

Gan, Y., T.E. McGraw, and E. Rodriguez-Boulan. 2002. The epithelial-specific adaptor AP1B mediates post-endocytic recycling to the basolateral membrane. *Nat Cell Biol*. 4:605-609.

Gao, L., I.G. Macara, and G. Joberty. 2002. Multiple splice variants of Par3 and of a novel related gene, Par3L, produce proteins with different binding properties. *Gene*. 294:99-107.

Garrard, S.M., C.T. Capaldo, L. Gao, M.K. Rosen, I.G. Macara, and D.R. Tomchick. 2003. Structure of Cdc42 in a complex with the GTPase-binding domain of the cell polarity protein, Par6. *EMBO J*. 22:1125-1133.

Geiss-Friedlander, R., and F. Melchior. 2007. Concepts in sumoylation: a decade on. *Nat Rev Mol Cell Biol*. 8:947-956.

Gonzalez, A., and E. Rodriguez-Boulan. 2009. Clathrin and AP1B: key roles in basolateral trafficking through trans-endosomal routes. *FEBS Lett*. 583:3784-3795.

Gough, N.R., and D.M. Fambrough. 1997. Different steady state subcellular distributions of the three splice variants of lysosome-associated membrane protein LAMP-2 are determined largely by the COOH-terminal amino acid residue. *The Journal of cell biology*. 137:1161-1169.

Gough, N.R., M.E. Zweifel, O. Martinez-Augustin, R.C. Aguilar, J.S. Bonifacino, and D.M. Fambrough. 1999. Utilization of the indirect lysosome targeting pathway by lysosome-associated membrane proteins (LAMPs) is influenced largely by the C-terminal residue of their GYXXphi targeting signals. *J Cell Sci*. 112 (Pt 23):4257-4269.

Gravotta, D., A. Deora, E. Perret, C. Oyanadel, A. Soza, R. Schreiner, A. Gonzalez, and E. Rodriguez-Boulan. 2007. AP1B sorts basolateral proteins in recycling and biosynthetic routes of MDCK cells. *Proceedings of the National Academy of Sciences of the United States of America*. 104:1564-1569.

Groenestege, W.M., S. Thebault, J. van der Wijst, D. van den Berg, R. Janssen, S. Tejpar, L.P. van den Heuvel, E. van Cutsem, J.G. Hoenderop, N.V. Knoers, and R.J. Bindels. 2007. Impaired basolateral sorting of pro-EGF causes isolated recessive renal hypomagnesemia. *The Journal of clinical investigation*. 117:2260-2267.

Harris, R.C., E. Chung, and R.J. Coffey. 2003. EGF receptor ligands. *Exp Cell Res*. 284:2-13.

Harter, C., and I. Mellman. 1992. Transport of the lysosomal membrane glycoprotein lgp120 (lgp-A) to lysosomes does not require appearance on the plasma membrane. *The Journal of cell biology*. 117:311-325.

Hartsock, A., and W.J. Nelson. 2008. Adherens and tight junctions: structure, function and connections to the actin cytoskeleton. *Biochim Biophys Acta*. 1778:660-669.

He, C., M. Hobert, L. Friend, and C. Carlin. 2002. The epidermal growth factor receptor juxtamembrane domain has multiple basolateral plasma membrane localization determinants, including a dominant signal with a polyproline core. *The Journal of biological chemistry*. 277:38284-38293.

Hicke, L. 2001. Protein regulation by monoubiquitin. *Nat Rev Mol Cell Biol*. 2:195-201.

Higginbotham, J.N., M. Demory Beckler, J.D. Gephart, J.L. Franklin, G. Bogatcheva, G.J. Kremers, D.W. Piston, G.D. Ayers, R.E. McConnell, M.J. Tyska, and R.J. Coffey. 2011. Amphiregulin Exosomes Increase Cancer Cell Invasion. *Curr Biol*.

Hirose, T., Y. Izumi, Y. Nagashima, Y. Tamai-Nagai, H. Kurihara, T. Sakai, Y. Suzuki, T. Yamanaka, A. Suzuki, K. Mizuno, and S. Ohno. 2002. Involvement of ASIP/PAR-3 in the promotion of epithelial tight junction formation. *J Cell Sci*. 115:2485-2495.

Hirst, J., N.A. Bright, B. Rous, and M.S. Robinson. 1999. Characterization of a fourth adaptor-related protein complex. *Molecular biology of the cell*. 10:2787-2802.

Hobbs, H.H., M.S. Brown, and J.L. Goldstein. 1992. Molecular genetics of the LDL receptor gene in familial hypercholesterolemia. *Hum Mutat*. 1:445-466.

Hobert, M., and C. Carlin. 1995. Cytoplasmic juxtamembrane domain of the human EGF receptor is required for basolateral localization in MDCK cells. *J Cell Physiol*. 162:434-446.

Hobert, M.E., S.J. Kil, M.E. Medof, and C.R. Carlin. 1997. The cytoplasmic juxtamembrane domain of the epidermal growth factor receptor contains a novel autonomous basolateral sorting determinant. *The Journal of biological chemistry*. 272:32901-32909.

Honing, S., D. Ricotta, M. Krauss, K. Spate, B. Spolaore, A. Motley, M. Robinson, C. Robinson, V. Haucke, and D.J. Owen. 2005. Phosphatidylinositol-(4,5)-bisphosphate regulates sorting signal recognition by the clathrin-associated adaptor complex AP2. *Mol Cell*. 18:519-531.

Hu, T., C. Li, Z. Cao, T.J. Van Raay, J.G. Smith, K. Willert, L. Solnica-Krezel, and R.J. Coffey. 2010. Myristoylated Naked2 antagonizes Wnt-beta-catenin activity by degrading Dishevelled-1 at the plasma membrane. *The Journal of biological chemistry*. 285:13561-13568.

Hunziker, W., C. Harter, K. Matter, and I. Mellman. 1991. Basolateral sorting in MDCK cells requires a distinct cytoplasmic domain determinant. *Cell*. 66:907-920.

Hurley, J.H. 2008. ESCRT complexes and the biogenesis of multivesicular bodies. *Curr Opin Cell Biol*. 20:4-11.

Hynes, R.O. 2002. Integrins: bidirectional, allosteric signaling machines. *Cell*. 110:673-687.

Iyer, K., L. Burkle, D. Auerbach, S. Thaminy, M. Dinkel, K. Engels, and I. Stagljar. 2005. Utilizing the split-ubiquitin membrane yeast two-hybrid system to identify protein-protein interactions of integral membrane proteins. *Sci STKE*. 2005:pl3.

Jareb, M., and G. Banker. 1998. The polarized sorting of membrane proteins expressed in cultured hippocampal neurons using viral vectors. *Neuron*. 20:855-867.

Johnson, K.F., and S. Kornfeld. 1992a. The cytoplasmic tail of the mannose 6-phosphate/insulin-like growth factor-II receptor has two signals for lysosomal enzyme sorting in the Golgi. *The Journal of cell biology*. 119:249-257.

Johnson, K.F., and S. Kornfeld. 1992b. A His-Leu-Leu sequence near the carboxyl terminus of the cytoplasmic domain of the cation-dependent mannose 6-phosphate receptor is necessary for the lysosomal enzyme sorting function. *The Journal of biological chemistry*. 267:17110-17115.

Johnsson, N., and A. Varshavsky. 1994. Split ubiquitin as a sensor of protein interactions in vivo. *Proceedings of the National Academy of Sciences of the United States of America*. 91:10340-10344.

Jost, M., C. Kari, and U. Rodeck. 2000. The EGF receptor - an essential regulator of multiple epidermal functions. *Eur J Dermatol*. 10:505-510.

Jost, M., F. Simpson, J.M. Kavran, M.A. Lemmon, and S.L. Schmid. 1998. Phosphatidylinositol-4,5-bisphosphate is required for endocytic coated vesicle formation. *Curr Biol*. 8:1399-1402.

Kallay, L.M., A. McNickle, P.J. Brennwald, A.L. Hubbard, and L.T. Braiterman. 2006. Scribble associates with two polarity proteins, Lgl2 and Vangl2, via distinct molecular domains. *J Cell Biochem*. 99:647-664.

Kang, R.S., and H. Folsch. 2011. ARH cooperates with AP-1B in the exocytosis of LDLR in polarized epithelial cells. *The Journal of cell biology*.

Kelly, B.T., A.J. McCoy, K. Spate, S.E. Miller, P.R. Evans, S. Honing, and D.J. Owen. 2008. A structural explanation for the binding of endocytic dileucine motifs by the AP2 complex. *Nature*. 456:976-979.

Kohler, K., and A. Zahraoui. 2005. Tight junction: a co-ordinator of cell signalling and membrane trafficking. *Biol Cell*. 97:659-665.

Koivisto, U.M., A.L. Hubbard, and I. Mellman. 2001. A novel cellular phenotype for familial hypercholesterolemia due to a defect in polarized targeting of LDL receptor. *Cell*. 105:575-585.

Konturek, P.C., S.J. Konturek, T. Brzozowski, and H. Ernst. 1995. Epidermal growth factor and transforming growth factor-alpha: role in protection and healing of gastric mucosal lesions. *Eur J Gastroenterol Hepatol*. 7:933-937.

Kuo, A., C. Zhong, W.S. Lane, and R. Derynck. 2000. Transmembrane transforming growth factor-alpha tethers to the PDZ domain-containing, Golgi membrane-associated protein p59/GRASP55. *EMBO J*. 19:6427-6439.

Lauwers, E., C. Jacob, and B. Andre. 2009. K63-linked ubiquitin chains as a specific signal for protein sorting into the multivesicular body pathway. *The Journal of cell biology*. 185:493-502.

Le Bivic, A., Y. Sambuy, A. Patzak, N. Patil, M. Chao, and E. Rodriguez-Boulan. 1991. An internal deletion in the cytoplasmic tail reverses the apical localization of human NGF receptor in transfected MDCK cells. *The Journal of cell biology*. 115:607-618.

Lee, D.C., S.E. Fenton, E.A. Berkowitz, and M.A. Hissong. 1995. Transforming growth factor alpha: expression, regulation, and biological activities. *Pharmacol Rev*. 47:51-85.

Letourneur, F., and R.D. Klausner. 1992. A novel di-leucine motif and a tyrosine-based motif independently mediate lysosomal targeting and endocytosis of CD3 chains. *Cell*. 69:1143-1157.

Li, C., J.L. Franklin, R. Graves-Deal, W.G. Jerome, Z. Cao, and R.J. Coffey. 2004a. Myristoylated Naked2 escorts transforming growth factor alpha to the basolateral plasma membrane of polarized epithelial cells. *Proceedings of the National Academy of Sciences of the United States of America*. 101:5571-5576.

Li, C., M. Hao, Z. Cao, W. Ding, R. Graves-Deal, J. Hu, D.W. Piston, and R.J. Coffey. 2007. Naked2 acts as a cargo recognition and targeting protein to ensure proper delivery and fusion of TGF-alpha containing exocytic vesicles at the lower lateral membrane of polarized MDCK cells. *Molecular biology of the cell*. 18:3081-3093.

Li, Y., D. Karnak, B. Demeler, B. Margolis, and A. Lavie. 2004b. Structural basis for L27 domain-mediated assembly of signaling and cell polarity complexes. *EMBO J*. 23:2723-2733.

Lodish, H.F. 2003. Molecular cell biology. W.H. Freeman and Company, New York. xxxiii, 973 , 979 p. pp.

Luetteke, N.C., T.H. Qiu, S.E. Fenton, K.L. Troyer, R.F. Riedel, A. Chang, and D.C. Lee. 1999. Targeted inactivation of the EGF and amphiregulin genes reveals distinct roles for EGF receptor ligands in mouse mammary gland development. *Development (Cambridge, England)*. 126:2739-2750.

Luetteke, N.C., T.H. Qiu, R.L. Peiffer, P. Oliver, O. Smithies, and D.C. Lee. 1993. TGF alpha deficiency results in hair follicle and eye abnormalities in targeted and waved-1 mice. *Cell*. 73:263-278.

Makarova, O., M.H. Roh, C.J. Liu, S. Laurinec, and B. Margolis. 2003. Mammalian Crumbs3 is a small transmembrane protein linked to protein associated with Lin-7 (Pals1). *Gene*. 302:21-29.

Mandai, K., H. Nakanishi, A. Satoh, H. Obaishi, M. Wada, H. Nishioka, M. Itoh, A. Mizoguchi, T. Aoki, T. Fujimoto, Y. Matsuda, S. Tsukita, and Y. Takai. 1997. Afadin: A novel actin filament-binding protein with one PDZ domain localized at cadherin-based cell-to-cell adherens junction. *The Journal of cell biology*. 139:517-528.

Marchiando, A.M., W.V. Graham, and J.R. Turner. 2010. Epithelial barriers in homeostasis and disease. *Annu Rev Pathol*. 5:119-144.

Margolis, B., and J.P. Borg. 2005. Apicobasal polarity complexes. *J Cell Sci*. 118:5157-5159.

Marks, M.S., P.A. Roche, E. van Donselaar, L. Woodruff, P.J. Peters, and J.S. Bonifacino. 1995. A lysosomal targeting signal in the cytoplasmic tail of the beta chain directs HLA-DM to MHC class II compartments. *The Journal of cell biology*. 131:351-369.

Martin-Belmonte, F., and K. Mostov. 2008. Regulation of cell polarity during epithelial morphogenesis. *Curr Opin Cell Biol*. 20:227-234.

Matsuda, S., E. Miura, K. Matsuda, W. Kakegawa, K. Kohda, M. Watanabe, and M. Yuzaki. 2008. Accumulation of AMPA receptors in autophagosomes in neuronal axons lacking adaptor protein AP-4. *Neuron*. 57:730-745.

Matsumine, A., A. Ogai, T. Senda, N. Okumura, K. Satoh, G.H. Baeg, T. Kawahara, S. Kobayashi, M. Okada, K. Toyoshima, and T. Akiyama. 1996. Binding of APC to the human homolog of the Drosophila discs large tumor suppressor protein. *Science*. 272:1020-1023.

Matter, K., W. Hunziker, and I. Mellman. 1992. Basolateral sorting of LDL receptor in MDCK cells: the cytoplasmic domain contains two tyrosine-dependent targeting determinants. *Cell*. 71:741-753.

Matter, K., E.M. Yamamoto, and I. Mellman. 1994. Structural requirements and sequence motifs for polarized sorting and endocytosis of LDL and Fc receptors in MDCK cells. *The Journal of cell biology*. 126:991-1004.

McCarthy, K.M., I.B. Skare, M.C. Stankewich, M. Furuse, S. Tsukita, R.A. Rogers, R.D. Lynch, and E.E. Schneeberger. 1996. Occludin is a functional component of the tight junction. *J Cell Sci*. 109 (Pt 9):2287-2298.

Mellman, I., and W.J. Nelson. 2008. Coordinated protein sorting, targeting and distribution in polarized cells. *Nat Rev Mol Cell Biol*. 9:833-845.

Miranda, K.C., T. Khromykh, P. Christy, T.L. Le, C.J. Gottardi, A.S. Yap, J.L. Stow, and R.D. Teasdale. 2001. A dileucine motif targets E-cadherin to the basolateral cell surface in Madin-Darby canine kidney and LLC-PK1 epithelial cells. *The Journal of biological chemistry*. 276:22565-22572.

Mobius, W., Y. Ohno-Iwashita, E.G. van Donselaar, V.M. Oorschot, Y. Shimada, T. Fujimoto, H.F. Heijnen, H.J. Geuze, and J.W. Slot. 2002. Immunoelectron microscopic localization of cholesterol using biotinylated and non-cytolytic perfringolysin O. *J Histochem Cytochem*. 50:43-55.

Monlauzeur, L., A. Rajasekaran, M. Chao, E. Rodriguez-Boulan, and A. Le Bivic. 1995. A cytoplasmic tyrosine is essential for the basolateral localization of mutants of the human nerve growth factor receptor in Madin-Darby canine kidney cells. *The Journal of biological chemistry*. 270:12219-12225.

Moreno-De-Luca, A., S.L. Helmers, H. Mao, T.G. Burns, A.M. Melton, K.R. Schmidt, P.M. Fernhoff, D.H. Ledbetter, and C.L. Martin. 2011. Adaptor protein complex-4 (AP-4) deficiency causes a novel autosomal recessive cerebral palsy syndrome with microcephaly and intellectual disability. *J Med Genet*. 48:141-144.

Mostov, K.E., M. Verges, and Y. Altschuler. 2000. Membrane traffic in polarized epithelial cells. *Curr Opin Cell Biol*. 12:483-490.

Musch, A., D. Cohen, C. Yeaman, W.J. Nelson, E. Rodriguez-Boulan, and P.J. Brennwald. 2002. Mammalian homolog of Drosophila tumor suppressor lethal (2) giant larvae interacts with basolateral exocytic machinery in Madin-Darby canine kidney cells. *Molecular biology of the cell*. 13:158-168.

Nakatsu, F., and H. Ohno. 2003. Adaptor protein complexes as the key regulators of protein sorting in the post-Golgi network. *Cell Struct Funct*. 28:419-429.

Nakatsu, F., M. Okada, F. Mori, N. Kumazawa, H. Iwasa, G. Zhu, Y. Kasagi, H. Kamiya, A. Harada, K. Nishimura, A. Takeuchi, T. Miyazaki, M. Watanabe, S. Yuasa, T. Manabe, K. Wakabayashi, S. Kaneko, T. Saito, and H. Ohno. 2004. Defective function of GABA-containing synaptic vesicles in mice lacking the AP-3B clathrin adaptor. *The Journal of cell biology*. 167:293-302.

Nakayama, M., T.M. Goto, M. Sugimoto, T. Nishimura, T. Shinagawa, S. Ohno, M. Amano, and K. Kaibuchi. 2008. Rho-kinase phosphorylates PAR-3 and disrupts PAR complex formation. *Dev Cell*. 14:205-215.

Nambiar, R., R.E. McConnell, and M.J. Tyska. 2010. Myosin motor function: the ins and outs of actin-based membrane protrusions. *Cell Mol Life Sci*. 67:1239-1254.

Navarro, C., S. Nola, S. Audebert, M.J. Santoni, J.P. Arsanto, C. Ginestier, S. Marchetto, J. Jacquemier, D. Isnardon, A. Le Bivic, D. Birnbaum, and J.P. Borg. 2005. Junctional recruitment of mammalian Scribble relies on E-cadherin engagement. *Oncogene*. 24:4330-4339.

Nelson, W.J. 2008. Regulation of cell-cell adhesion by the cadherin-catenin complex. *Biochem Soc Trans*. 36:149-155.

Nishimura, T., A. Andoh, O. Inatomi, M. Shioya, Y. Yagi, T. Tsujikawa, and Y. Fujiyama. 2008. Amphiregulin and epiregulin expression in neoplastic and inflammatory lesions in the colon. *Oncol Rep*. 19:105-110.

Ohno, H., J. Stewart, M.C. Fournier, H. Bosshart, I. Rhee, S. Miyatake, T. Saito, A. Gallusser, T. Kirchhausen, and J.S. Bonifacino. 1995. Interaction of tyrosine-based sorting signals with clathrin-associated proteins. *Science*. 269:1872-1875.

Ohno, H., T. Tomemori, F. Nakatsu, Y. Okazaki, R.C. Aguilar, H. Folsch, I. Mellman, T. Saito, T. Shirasawa, and J.S. Bonifacino. 1999. Mu1B, a novel adaptor medium chain expressed in polarized epithelial cells. *FEBS Lett*. 449:215-220.

Olusanya, O., P.D. Andrews, J.R. Swedlow, and E. Smythe. 2001. Phosphorylation of threonine 156 of the mu2 subunit of the AP2 complex is essential for endocytosis in vitro and in vivo. *Curr Biol*. 11:896-900.

Ong, L.L., C.P. Er, A. Ho, M.T. Aung, and H. Yu. 2003. Kinectin anchors the translation elongation factor-1 delta to the endoplasmic reticulum. *The Journal of biological chemistry*. 278:32115-32123.

Ong, L.L., A.P. Lim, C.P. Er, S.A. Kuznetsov, and H. Yu. 2000. Kinectin-kinesin binding domains and their effects on organelle motility. *The Journal of biological chemistry*. 275:32854-32860.

Ooi, C.E., E.C. Dell'Angelica, and J.S. Bonifacino. 1998. ADP-Ribosylation factor 1 (ARF1) regulates recruitment of the AP-3 adaptor complex to membranes. *The Journal of cell biology*. 142:391-402.

Owen, D.J., B.M. Collins, and P.R. Evans. 2004. Adaptors for clathrin coats: structure and function. *Annu Rev Cell Dev Biol*. 20:153-191.

Owen, D.J., and P.R. Evans. 1998. A structural explanation for the recognition of tyrosine-based endocytotic signals. *Science*. 282:1327-1332.

Paladino, S., T. Pocard, M.A. Catino, and C. Zurzolo. 2006. GPI-anchored proteins are directly targeted to the apical surface in fully polarized MDCK cells. *The Journal of cell biology*. 172:1023-1034.

Paladino, S., D. Sarnataro, R. Pillich, S. Tivodar, L. Nitsch, and C. Zurzolo. 2004. Protein oligomerization modulates raft partitioning and apical sorting of GPI-anchored proteins. *The Journal of cell biology*. 167:699-709.

Paladino, S., D. Sarnataro, S. Tivodar, and C. Zurzolo. 2007. Oligomerization is a specific requirement for apical sorting of glycosyl-phosphatidylinositol-anchored proteins but not for non-raft-associated apical proteins. *Traffic*. 8:251-258.

Patel, S.D., C. Ciatto, C.P. Chen, F. Bahna, M. Rajebhosale, N. Arkus, I. Schieren, T.M. Jessell, B. Honig, S.R. Price, and L. Shapiro. 2006. Type II cadherin ectodomain structures: implications for classical cadherin specificity. *Cell*. 124:1255-1268.

Paulhe, F., M. Wehrle-Haller, M.C. Jacquier, B.A. Imhof, S. Tabone-Eglinger, and B. Wehrle-Haller. 2009. Dimerization of Kit-ligand and efficient cell-surface presentation requires a conserved Ser-Gly-Gly-Tyr motif in its transmembrane domain. *FASEB J*. 23:3037-3048.

Peden, A.A., V. Oorschot, B.A. Hesser, C.D. Austin, R.H. Scheller, and J. Klumperman. 2004. Localization of the AP-3 adaptor complex defines a novel endosomal exit site for lysosomal membrane proteins. *The Journal of cell biology*. 164:1065-1076.

Peeters, M., T. Price, and J.L. Van Laethem. 2009. Anti-epidermal growth factor receptor monotherapy in the treatment of metastatic colorectal cancer: where are we today? *Oncologist*. 14:29-39.

Peschon, J.J., J.L. Slack, P. Reddy, K.L. Stocking, S.W. Sunnarborg, D.C. Lee, W.E. Russell, B.J. Castner, R.S. Johnson, J.N. Fitzner, R.W. Boyce, N. Nelson, C.J. Kozlosky, M.F. Wolfson, C.T. Rauch, D.P. Cerretti, R.J. Paxton, C.J. March, and R.A. Black. 1998. An essential role for ectodomain shedding in mammalian development. *Science*. 282:1281-1284.

Pieczynski, J., and B. Margolis. 2011. Protein complexes that control renal epithelial polarity. *Am J Physiol Renal Physiol*. 300:F589-601.

Piepkorn, M., R.A. Underwood, C. Henneman, and L.T. Smith. 1995. Expression of amphiregulin is regulated in cultured human keratinocytes and in developing fetal skin. *J Invest Dermatol*. 105:802-809.

Plant, P.J., J.P. Fawcett, D.C. Lin, A.D. Holdorf, K. Binns, S. Kulkarni, and T. Pawson. 2003. A polarity complex of mPar-6 and atypical PKC binds, phosphorylates and regulates mammalian Lgl. *Nat Cell Biol*. 5:301-308.

Plowman, G.D., J.M. Green, V.L. McDonald, M.G. Neubauer, C.M. Disteche, G.J. Todaro, and M. Shoyab. 1990. The amphiregulin gene encodes a novel epidermal growth factor-related protein with tumor-inhibitory activity. *Molecular and cellular biology*. 10:1969-1981.

Pokutta, S., K. Herrenknecht, R. Kemler, and J. Engel. 1994. Conformational changes of the recombinant extracellular domain of E-cadherin upon calcium binding. *Eur J Biochem*. 223:1019-1026.

Pond, L., L.A. Kuhn, L. Teyton, M.P. Schutze, J.A. Tainer, M.R. Jackson, and P.A. Peterson. 1995. A role for acidic residues in di-leucine motif-based targeting to the endocytic pathway. *The Journal of biological chemistry*. 270:19989-19997.

Potter, B.A., R.P. Hughey, and O.A. Weisz. 2006. Role of N- and O-glycans in polarized biosynthetic sorting. *Am J Physiol Cell Physiol*. 290:C1-C10.

Puertollano, R., R.C. Aguilar, I. Gorshkova, R.J. Crouch, and J.S. Bonifacino. 2001. Sorting of mannose 6-phosphate receptors mediated by the GGAs. *Science*. 292:1712-1716.

Qin, Y., C. Capaldo, B.M. Gumbiner, and I.G. Macara. 2005. The mammalian Scribble polarity protein regulates epithelial cell adhesion and migration through E-cadherin. *The Journal of cell biology*. 171:1061-1071.

Raiborg, C., and H. Stenmark. 2009. The ESCRT machinery in endosomal sorting of ubiquitylated membrane proteins. *Nature*. 458:445-452.

Raleigh, D.R., D.M. Boe, D. Yu, C.R. Weber, A.M. Marchiando, E.M. Bradford, Y. Wang, L. Wu, E.E. Schneeberger, L. Shen, and J.R. Turner. 2011. Occludin S408 phosphorylation regulates tight junction protein interactions and barrier function. *The Journal of cell biology*. 193:565-582.

Reymond, N., S. Fabre, E. Lecocq, J. Adelaide, P. Dubreuil, and M. Lopez. 2001. Nectin4/PRR4, a new afadin-associated member of the nectin family that trans-interacts with nectin1/PRR1 through V domain interaction. *The Journal of biological chemistry*. 276:43205-43215.

Ricotta, D., S.D. Conner, S.L. Schmid, K. von Figura, and S. Honing. 2002. Phosphorylation of the AP2 mu subunit by AAK1 mediates high affinity binding to membrane protein sorting signals. *The Journal of cell biology*. 156:791-795.

Rimm, D.L., E.R. Koslov, P. Kebriaei, C.D. Cianci, and J.S. Morrow. 1995. Alpha 1(E)-catenin is an actin-binding and -bundling protein mediating the attachment of F-actin to the membrane adhesion complex. *Proceedings of the National Academy of Sciences of the United States of America*. 92:8813-8817.

Ringwald, M., R. Schuh, D. Vestweber, H. Eistetter, F. Lottspeich, J. Engel, R. Dolz, F. Jahnig, J. Epplen, S. Mayer, and et al. 1987. The structure of cell adhesion molecule uvomorulin. Insights into the molecular mechanism of Ca2+-dependent cell adhesion. *EMBO J*. 6:3647-3653.

Robinson, M.S. 2004. Adaptable adaptors for coated vesicles. *Trends Cell Biol*. 14:167-174.

Rodriguez-Boulan, E., and A. Musch. 2005. Protein sorting in the Golgi complex: shifting paradigms. *Biochim Biophys Acta*. 1744:455-464.

Rodriguez-Boulan, E., and W.J. Nelson. 1989. Morphogenesis of the polarized epithelial cell phenotype. *Science*. 245:718-725.

Roh, M.H., S. Fan, C.J. Liu, and B. Margolis. 2003. The Crumbs3-Pals1 complex participates in the establishment of polarity in mammalian epithelial cells. *J Cell Sci*. 116:2895-2906.

Roh, M.H., C.J. Liu, S. Laurinec, and B. Margolis. 2002a. The carboxyl terminus of zona occludens-3 binds and recruits a mammalian homologue of discs lost to tight junctions. *The Journal of biological chemistry*. 277:27501-27509.

Roh, M.H., O. Makarova, C.J. Liu, K. Shin, S. Lee, S. Laurinec, M. Goyal, R. Wiggins, and B. Margolis. 2002b. The Maguk protein, Pals1, functions as an adapter, linking mammalian homologues of Crumbs and Discs Lost. *The Journal of cell biology*. 157:161-172.

Rohde, G., D. Wenzel, and V. Haucke. 2002. A phosphatidylinositol (4,5)-bisphosphate binding site within mu2-adaptin regulates clathrin-mediated endocytosis. *The Journal of cell biology*. 158:209-214.

Rous, B.A., B.J. Reaves, G. Ihrke, J.A. Briggs, S.R. Gray, D.J. Stephens, G. Banting, and J.P. Luzio. 2002. Role of adaptor complex AP-3 in targeting wild-type and mutated CD63 to lysosomes. *Molecular biology of the cell*. 13:1071-1082.

Rousset, R., J.A. Mack, K.A. Wharton, Jr., J.D. Axelrod, K.M. Cadigan, M.P. Fish, R. Nusse, and M.P. Scott. 2001. Naked cuticle targets dishevelled to antagonize Wnt signal transduction. *Genes Dev*. 15:658-671.

Ryan, S., S. Verghese, N.L. Cianciola, C.U. Cotton, and C.R. Carlin. 2010. Autosomal recessive polycystic kidney disease epithelial cell model reveals multiple basolateral epidermal growth factor receptor sorting pathways. *Molecular biology of the cell*. 21:2732-2745.

Sahin, U., G. Weskamp, K. Kelly, H.M. Zhou, S. Higashiyama, J. Peschon, D. Hartmann, P. Saftig, and C.P. Blobel. 2004. Distinct roles for ADAM10 and ADAM17 in ectodomain shedding of six EGFR ligands. *The Journal of cell biology*. 164:769-779.

Saitou, M., M. Furuse, H. Sasaki, J.D. Schulzke, M. Fromm, H. Takano, T. Noda, and S. Tsukita. 2000. Complex phenotype of mice lacking occludin, a component of tight junction strands. *Molecular biology of the cell*. 11:4131-4142.

Sakakibara, A., M. Furuse, M. Saitou, Y. Ando-Akatsuka, and S. Tsukita. 1997. Possible involvement of phosphorylation of occludin in tight junction formation. *The Journal of cell biology*. 137:1393-1401.

Sanderson, M.P., S. Keller, A. Alonso, S. Riedle, P.J. Dempsey, and P. Altevogt. 2008. Generation of novel, secreted epidermal growth factor receptor (EGFR/ErbB1) isoforms via metalloprotease-dependent ectodomain shedding and exosome secretion. *J Cell Biochem*. 103:1783-1797.

Satoh-Horikawa, K., H. Nakanishi, K. Takahashi, M. Miyahara, M. Nishimura, K. Tachibana, A. Mizoguchi, and Y. Takai. 2000. Nectin-3, a new member of immunoglobulin-like cell adhesion molecules that shows homophilic and heterophilic cell-cell adhesion activities. *The Journal of biological chemistry*. 275:10291-10299.

Scheiffele, P., J. Peranen, and K. Simons. 1995. N-glycans as apical sorting signals in epithelial cells. *Nature*. 378:96-98.

Schlessinger, J. 2000. Cell signaling by receptor tyrosine kinases. *Cell*. 103:211-225.

Schneeberger, E.E., and R.D. Lynch. 2004. The tight junction: a multifunctional complex. *Am J Physiol Cell Physiol*. 286:C1213-1228.

Schroer, T.A., B.J. Schnapp, T.S. Reese, and M.P. Sheetz. 1988. The role of kinesin and other soluble factors in organelle movement along microtubules. *The Journal of cell biology*. 107:1785-1792.

Schuger, L., G.R. Johnson, K. Gilbride, G.D. Plowman, and R. Mandel. 1996. Amphiregulin in lung branching morphogenesis: interaction with heparan sulfate proteoglycan modulates cell proliferation. *Development (Cambridge, England)*. 122:1759-1767.

Shirasawa, S., M. Furuse, N. Yokoyama, and T. Sasazuki. 1993. Altered growth of human colon cancer cell lines disrupted at activated Ki-ras. *Science*. 260:85-88.

Shoyab, M., V.L. McDonald, J.G. Bradley, and G.J. Todaro. 1988. Amphiregulin: a bifunctional growth-modulating glycoprotein produced by the phorbol 12-myristate 13-acetate-treated human breast adenocarcinoma cell line MCF-7. *Proceedings of the National Academy of Sciences of the United States of America*. 85:6528-6532.

Shoyab, M., G.D. Plowman, V.L. McDonald, J.G. Bradley, and G.J. Todaro. 1989. Structure and function of human amphiregulin: a member of the epidermal growth factor family. *Science*. 243:1074-1076.

Shum, L., C.W. Turck, and R. Derynck. 1996. Cysteines 153 and 154 of transmembrane transforming growth factor-alpha are palmitoylated and mediate cytoplasmic protein association. *The Journal of biological chemistry*. 271:28502-28508.

Simmen, T., S. Honing, A. Icking, R. Tikkanen, and W. Hunziker. 2002. AP-4 binds basolateral signals and participates in basolateral sorting in epithelial MDCK cells. *Nat Cell Biol*. 4:154-159.

Simons, K., and G. van Meer. 1988. Lipid sorting in epithelial cells. *Biochemistry*. 27:6197-6202.

Simons, M., and G. Raposo. 2009. Exosomes--vesicular carriers for intercellular communication. *Curr Opin Cell Biol*. 21:575-581.

Simpson, F., N.A. Bright, M.A. West, L.S. Newman, R.B. Darnell, and M.S. Robinson. 1996. A novel adaptor-related protein complex. *The Journal of cell biology*. 133:749-760.

Singla, V., and J.F. Reiter. 2006. The primary cilium as the cell's antenna: signaling at a sensory organelle. *Science*. 313:629-633.

Smith, A.L., D.B. Friedman, H. Yu, R.H. Carnahan, and A.B. Reynolds. 2011. ReCLIP (reversible cross-link immuno-precipitation): an efficient method for interrogation of labile protein complexes. *PLoS One*. 6:e16206.

Sorkin, A., M. Mazzotti, T. Sorkina, L. Scotto, and L. Beguinot. 1996. Epidermal growth factor receptor interaction with clathrin adaptors is mediated by the Tyr974-containing internalization motif. *The Journal of biological chemistry*. 271:13377-13384.

St Johnston, D., and J. Ahringer. 2010. Cell polarity in eggs and epithelia: parallels and diversity. *Cell*. 141:757-774.

Stamnes, M.A., and J.E. Rothman. 1993. The binding of AP-1 clathrin adaptor particles to Golgi membranes requires ADP-ribosylation factor, a small GTP-binding protein. *Cell*. 73:999-1005.

Straight, S.W., K. Shin, V.C. Fogg, S. Fan, C.J. Liu, M. Roh, and B. Margolis. 2004. Loss of PALS1 expression leads to tight junction and polarity defects. *Molecular biology of the cell*. 15:1981-1990.

Sugimoto, H., M. Sugahara, H. Folsch, Y. Koide, F. Nakatsu, N. Tanaka, T. Nishimura, M. Furukawa, C. Mullins, N. Nakamura, I. Mellman, and H. Ohno. 2002. Differential recognition of tyrosine-based basolateral signals by AP-1B subunit mu1B in polarized epithelial cells. *Molecular biology of the cell*. 13:2374-2382.

Swaminathan, S., A.Y. Amerik, and M. Hochstrasser. 1999. The Doa4 deubiquitinating enzyme is required for ubiquitin homeostasis in yeast. *Molecular biology of the cell*. 10:2583-2594.

Tachibana, K., H. Nakanishi, K. Mandai, K. Ozaki, W. Ikeda, Y. Yamamoto, A. Nagafuchi, S. Tsukita, and Y. Takai. 2000. Two cell adhesion molecules, nectin and cadherin, interact through their cytoplasmic domain-associated proteins. *The Journal of cell biology*. 150:1161-1176.

Takahashi, K., H. Nakanishi, M. Miyahara, K. Mandai, K. Satoh, A. Satoh, H. Nishioka, J. Aoki, A. Nomoto, A. Mizoguchi, and Y. Takai. 1999. Nectin/PRR: an immunoglobulin-like cell adhesion molecule recruited to cadherin-based adherens junctions through interaction with Afadin, a PDZ domain-containing protein. *The Journal of cell biology*. 145:539-549.

Takai, Y., and H. Nakanishi. 2003. Nectin and afadin: novel organizers of intercellular junctions. *J Cell Sci*. 116:17-27.

Takatsu, H., Y. Katoh, Y. Shiba, and K. Nakayama. 2001. Golgi-localizing, gamma-adaptin ear homology domain, ADP-ribosylation factor-binding (GGA) proteins interact with acidic dileucine sequences within the cytoplasmic domains of sorting receptors through their Vps27p/Hrs/STAM (VHS) domains. *The Journal of biological chemistry*. 276:28541-28545.

Thebault, S., R.T. Alexander, W.M. Tiel Groenestege, J.G. Hoenderop, and R.J. Bindels. 2009. EGF increases TRPM6 activity and surface expression. *J Am Soc Nephrol*. 20:78-85.

Thery, C., S. Amigorena, G. Raposo, and A. Clayton. 2006. Isolation and characterization of exosomes from cell culture supernatants and biological fluids. *Curr Protoc Cell Biol*. Chapter 3:Unit 3 22.

Thomas, D.C., C.B. Brewer, and M.G. Roth. 1993. Vesicular stomatitis virus glycoprotein contains a dominant cytoplasmic basolateral sorting signal critically dependent upon a tyrosine. *The Journal of biological chemistry*. 268:3313-3320.

Thoreson, M.A., and A.B. Reynolds. 2002. Altered expression of the catenin p120 in human cancer: implications for tumor progression. *Differentiation*. 70:583-589.

Thorne, B.A., and G.D. Plowman. 1994. The heparin-binding domain of amphiregulin necessitates the precursor pro-region for growth factor secretion. *Molecular and cellular biology*. 14:1635-1646.

Tomko, R.P., R. Xu, and L. Philipson. 1997. HCAR and MCAR: the human and mouse cellular receptors for subgroup C adenoviruses and group B coxsackieviruses. *Proceedings of the National Academy of Sciences of the United States of America*. 94:3352-3356.

Toyoshima, I., H. Yu, E.R. Steuer, and M.P. Sheetz. 1992. Kinectin, a major kinesin-binding protein on ER. *The Journal of cell biology*. 118:1121-1131.

Trajkovic, K., C. Hsu, S. Chiantia, L. Rajendran, D. Wenzel, F. Wieland, P. Schwille, B. Brugger, and M. Simons. 2008. Ceramide triggers budding of exosome vesicles into multivesicular endosomes. *Science*. 319:1244-1247.

Traub, L.M. 2009. Tickets to ride: selecting cargo for clathrin-regulated internalization. *Nat Rev Mol Cell Biol*. 10:583-596.

Tsukita, S., M. Furuse, and M. Itoh. 2001. Multifunctional strands in tight junctions. *Nat Rev Mol Cell Biol*. 2:285-293.

Urbanowski, J.L., and R.C. Piper. 2001. Ubiquitin sorts proteins into the intralumenal degradative compartment of the late-endosome/vacuole. *Traffic*. 2:622-630.

van Meer, G., and K. Simons. 1988. Lipid polarity and sorting in epithelial cells. *J Cell Biochem*. 36:51-58.

Vignal, E., A. Blangy, M. Martin, C. Gauthier-Rouviere, and P. Fort. 2001. Kinectin is a key effector of RhoG microtubule-dependent cellular activity. *Molecular and cellular biology*. 21:8022-8034.

Wang, Q., T.W. Hurd, and B. Margolis. 2004. Tight junction protein Par6 interacts with an evolutionarily conserved region in the amino terminus of PALS1/stardust. *The Journal of biological chemistry*. 279:30715-30721.

Wang, Y.J., J. Wang, H.Q. Sun, M. Martinez, Y.X. Sun, E. Macia, T. Kirchhausen, J.P. Albanesi, M.G. Roth, and H.L. Yin. 2003. Phosphatidylinositol 4 phosphate regulates targeting of clathrin adaptor AP-1 complexes to the Golgi. *Cell*. 114:299-310.

Wehrle-Haller, B., and B.A. Imhof. 2001. Stem cell factor presentation to c-Kit. Identification of a basolateral targeting domain. *The Journal of biological chemistry*. 276:12667-12674.

Weissman, A.M. 2001. Themes and variations on ubiquitylation. *Nat Rev Mol Cell Biol*. 2:169-178.

Weisz, O.A., and E. Rodriguez-Boulan. 2009. Apical trafficking in epithelial cells: signals, clusters and motors. *J Cell Sci*. 122:4253-4266.

Wells, A. 1999. EGF receptor. *Int J Biochem Cell Biol*. 31:637-643.

Wells, C.D., J.P. Fawcett, A. Traweger, Y. Yamanaka, M. Goudreault, K. Elder, S. Kulkarni, G. Gish, C. Virag, C. Lim, K. Colwill, A. Starostine, P. Metalnikov, and T. Pawson. 2006. A Rich1/Amot complex regulates the Cdc42 GTPase and apical-polarity proteins in epithelial cells. *Cell*. 125:535-548.

White, I.J., L.M. Bailey, M.R. Aghakhani, S.E. Moss, and C.E. Futter. 2006. EGF stimulates annexin 1-dependent inward vesiculation in a multivesicular endosome subpopulation. *EMBO J*. 25:1-12.

Williams, M.A., and M. Fukuda. 1990. Accumulation of membrane glycoproteins in lysosomes requires a tyrosine residue at a particular position in the cytoplasmic tail. *The Journal of cell biology*. 111:955-966.

Wolff, S.C., A.D. Qi, T.K. Harden, and R.A. Nicholas. 2010. Charged residues in the C-terminus of the P2Y1 receptor constitute a basolateral-sorting signal. *J Cell Sci*. 123:2512-2520.

Yamada, S., S. Pokutta, F. Drees, W.I. Weis, and W.J. Nelson. 2005. Deconstructing the cadherin-catenin-actin complex. *Cell*. 123:889-901.

Yamanaka, T., Y. Horikoshi, Y. Sugiyama, C. Ishiyama, A. Suzuki, T. Hirose, A. Iwamatsu, A. Shinohara, and S. Ohno. 2003. Mammalian Lgl forms a protein complex with PAR-6 and aPKC independently of PAR-3 to regulate epithelial cell polarity. *Curr Biol*. 13:734-743.

Yamanaka, T., Y. Horikoshi, A. Suzuki, Y. Sugiyama, K. Kitamura, R. Maniwa, Y. Nagai, A. Yamashita, T. Hirose, H. Ishikawa, and S. Ohno. 2001. PAR-6 regulates aPKC activity in a novel way and mediates cell-cell contact-induced formation of the epithelial junctional complex. *Genes Cells*. 6:721-731.

Yang, S.H., A. Galanis, J. Witty, and A.D. Sharrocks. 2006. An extended consensus motif enhances the specificity of substrate modification by SUMO. *EMBO J*. 25:5083-5093.

Yap, A.S., C.M. Niessen, and B.M. Gumbiner. 1998. The juxtamembrane region of the cadherin cytoplasmic tail supports lateral clustering, adhesive strengthening, and interaction with p120ctn. *The Journal of cell biology*. 141:779-789.

Yeaman, C., A.H. Le Gall, A.N. Baldwin, L. Monlauzeur, A. Le Bivic, and E. Rodriguez-Boulan. 1997. The O-glycosylated stalk domain is required for apical sorting of neurotrophin receptors in polarized MDCK cells. *The Journal of cell biology*. 139:929-940.

Zaidel-Bar, R., S. Itzkovitz, A. Ma'ayan, R. Iyengar, and B. Geiger. 2007. Functional atlas of the integrin adhesome. *Nat Cell Biol*. 9:858-867.

Zamir, E., and B. Geiger. 2001. Molecular complexity and dynamics of cell-matrix adhesions. *J Cell Sci*. 114:3583-3590.

Zhu, Y., B. Doray, A. Poussu, V.P. Lehto, and S. Kornfeld. 2001. Binding of GGA2 to the lysosomal enzyme sorting motif of the mannose 6-phosphate receptor. *Science*. 292:1716-1718.